Università degli Studi di Cagliari

PhD PROGRAM in:

SCIENZE E TECNOLOGIE FARMACEUTICHE

Ciclo XXIII

S.S.D: CHIM/09

PREPARATION, DEVELOPMENT AND EVALUATION OF NOVEL DRUG DELIVERY SYSTEMS FOR COLON TARGETING

PhD candidate: *Carla Mura*

PhD program coordinator: *Prof. Elias Maccioni*

Supervisors: *Prof. Giuseppe Loy*
Prof. Octavio Diez

TABLE OF CONTENTS

1. INTRODUCTION

1.1. Colon anatomy

The colon is the last part of the digestive system; it extracts water and salt from solid wastes before they are eliminated from the body, and is the site in which flora-aided (largely bacteria) fermentation of unabsorbed material occurs. Unlike the small intestine, the colon does not play a major role in absorption of foods and nutrients. However, the colon does absorb water, potassium and some fat soluble vitamins. Anatomically it consists of four sections (Figure 1) [1]: the ascending colon, the transverse colon, the descending colon, and the sigmoid colon (the proximal colon usually refers to the ascending colon and transverse colon). The colon, cecum, and rectum make up the large intestine.

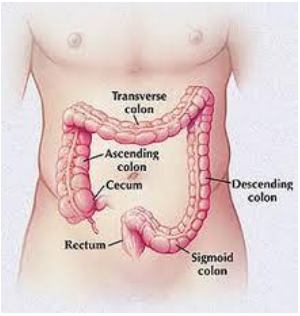

Figure 1. Colon anatomy

Histologically the colon can be divided into four layers (Figures 2A and B) [2,3]: mucosa, submucosa, muscularis externa and serosa.

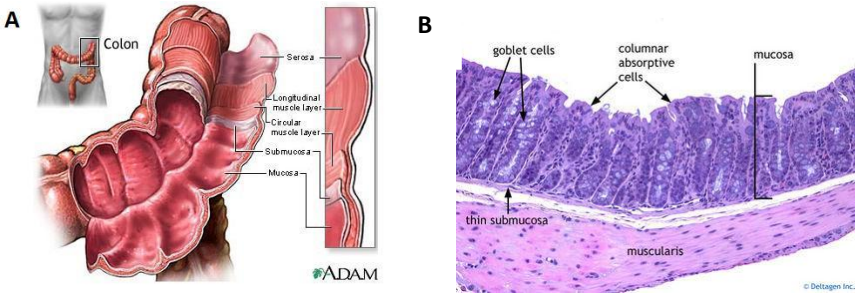

Figures 2A and B. Colon structure.

The mucosa is composed by the epithelium, lamina propria and muscularis mucosae (Figures 3A and B) [4]. It has a simple columnar epithelium shaped into straight

tubular crypts, which are short invaginations of mucosal epithelium and provide protected pockets for special cellular functions. There are no villi. In cellular composition, the epithelium resembles that of the small intestine, but with a higher proportion of goblet cells interspersed among the absorptive cells (enterocytes). Goblet cells are specialized for secretion of mucus, which facilitates passage of material through the bowel, while enterocytes are specialized for absorption of nutrients across the apical plasma membrane and export of these same nutrients across the basal plasma membrane. The crypt epithelium also includes stem cells which replenish the epithelium every few days, enteroendocrine cells, and Paneth cells (secretory epithelial cells located at the ends of intestinal crypts. The function for these cells is secretion of anti-bacterial proteins into the crypt lumen, thereby providing protection for the stem cells which line the crypt walls). The crypts are separated by conspicuous lamina propria, the loose connective tissue in a mucosa. Lamina propria supports the delicate mucosal epithelium, allows the epithelium to move freely with respect to deeper structures, and provides for immune defense, it is composed by connective tissue infiltrated by many white blood cells, with capillaries and thin strands of smooth muscle.

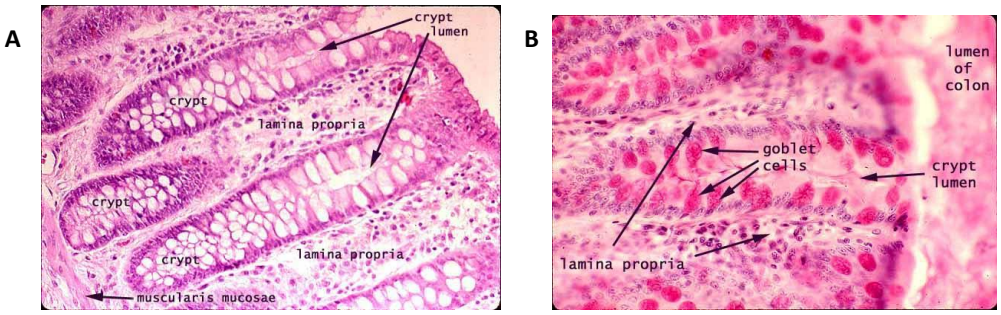

Figure 3A and B. Colon mucosa structure.

The muscularis mucosa of the lower tract forms a thin layer (only a few muscle fibers in thickness) beneath the deep ends of the crypts. The submucosa is a connective tissue layer deep to and supporting the mucosa. The muscularis externa of the colon has the standard layers of inner circular and outer longitudinal smooth muscle. The outer layer of the colon is a serosa attached to mesentery, ordinary connective tissue with a surface of mesothelium.

1.2. Colon specific delivery

The oral route is considered to be the most convenient for administration of drugs to patients. The conventional oral dosage forms normally dissolve in the stomach fluid or intestinal fluid and are absorbed from these regions of the gastrointestinal (GI) tract, which depend upon the physicochemical properties of the drug. Localized delivery of the drugs in the colon region is possible only when the drug is protected from the hostile environment of upper GI tract. Dosage forms that deliver drugs into the colon region rather than upper GI tract proffers number of advantages. Oral delivery of drugs to the colon is valuable in the treatment of diseases of colon (ulcerative colitis, Crohn's disease, carcinomas and infections) whereby high local concentration can be achieved while minimizing side effects that occur because of release of drugs in the upper GI tract or unnecessary systemic absorption. Specific systemic absorption of drugs and protein/peptides in the colonic region offers interesting possibilities for the treatment of disease susceptible to diurnal rhythm such as asthma, arthritis or inflammation [5-7]. The colon is considered to be more suitable for delivery of peptides and protein in comparison to small intestine because proteolytic enzyme activity in the colon, such as digestive enzyme and metabolic enzyme activity, is lower than in the small intestine [8-11]. Because of the distal location of colon in the GI tract, a colon-specific drug delivery system should prevent drug release in the stomach and small intestine, and affect an abrupt onset of drug release upon entry into the colon. This necessitates a triggering element in the system that can respond to physiological changes in the colon. Three strategies are currently being pursued to achieve drug release specifically in the colon [12-14].

1) The fact that the luminal pH of the distal colon is slightly higher than that of the proximal small intestine has led to the development of oral dosage forms that are intended to release the drug at the colonic pH (pH controlled drug delivery). An overview of the pH details of the GIT is shown in Table 1 [15].

2) The colonic microflora produce a variety of enzymes that are not present in the stomach or the small intestine and could therefore be used to deliver drugs to the colon after enzymatic cleavage of degradable formulation components or drug carrier bonds (enzyme controlled drug delivery).

3) The relatively constant transit time in the small intestine – approximately 3–5 h – is another physiological characteristic that can be taken advantage of to achieve colon specificity (time-controlled drug delivery). After gastric emptying, a time-controlled drug delivery system is intended to release the drug after a predetermined lag phase. Gastric emptying of dosage forms is highly variable and depends primarily on whether the subject is fed or fasted and on the properties of the dosage form such as size and density. The transit times of small dosage forms in GI tract is shown in Table 2 [15].

Table 1. Average pH in the GI tract

Location	pH
Oral cavity	6.2-7.4
Oesophagus	5.0-6.0
Stomach	
• **Fasted condition**	1.5-3.0
• **Fed condition**	3.0
Small intestine	
• **Duodenum**	4.5-5.0
• **Jejunum**	5.0-6.5
• **Ileum**	6.0-7.0
Large intestine	7.5

Table 2. Transit time in the GI tract

Organ	Transit time (h)
Stomach	
• **Fasting**	<1
• **Fed**	>2
Small intestine	3-4
Large intestine	20-30

1.2.1. pH-dependent systems

The pH-dependent systems rely on the physiological difference between the luminal pH of the acidic stomach and that of the large intestine. The pH of the human GI tract increases progressively from the stomach (pH=1-2, which increases to 3 during digestion), small intestine (pH=5-6) at the site of digestion and it increases to 7-8 in the distal ileum [15]. The coating of pH-sensitive polymers to the tablets capsules or pellets provide delayed release and protect the active drug from gastric fluid. The polymers used for colon targeting, however, should be able to withstand the lower

pH values of the stomach and of the proximal part of the small intestine and also be able to disintegrate at the neutral of slightly alkaline pH of the terminal ileum and preferably at the ileocecal junction. These processes distribute the drug throughout the large intestine and improve the potential of colon targeted delivery systems. Most commonly used pH-dependent coating polymers are methacrylic acid copolymers commonly known as Eudragit®, more specifically Eudragit® L and Eudragit® S (Figure 4) [14]. Eudragit® L 100 and S 100 are copolymers of methacrylic acid and methyl methacrilate. The ratio of carboxyl to ester groups is approximately 1:1 in Eudragit® L 100 and 1:2 in Eudragit® S 100. The polymers form salts and dissolve above pH 5.5 and disperse in water to form latex and thus avoid the use of organic solvents in the coating process. The water solubility of the Eudragit® S depends on the ratio of free carboxyl groups to the esterified groups. The critical factor that influences the performance of these polymers is the pH value at which dissolution occurs.

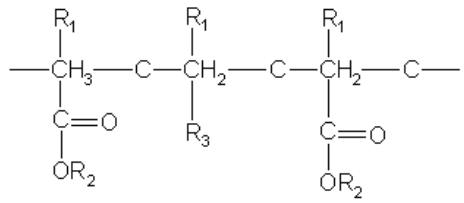

R1 = CH3; H
R2 = CH3, CH3CH2
R3 = COOH (Eudragit® L and S)
R3 = COOCH2CH2N (CH3)3Cl- (Eudragit® RL and RS)

Figure 4. Chemical structures of various formulations of Eudragit®

1.2.2. Time-release-dependent systems

This approach is based on the principle of delaying the release of the drug until it enters into the colon. The strategy in designing timed release systems is to resist the acidic environment of the stomach and to undergo a lag time of predetermined span of time, after which release of drug takes place. The lag time in this case is the time requires to transit from the mouth to the colon. The first formulation introduced based on this principle was Pulsincap® (Figure 5) [16]. It is similar in appearance to hard gelatin capsule; the main body is made water insoluble. The contents are contained within a body by a hydrogel plug, which is covered by a water-soluble

cap. The whole unit is coated with an enteric polymer to avoid the problem of variable gastric emptying. When the capsule enters the small intestine the enteric coating dissolves and the hydrogel plug starts to swell, the amount of hydrogel is such adjusted that it pops out only after the stipulated period of time to the release contents.

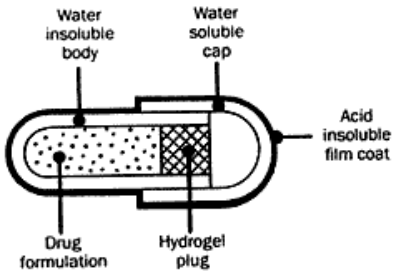

Figure 5. Pulsincap® system

A delivery system called Time Clock® has been exploited to deliver the drug to the colon. It is composed of a solid dosage form coated with a hydrophobic coating layer which consists of wax, Tween-80 and hydroxypropylmethylcellulose (HPMC). The lag time observed with this system is caused by slow hydratation of the coating layer in a time proportional to the thickness of the film and the core is then available for dispersion.

Pressure controlled drug delivery systems have been developed to target the drugs to the colon [17,18]. The OROS-CT can be used to target the drug locally to the colon for the treatment of disease or to achieve systemic absorption. The OROS-CT system can be a single osmotic unit or may incorporate as many as 5-6 push-pull units, encapsulated within a hard gelatin capsule. Each bilayer push pull unit contains an osmotic push layer and a drug layer, both surrounded by a semipermeable membrane. An orifice is drilled through the membrane next to the drug layer. Immediately after the OROS-CT is swallowed, the gelatin capsule containing the push pull units dissolves. Because of its drug-permeable enteric coating, each push pull unit is prevented from absorbing water in the acidic aqueous environment of the stomach and hence no drug is delivered. As the unit enters the small intestine, the coating dissolves in this larger pH environment (pH>7), water enters the unit, causing the osmotic push compartment to swell and concomitantly

creates a flowable gel in the drug compartment. Swelling of the osmotic push compartment forces drug gel out of the orifice at a rate precisely controlled by the rate of water transport through the semipermeable membrane.

For treating ulcerative colitis each push pull unit is designed with a 3-4 hours post gastric delay to prevent drug delivery in the small intestine. Drug release begins when the unit reaches the colon. OROS-CT units can maintain a constant release rate for up to 24 hours in the colon or can deliver drug over an internal as short as 4 hours. The results showed the capability of the system in delaying drug release for a programmable period of time and the possibility of exploiting such delay to attain colon targeted delivery according to a time-dependent approach.

1.2.3. Enzyme-dependent systems

The gastrointestinal tract is inhabited by a variant microflora all along. The bacteria distribution within the gastro-intestinal tract is different and depends on the part of the GIT considered.

In Figure 6 [19] the concentration of bacterial flora in different regions of the gastrointestinal tract is presented. The microflora of the stomach is normally sparse and bacterial concentration is less than 10^3 CFU (colony forming unit) ml^{-1}. The bacterial concentration in the small intestine is of the order of 10^3–10^4 CFU ml^{-1}, while in the large intestine it increases sharply and the colon has a microflora of 10^{11}–10^{12} CFU ml^{-1} [20].

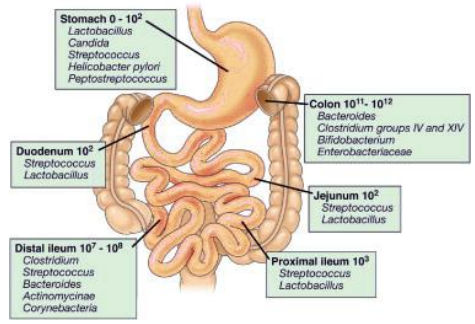

Figure 6. Microflora distribution in GI tract

One of the main function of the colonic microflora is the carbohydrate fermentation and absorption; bacteria produce a wide range of reductive and hydrolytic enzymes (amidase, esterase, reductase, deaminase), that ferment the various types of substrate

that have been indigested in the small intestine like glucose, bi- and tri-saccharide and other polysaccharide (starch, pectin, dextran, chitosan, guar gum). The large and specific colonic enzyme concentration, which is not present in the rest of the GI tract, can be used to deliver drugs to the large intestine. Enzyme-dependent systems can be divided in two groups: prodrugs and biodegradable polysaccharides.

Prodrug is pharmacologically inactive derivative of a parent drug molecule that requires spontaneous or enzymatic transformation in vivo to release the active drug. For colonic delivery of drugs, prodrugs are designed to undergo minimal absorption and hydrolysis in the upper GI tract and undergo enzymatic hydrolysis in the colon, there by releasing the active drug moiety from the carrier. A considerable number of linkages susceptible to bacterial hydrolysis specifically in the colon have been prepared where the drug is covalently attached to hydrophilic moieties of carriers like amino acid, glucuronic acid, monosaccharide, polymers.

The metabolism of azo compounds by the intestinal bacteria is one of the most extensively studied bacterial metabolic processes. Both intracellular and extracellular reduction has been observed. In 1942 sulfasalazine (Figure 7) was prepared: it is formed by 5-aminosalycilic acid bound with a carrier (sulfapyridine, SP) through an azo-bond, which undergoes reduction in the colon. However, due to a number of side effects associated with SP studies, other carriers were studied to deliver 5-ASA to the large intestine with minimal side effects. This lead to formation of ipsalazide, balsalazide, and finally to olsalazide, where two molecules of 5-ASA were joined together [21].

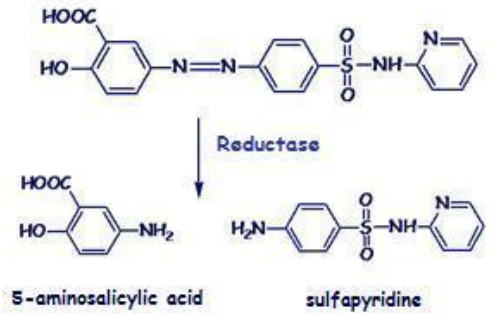

Figure 7. Sulfasalazine chemical structure and mechanism of drug release by reductase enzyme

Macromolecular prodrugs were also prepared, for istance dextran [22,23] or cyclodextrin [24-27] conjugates.

Newer approaches are aimed at use of polymers as drug carriers for drug delivery to the colon. Both synthetic as well as naturally occurring polymers are used for this purpose. Use of naturally occurring polysaccharides have also been investigated for colonic delivery of drugs, since these polymers of monosaccharide are found in abundance have wide availability, are inexpensive and are available in variety of structures with varied properties. They can be easily modified chemically and biochemically and are highly stable, safe, non- toxic, hydrophilic and gel forming and in addition biodegradable. These include naturally occurring polysaccharides obtained from plant (guar gum, inulin), animal (chitosan, chondroitin sulphate), algal (alginates) or microbial (dextran) origin [28-30]. These are selectively broken down by the colonic microflora to simple saccharides.

Many of the polysaccharide-based delivery systems shield the drug from the hostile environments of the upper GIT. When these delivery systems arrive into the colon the glycosidic linkages within the polysaccharides are hydrolyzed releasing the drug candidate.

1.2.4. Drugs used to colon delivery

Drugs which show poor absorption or degrade in the stomach or intestine including peptide are most suitable for colon specific drug delivery systems [31-36].

The drugs used in the treatment of inflammatory bowel disease and colon cancer are ideal candidates for local colon delivery [37-39].

In addition colonic targeting of drugs would prove useful where an intentional delay in absorption is desirable from a therapeutic point of view as for the treatment of diseases that have peak symptoms in the early morning and that exhibit circadian rhythm, such as nocturnal asthma, angina and rheumatoid arthritis [7].

The criteria for the selection of drugs for colon specific drug delivery systems are shown in Table 3.

Table 3. Drugs used for colon specific delivery.

Criteria	Drugs
Drugs for disease that exhibit circardian rhytm	Theophylline Ibuprofen Verapamil
Drugs poorly absorbed from upper GIT	Cyclosporine Desmopressin
Drugs for colon cancer	5-Fluorouracil
Drugs that degrade in stomach and small intestine	5-Fluorouracil Calcitonin Insulin
Drugs for targeting	5-Aminosalicylic-acid Prednisolone Metronidazole

1.3. Colon diseases

Site specific drug delivery to the colon is important for the treatment of diseases associated with the colon, reducing the side effects of the drug and reducing the administered dose. The most important colon-associated diseases are: inflammatory bowel disease (Crohn's disease and ulcerative colitis), colon cancer, irritable bowel syndrome, diverticulitis and amoebiasis.

1.3.1. Inflammatory bowel disease

The term inflammatory bowel disease (IBD) covers a group of disorders in which the intestine become inflamed, probably as a result of an immune reaction of the body against its own intestinal tissue. Two major types of IBD have been described: ulcerative colitis (UC) and Crohn's disease (CD) [40,41].

Table 4. Main differences between Ulcerative colitis and Crohn's disease.

	Ulcerative colitis	Crohn's disease
Areas of involvement	Involves the rectum and extends proximally in a continuous fashion, and always remains restricted to the colon. Is sometimes restricted to the rectum as 'ulcerative proctitis.	Most commonly the terminal ileum, cecum, perianal area and colon, but any part of the GI tract can be affected. Characterized by segments of normal bowel between affected regions, known as 'skip lesions'.
Histology of inflammation type	An inflammation affecting the superficial (mucosal) layers of the bowel wall, infiltration of lymphocytes and granulocytes and loss of Goblet cells, accompanied by ulcerations and crypt abscesses.	A transmural inflammation (affecting all layers of the bowel wall), dense infiltration of lymphocytes and macrophages; granulomas in up to 60% of the patients; fissuring ulceration and submucosal fibrosis.
Characterization of inflammation type	The inflammation is characterized by a more Th2 type response, with high levels of IL-5 and IL-13 (but not IL-4), high levels of autoantibodies (anti-neutrophil cytoplasmic antibodies (pANCA), indicative of B-cell activation).	The inflammation is characterized by a Th1 type response, with high levels of IL-12, IFN-g and TNF-a.

As the name suggests, ulcerative colitis is limited to the colon (large intestine), although Crohn's disease can involve any part of the gastrointestinal tract from the mouth to the anus; it most commonly affects the small intestine and/or the colon. The main differences between them are shown in Table 4 [42].

Because inflammatory bowel disease is a chronic disease (lasting a long time), it goes through periods in which the disease flares up and is considered to be in an active stage and severe inflammation; these periods are followed by remission, in which symptoms disappear or decrease and normal conditions return [43]. Symptoms may range from mild to severe and generally depend upon the part of the intestinal tract involved. They include the following: abdominal cramps and pain, bloody diarrhea, severe urgency to have a bowel movement, fever, loss of appetite, weight loss, anemia (due to blood loss).

Researchers do not yet know what causes inflammatory bowel disease [44,45]. Therefore, IBD is called an idiopathic disease (disease with an unknown cause). An unknown factor/agent (or a combination of factors) triggers the body's immune system to produce an inflammatory reaction in the intestinal tract that continues without control. As a result of the inflammatory reaction, the intestinal wall is damaged leading to bloody diarrhea and abdominal pain.

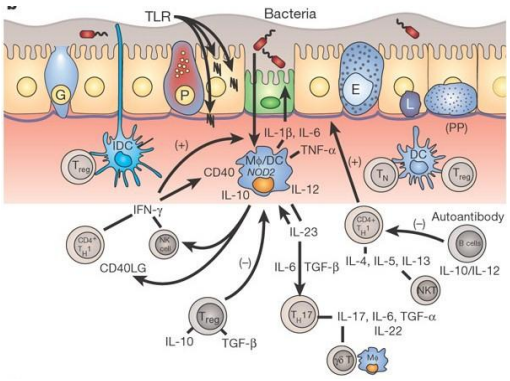

Figure 8. Mucosal immune response initiated by microbial sensing systems activates adaptive immune responses. Pathogenic bacteria or commensal microbes in genetically susceptible hosts disrupt epithelial barrier function, triggering the recruitment and activation of innate immune responses and colitogenic $CD4^+$ T cells. Depicted cells and cytokines imply that multiple components are involved in controlling mucosal immune responses in physiological and pathological states of inflammation. NK, natural killer.

Genetic, infectious, immunologic, and psychological factors have all been implicated in influencing the development of IBD. There is a genetic predisposition (or perhaps susceptibility) to the development of IBD. However, the triggering factor for activation of the body's immune system has yet to be identified. Factors that can turn on the body's immune system include an infectious agent, an immune response to an antigen, or an autoimmune process. Genetic susceptibility is influenced by the luminal microbiota, which provides antigens and adjuvants that stimulate either pathogenic or protective immune responses. Environmental triggers are necessary to initiate or reactivate disease expression. In inflammatory bowel disease, the well-controlled balance of the intestinal immune system is disturbed at all levels (Figure 8) [46].

Standard treatment for ulcerative colitis depends on extent of involvement and disease severity [47-49]. The goal is to induce remission initially with medications, followed by the administration of maintenance medications to prevent a relapse of the disease. Aminosalicylate, corticosteroids, immunosuppressive drugs and TNF-inhibitors are commonly used in the treatment of IBD.

- Aminosalicylate: 5-ASA compounds (mesalazine, osalazine, sulfasalazine, balsalazide) [50] have been shown to be useful in the treatment of mild-to-moderate Crohn's disease and ulcerative colitis and as maintenance therapy.
- Corticosteroids: They are a class of anti-inflammatory drug that are used primarily for treatment of moderate to severe IBD. The most commonly prescribed oral steroid is prednisone, but the following corticosteroids are also used as immune system suppressants in treatment of ulcerative colitis: cortisone, hydrocortisone and budesonide [51].
- Immunosuppressive drugs. They inhibit the immune system generally. These include the cytostatic drugs that inhibit cell division, including the cloning of white blood cells that is a part of the immune response. Immunosuppressive drugs used with ulcerative colitis include: mercaptopurine (6-MP, it is a cytostatic drug that is an antimetabolite, it mimics purine, which is necessary for the synthesis of DNA, with mercaptopurine present, cells are not able to make DNA, and cell division is inhibited); azathioprine (which metabolises to 6-MP) and methotrexate (which inhibits folic acid) [52].

- TNF inhibitors: They are monoclonal antibodies that inhibit the pro-inflammatory cytokine tumour necrosis factor (TNF). The most important are infliximab and adalimubab [53].
- Antibiotics: Metronidazole and ciprofloxacin are antibiotics which are used to treat IBD. They are also used for treatment of complications, including abscesses and other infections.

1.3.1.1. 5-Aminosalycilic acid

5-Aminosalicylic acid (5-ASA), also known as mesalazine or mesalamine, is an anti-inflammatory drug used to treat inflammation of the digestive tract, ulcerative colitis and Crohn's disease (Inflammatory Bowel Disease, IBD). It is a bowel-specific aminosalicylate drug that acts locally in the gut and has its predominant actions there [50].

The precise mechanism of action of 5-ASA is not known, but is likely due to a combination of anti-inflammatory properties [54,55].

Table 5. 5-ASA chemical properties.

CHEMICAL STRUCTURE	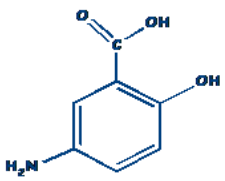
IUPAC name	5-amino-2-hydroxybenzoic acid
Formula	$C_7H_7NO_3$
Mol. mass	**153,135 g/mol**
Water Solubility	**0.84 mg/ml**
Log P	**1.3**

It has been shown to block the production of interleukin-1 (IL-1) and tumor necrosis factor-α (TNF-α) [56,57] and it is a potent inhibitor of the cyclooxygenase pathway, inhibiting the production of prostaglandin E2 in inflamed intestinal specimens [58].

Blockage of the lipooxygenase pathway has also been shown [59,60] inhibiting both 5-lipooxygenase and 5-lipooxygenase-activating protein. It is also one of the most potent known free radical scavengers and antioxidants [61-64]. Many of the effects of 5-ASA may also be explained by inhibition of activation of nuclear factor-κB (NF-κB), a central transcription regulatory factor involved in mediating the initiation and perpetuation of inflammatory processes [65,66]. Activated NF-κB has been detected in macrophages and epithelial cells in inflamed mucosa from Crohn's disease and ulcerative colitis [67].

5-ASA is rapidly and completely absorbed from the upper intestine when administered orally, [68,69]. Free 5-ASA undergoes rapid and nearly complete systemic absorption from the proximal intestine depending on its concentration and the local pH, followed by extensive metabolism to N-acetyl-5-ASA, by the N-acetyltransferase 1 (NAT 1) enzyme [70,71] in both intestinal epithelial cells and the liver, and then excretion in the urine as a mixture of free 5-ASA and N-acetyl-5-ASA [72,73]. To prevent proximal small intestinal absorption and allow the drug to reach the inflamed small bowel and/or colon, a variety of 5-ASA delivery systems have been developed [74]. These include:

1) Creating a larger unabsorbing molecule (prodrug) by binding it to a carrier or another 5-ASA via an azo-bond, this subsequently undergoes cleavage in the colon releasing the active drug. Examples include sulfasalazine (Azulfidine®), olsalazide sodium (Dipentum®), and balsalazide disodium (Colazalk™).

2) Coating mesalamine with a pH-sensitive polymer, which dissolves in the basic environment of the distal ileum and colon (Asacol®).

(3) Coating mesalamine with a moisture-sensitive coating (ethyl-cellulose) to release mesalamine upon contact with moisture throughout the GI tract (Pentasa®).

(4) Administrating mesalamine as an enema (Rowasa®) or suppository (Canasa™), effectively by passing the threat of small bowel absorption.

1.3.2. Amoebiasis

Amoebiasis refers to infection caused by the amoeba *Entamoeba histolytica*, that is an anaerobic parasitic protozoan, part of the genus *Entamoeba* [75,76].

The active (trophozoite) stage exists only in the host and in fresh loose feces; cysts survive outside the host in water, soils and on foods, especially under moist conditions on the latter. The cysts are readily killed by heat and by freezing temperatures, and survive for only a few months outside of the host. When cysts are swallowed they cause infections by excysting (releasing the trophozoite stage) in the digestive tract.

The life cycle of the protozoa [77] is shown in Figure 9 [78]: cysts with four nuclei (metacysts) are ingested orally with contaminated food or drinking water. After excysting in the small intestine, both the cytoplasm and nuclei divide to form eight small amebulae (metacystic trophozoites). Mature trophozoites (minuta forms) reproduce by constant binary fission. Some of the minuta forms may grow to magna forms, which enter the intestinal wall and, via the bloodstream, other organs such as liver, lung, and brain, where they lead to abscesses (amoebomae).

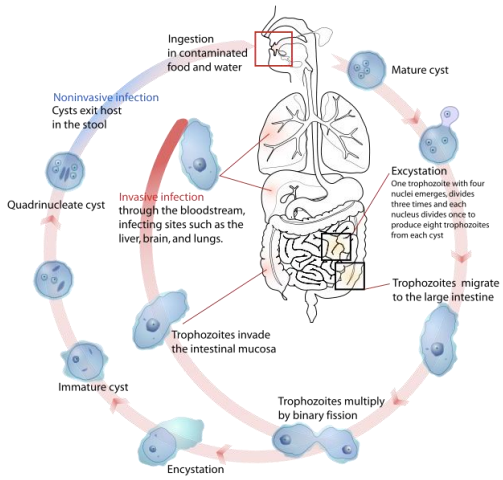

Figure 9. Life cycle of protozoa.

Symptoms can range from mild diarrhea to dysentery with blood and mucus in the stool.

E. histolytica is usually a commensal organism.[79] Severe amoebiasis infections (known as invasive or fulminant amoebiasis) occur in two major forms. Invasion of the intestinal lining causes amoebic dysentery or amoebic colitis [80]. If the parasite reaches the bloodstream it can spread through the body, most frequently ending up in the liver where it causes amoebic liver abscesses [81]. Liver abscesses can occur

without previous development of amoebic dysentery. When no symptoms are present, the infected individual is still a carrier, able to spread the parasite to others through poor hygienic practices.

Because of *E. histolytica* infections occur in both the intestine and in tissue of the intestine and/or liver, as a result, two different classes of drugs are needed to treat the infection, one for each location [82]. Such anti-amoebic drugs are known as amoebicides. Both tissue and lumenal drugs must be used to treat infections, with metronidazole usually being given first, followed by paromomycin or diloxanide.

- Tissue amebicides: Metronidazole [83], or a related drug such as tinidazole [84], secnidazole or ornidazole, is used to destroy amoebae that have invaded tissue. These are rapidly absorbed into the bloodstream and transported to the site of infection. Because they are rapidly absorbed there is almost none remaining in the intestine.
- Luminal amebicides: Since most of the amoebae remain in the intestine when tissue invasion occurs, it is important to get rid of those also or the patient will be at risk of developing another case of invasive disease. Several drugs are available for treating intestinal infections, the most effective of which has been shown to be paromomycin [85], diloxanide furoate and iodoquinol.

1.3.2.1. Metronidazole

Metronidazole is a nitroimidazole compound active in the treatment of anaerobic protozoan and bacterial infections [86,87].

Metronidazole is bactericidal against the majority of anaerobic bacteria like *Gardnerella, Bacteroides fragilis, Fusobacterium, Clostridium, Peptococcus, Peptostreptococcus, Clostridium difficile* [88,89] and against some microaerophilic organisms and anaerobic protozoa [90,91]. These include *Entamoeba histolytica*, *Giardia lamblia*, and *Balantidium coli*.

It is used in the treatment of: Trichomoniasis, pseudomembranous colitis, bacterial vaginosis, upper genital tract infections, Amoebiasis and Giardiasis.

Table 6. Metronidazole chemical properties.

CHEMICAL STRUCTURE	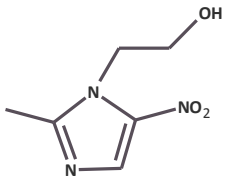
IUPAC name	2-(2-methyl-5-nitro-1*H*-imidazol-1-yl)ethanol
Formula	$C_6H_9N_3O_3$
Mol. mass	171,15 g/mol
Water solubility	10.0 mg/ml
Log P	-0.1

The proposed mechanism of action of metronidazole consists of a four-step process [86]: entry into a target cell, activation, generation of free radicals, and, finally, cell death resulting from damage to DNA. Metronidazole enters aerobic and anaerobic bacteria, protozoa, and mammalian cells through passive diffusion. In anaerobic bacteria, metronidazole is converted to an active metabolite that has not been characterized completely. This conversion creates a concentration gradient, promoting the further diffusion of the parent compound into the cell. In aerobic organisms, conversion does not occur, and the concentration of metronidazole within the cell equilibrates with the serum concentration. Activation of metronidazole in anaerobic organisms occurs through reduction of the nitro group [92]. The reduction is thought to be mediated through donation of electrons by ferredoxin-like transport proteins. These proteins are an integral part of the normal metabolism of anaerobic organisms but have a limited role in aerobic organism metabolism. The intermediate compounds generated by activation of metronidazole are free radicals, which are believed to be the source of the cytotoxicity of this compound. These free radicals consist of nitro, nitroso, and hydroxylamine derivatives. These compounds are short lived and are quickly metabolized to inactive end products. The free radical intermediate compounds are thought to

interact with and/or destroy directly cellular DNA. The generation of free radicals is the source of concern regarding the teratogenic and carcinogenic potential of metronidazole.

The use of metronidazole in the treatment of amoebiasis (amebic dysentery) requires high drug doses: 750 mg orally 3 times daily for 5-10 days, because it is completely absorbed before it reaches the site of action (colon). For this reason it is necessary to develop a new drug delivery system that protects the drug from the absorption in the upper part of the gastrointestinal tract and releases metronidazole in the colon.

1.4. Carrier systems

1.4.1. Chitosan

Chitosan is a linear polysaccharide composed of randomly distributed β-(1-4)-linked D-glucosamine (deacetylated unit) and N-acetyl-D-glucosamine (acetylated unit) (Figure 10). Chitosan is produced commercially by deacetylation of chitin, which is the second most abundant polysaccharide in nature and the structural element in the exoskeleton of crustaceans (crabs, shrimp) and cell walls of fungi [93,94].

Chitosan refers to a large number of polymers, which differ in their degree of N-deacetylation (40-98%) and molecular weight (50,000-2,000,000 Dalton). These two characteristics are very important to the physic-chemical properties of the chitosan and hence, it has a major effect on the biological properties.

Chitosan is a weak base with a pk_a value of the D-glucosamine unit of about 6.5 and therefore is insoluble at neutral and alkaline pH values. It is insoluble in water and organic solvent but it dissolves at acidic pH. Indeed in acidic medium the amine groups of the polymer are protonated resulting in a soluble positively charged polysaccharide.

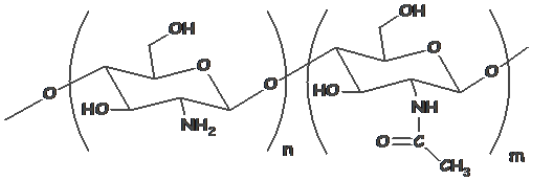

Figure 10. Chitosan structure.

Because chitosan has favorable biological properties such as biodegradability [95] and biocompatibility [96] it has attracted a lot of attention in the pharmaceutical and medical fields. Chitosan's main properties are as follows: gel-forming behaviour, mucoadhesion, absorption enhancer [97].

Chitosan has been shown to possess mucoadhesive properties [98-100] due to molecular attractive forces formed by electrostatic interaction between positively charged chitosan and negatively charged mucosal surfaces. These properties may be attributed to: strong hydrogen bonding groups like –OH, –COOH, sufficient chain flexibility and positive charge on chitosan polymer gives rise to strong electrostatic

interaction with mucus or negatively charged sialic acid residues on the mucosal surface.

Chitosan hydrogels have been prepared [101] with a variety of different shapes, geometries, and formulations that include liquid gels, powders, beads, films, tablets, capsules, microparticles, textile fibers, and inorganic composites. In each preparation chitosan is either physically associated or chemically cross-linked to form the hydrogel [102,103]. There are four major physical interactions (ionic, polyelectrolyte, interpolymer complex, and hydrophobic associations) that lead to the gelation of a chitosan solution.

Chitosan can be chemically modified in a lot of different ways, since it provides functional groups as primary amine as well as a secondary hydroxyl groups in its monomers [104,105]. Quaternized derivatives [106,107], carboxymethyl chitosan [108], N-Acyl derivatives (for instance N-Succinyl-chitosan) [109], thiolated chitosans [110,111] were prepared. Due to its favourable properties chitosan-based systems have gained a lot of attention in pharmaceutical field [112,113]. They are widely used for ophthalmic [114], nasal [115], buccal [116], intestinal [117], vaginal [118], vaccine [119] and colon delivery.

Chitosan is used in oral drug formulations to provide sustained release of drugs. It was found that chitosan is degraded by the microflora, which is available in the colon. As a result, this compound could be promising for colon-specific drug delivery. Enteric coated capsules have been prepared [120]. Different salts of chitosan were synthesized and evaluated [121,122], pH sensitive based chitosan hydrogels drug delivery system have been developed [123]. Chitosan-based microspheres [124] and polyelectrolyte complexes [125] were also prepared for colon targeted drug delivery. Chitosan derivatives were prepared and proved for colon-specific, orally administered drug delivery systems [126].

1.5.2. Cyclodextrin

Cyclodextrins are cyclic oligosaccharides containing at least 6 D-(+) glucopyranose units attached by α-(1, 4) glucosidic bonds (Figure 11) [127]. The three natural CDs: α-, β-, and γ-CD possess 6, 7, or 8 glucose units respectively [128]. They are

produced from starch by means of enzymatic conversion; commonly cyclodextrin glycosyltransferase (CGTase) is employed along with α-amylase [129].

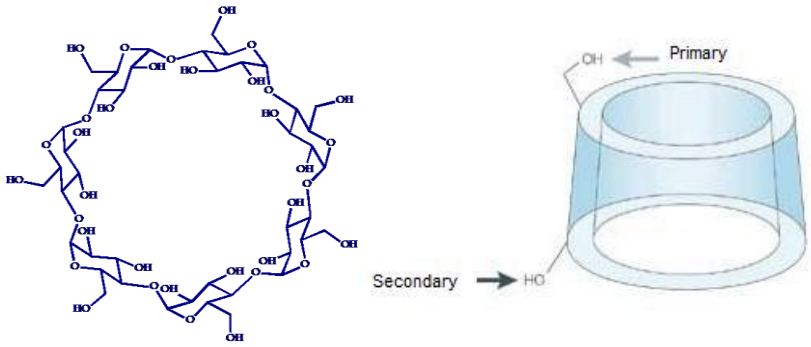

Figure 11. β-cyclodextrin structures.

The three kinds of cyclodextrin differ from ring size, number of glucopyranose units, molecular weight and solubility in water [130]. α-CD has 6 glucopyranose units, its molecular weight is 972 g/mol and the solubility in water at 25°C is 14.5 % w/w. β-CD has 7 glucopyranose units, the molecular weight is 1135 g/mol and the solubility is 1,85 %w/w. γ-CD is the most soluble (23.2% w/w) and has 8 glucopyranose unit, the molecular weight is 1297 g/mol.

They can be topologically represented as toroids with the larger and the smaller openings of the toroid exposing to the solvent secondary and primary hydroxyl groups respectively. The interior of the toroids is not hydrophobic, but considerably less hydrophilic than the aqueous environment and thus able to host other hydrophobic molecules. In contrast, the exterior is sufficiently hydrophilic to impart cyclodextrins (or their complexes) water solubility.

These properties make CD capable to form complexes with lipophilic molecules called inclusion complex [130]. The formation of the inclusion complex greatly modifies the physical and chemical properties of the guest molecule, mostly in terms of water solubility and stability. This is the reason why cyclodextrins have attracted much interest in many fields, especially pharmaceutical applications [131].

Moreover CD–drug conjugates, in which a drug is covalently bound to CD, were prepared because they could be used as colon-targeting. CDs are known to be barely capable of being hydrolyzed and only slightly absorbed in passage through the stomach and small intestine, while they are specifically degraded by the enzymatic

microflora [132-134]. This property of CDs may be exploited for the formation of colon targeted drug delivery system. Several drug-CD conjugates have been prepared and studied. Orally administered drug-CD conjugates can survive passage through the stomach and small intestine. However drug release will be triggered by enzymatic degradation of CDs in the colon [24-27].

1.6. References

[1] http://www.wanitaindonesia-ifs.com/2009_10_01_archive.html

[2] http://adam.about.com/reports/Structure-of-the-colon.htm

[3] http://histology-world.com/photoalbum/displayimage.php?album=5&pos=52

[4] http://www.siumed.edu/~dking2/erg/GI111b.htm

[5] B.C. Youan. Chronopharmaceutics: gimmick or clinically relevant approach to drug delivery? J. Controlled Release 98 (2004) 337– 353.

[6] A.S. Mandal, N. Biswas, K.M. Karim, A. Guha, S. Chatterjee, M. Behera, K. Kuotsu. Drug delivery system based on chronobiology-A review. J. Controlled Release 147 (2010) 314–325.

[7] V.S. Mastiholimath, P.M. Dandagi, S.S. Jain, A.P. Gadad, A.R. Kulkarni. Time and pH dependent colon specific, pulsatile delivery of theophylline for nocturnal asthma. Int. J. Pharm. 328 (2007) 49–56.

[8] M. Mackay, J. Phillips, J. Hastewell. Peptide drug delivery: Colonic and rectal absorption. Adv. Drug Deliv. Rev. 28 (1997) 253-273.

[9] M. Katsum, S. Watanabe, H. Kawai, S. Takemura, K. Sako. Effects of absorption promoters on insulin absorption through colon-targeted delivery. Int. J. Pharm. 307 (2006) 156–162.

[10] P. Langguth, V. Bohner, J. Heizmann, H.P. Merkle, S. Wolffram, S. Amidon, S. Yamashita. The challenge of proteolytic enzymes in intestinal peptide delivery. J. Controlled Release 46 (1997) 39-57.

[11] J.A. Fix. Oral controlled release technology for peptides: status and future prospects. Pharm. Res. 13 (1996) 1760–1764.

[12] C. S. Leopold. Coated dosage forms for colon-specific drug delivery. PSTT 2(5) (1999) 197-204.

[13] L. Yang, J.S. Chu, J.A. Fix. Colon-specific drug delivery: new approaches and in vitro/in vivo evaluation. Int. J. Pharm. 235 (2002) 1–15.

[14] M.K. Chourasia, S.K. Jain. Pharmaceutical approaches to colon targeted drug delivery systems. J. Pharm. Pharm. Sci. 6 (2003) 33-66.

[15] R. Kumar, M.B. Patil, S.R. Patil, M.S. Paschapur. Polysaccharides Based Colon Specific Drug delivery: A Review. Int. J. Pharm. Tech. Res. 2 (2009) 334-346.

[16] S.M. Reddy, V.R. Sinha, D.S. Reddy. Novel oral colon-specific drug delivery systems for pharmacotherapy of peptides and nonpeptide drugs. Drugs Today 35 (1999) 537-580.

[17] T. Takaya, K. Niwa, M. Muraoka, I. Ogita, N. Nagai, R. Yano, G. Kimura, Y. Yoshikawa, H. Yoshikawa, K. Tajada. Importance of dissolution process on systemic

availability of drugs delivered by colon delivery system. J Controlled Release 50 (1998) 111-122.

[18] M. Muraoka, Z. Hu, T. Shimokawa, S. Sekino, R. Kurogoshi, Y. Kuboi, Y. Yoshikawa, K. Takada. Evaluation of intestinal pressure controlled colon delivery capsule containing caffeine as a model drug in human volunteers. J. Controlled Release 52 (1998) 119-129.

[19] R.B. Sartor. Microbial Influences in Inflammatory Bowel Diseases. Gastroenterol. 134 (2008)577–594.

[20]V.R. Sinha, R. Kumria. Microbially triggered drug delivery to the colon. Eur. J. Pharm. Sci. 18 (2003) 3-18.

[21] C.P. Willoughby, J.K. Aronson, H. Agback, N.O. Bodin, S.C. Truelove S.C. Distribution and metabolism in healthy volunteers of disodium azodisalicylate a potential therapeutic agent for ulcerative colitis. Gut 23 (1982) 1081–1087.

[22] S. Ahmad, R.F. Tester, A. Corbett, J. Karkalas. Dextran and 5-aminosalicylic acid (5-ASA) conjugates: synthesis, characterization and enzymic hydrolysis. Carbohydr. Res. 341 (2006) 2694–2701.

[23] J. Varshosaz, J. Emami, Naser Tavakoli, A. Fassihi, M. Minaiyan, F. Ahmadi, F. Dorkoosh. Synthesis and evaluation of dextran–budesonide conjugates as colon specific prodrugs for treatment of ulcerative colitis. Int. J. Pharm. 365 (2009) 69-76.

[24] K. Uekama, K. Minami, F. Hirayama. 6^{A}-*O*-[(4-Biphenylyl)acetyl]-α-, -*β*-, and -*γ*-cyclodextrins and 6^{A}-Deoxy-6^{A}-[[(4-biphenylyl)acetyl]amino]-α-,-*β*-, and -*γ*-cyclodextrins: Potential Prodrugs for Colon-Specific Delivery. J. Med. Chem. 40 (1997) 2755-2761

[25] H. Yano, F. Hirayama, M. Kamada, H. Arima, K. Uekama. Colon-specific delivery of prednisolone-appended α-cyclodextrin conjugate: alleviation of systemic side effect after oral administration. J. Controlled Release 79 (2002) 103–112.

[26] A.H. El-Kamel, A.A.-M. Abdel-Aziz, A.J. Fatani, H.I. El-Subbagh. Oral colon targeted delivery systems for treatment of inflammatory bowel diseases: Synthesis, in vitro and in vivo assessment. Int. J. Pharm. 358 (2008) 248–255.

[27] M. Zou, H. Okamoto, G. Cheng, X. Hao, J. Sun, F. Cui, K. Danjo. Synthesis and properties of polysaccharide prodrugs of 5-aminosalicylic acid as potential colon-specific delivery systems. Eur. J. Pharm. Biopharm. 59 (2005) 155–160.

[28] L. Liu, M.L. Fishman, J. Kost, K.B. Hick. Pectin-based systems for colon-specific drug delivery via oral route. Biomaterials 24 (2003) 3333–3343.

[29] S.F. Ahrabi, G. Madsen, K. Dyrstad, S.A. Sande, C. Graffner. Development of pectin matrix tablets for colonic delivery of model drug ropivacaine. Eur. J. Pharm. Sci. 10 (2000) 43–52.

[30] P. Sriamornsak, J. Nunthanid. Calcium pectinate gel beads for controlled release drug delivery:I. Preparation and in vitro release studies. Int. J. Pharm. 160 (1998) 207–212.

[31] A. Lamprecht, H. Yamamoto, H. Takeuchi, Y. Kawashima. pH-sensitive microsphere delivery increases oral bioavailability of calcitonin. J. Controlled Release 98 (2004) 1– 9.

[32] P. Nykanen, K. Krogars, M. Sakkinen, J. Heinamaki, H. Jurjensson, P. Veski, M. Marvola. Organic acids as excipients in matrix granules for colon-specific drug delivery. Int. J. Pharm. 184 (1999) 251–261.

[33] G.V. den Mooter, C. Samyn, R. Kinget. In vivo evaluation of a colon specific drug delivery system: an absorption study of theophylline from capsules coated with azo polymers in rats, Pharm. Res. 12 (1995) 244-247.

[34] H. Tozaki, J. Nishioka, J. Komoike, N. Okada, T. Fujita, S. Muranishi, S. Kim, H. Terashima, A. Yamamoto. Enhanced Absorption of Insulin and (Asu1,7) Eel-Calcitonin using Novel Azopolymer-Coated Pellets for Colon-Specific Drug Delivery. J. Pharm. Sci. 90 (2001) 89–97.

[35] M.L. Lorenzo-Lamosa, C. Remunan-Lopez, J.L. Vila-Jato, M.J. Alonso. Design of microencapsulated chitosan microspheres for colonic drug delivery. J. Controlled Release 52 (1998) 109–118.

[36] , W. Kalala, R. Kinget, G. Van den Mooter, C. Samyn. Colonic drug-targeting: in vitro release of ibuprofen from capsules coated with poly(ether-ester) azopolymers. Int. J. Pharm. 139 (1996) 187-195.

[37] V.R. Sinha, B.R. Mittal, K.K. Bhutani, Rachna Kumria. Colonic drug delivery of 5-fluorouracil: an in vitro evaluation. Int. J. Pharm. 269 (2004) 101–108.

[38] Y.S.R. Krishnaiah, V. Satyanarayana, B. Dinesh Kumar, R.S. Karthikeyan. In vitro drug release studies on guar gum-based colon targeted oral drug delivery systems of 5-fluorouracil. Eur. J. Pharm. Sci. 16 (2002) 185–192.

[39] K. Philip, B.Philip. Colon Targeted Drug Delivery Systems: A Review on Primary and Novel Approaches A. Oman Medical Journal 25 (2010) 70-78.

[40] R.B. Sartor. Mechanisms of Disease: pathogenesis of Crohn's disease and ulcerative colitis. Gastroenterol. Hepatol. 3 (2006) 390-407.

[41] D.C Baumgart, S.R Carding. Inflammatory bowel disease: cause and immunobiology. Gastroenterol. 369 (2007) 1627–1640.

[42] M.E.A. Borm, G. Bouma. Animal models of inflammatory bowel disease. Drug Discovery Today 4 (2004) 437-443.

[43] D.C. Baumgart, W.J. Sandborn. Inflammatory bowel disease: clinical aspects and established and evolving therapies Lancet 369 (2007) 1641–57.

[44] T. Hibi, H. Ogata. Novel pathophysiological concepts of inflammatory bowel disease J. Gastroenterol. 41 (2006) 10–16.

[45] W. Strober, I. Fuss, P. Mannon. The fundamental basis of inflammatory bowel disease J. Clin. Invest. 117 (2007) 514–521.

[46] R.J. Xavier, D.K. Podolsky. Unravelling the pathogenesis of inflammatory bowel disease**.** Nature 448 (2007) 427-434.

[47] B.E. Sands. Therapy of Inflammatory Bowel Disease. Gastroenterol. 118 (2000) S68–S82.

[48] C. Xu, S. Meng, B. Pan. Drug therapy for ulcerative colitis. World J Gastroenterol 10 (2004) 2311-2317.

[49] M Campieri. New steroids and new salicylates in inflammatory bowel disease: a critical appraisal. Gut 50 (2002) 43–46.

[50] R. Bergman, M. Parkes. Systematic review: the use of mesalazine in inflammatory bowel disease. Aliment. Pharmacol. Ther. 23 (2006) 841–855.

[51] S.V. Kane, P. Schoenfeld, W.J. Sandborn, W. Tremaine, T. Hofer, B.G. Fegan. Systematic review: the effectiveness of budesonide therapy for Crohn's Disease. Aliment. Pharmacol. Ther. 16 (2002) 1509–1517.

[52] P.M. Choi, S.R. Targan. Immunomodulator therapy in Inflammatory bowel disease. Dig. Dis. Sci. 39 (1994) 1885-1892.

[53] A. Noble, R. Baldassano, P. Mamula. Novel therapeutic options in the inflammatory bowel disease world. Dig. Liver Dis. 40 (2008) 22–31.

[54] N.A. Punchard, S.M. Greenfield, R.P.H. Thompson. Mechanism of action of 5-aminosalicylic acid. Mediators Inflamm. 1 (1992) 151-165.

[55] S.M. Greenfield, N.A. Punchard, J.P. Teare, R.P.H. Thompson. Review article: the mode of action of the aminosalicylates in inflammatory bowel disease. Aliment. Pharmacol. Ther. 7 (1993) 369-383.

[56] D. Rachmilewitz, F. Karmeli, L.W. Schwartz, P.L. Simon. Effect of aminophenols (5-ASA and 4-ASA) on colonic interleukin-1 generation. Gut 33 (1992) 929–932.

[57] Y.R. Mahida, C.E. Lamming, A. Gallagher, A.B. Hawthorne, C.J. Hawkey. 5-Aminosalicylic acid is a potent inhibitor of interleukin 1β production in organ culture of colonic biopsy specimens from patients with inflammatory bowel disease. Gut 32 (1991) 50-54.

[58] J.R.S. Hoult, P.K. Moore. Effects of sulfasalazine and its metabolites on prostaglandin synthesis, inactivation and actions on smooth muscle. Br. J. Pharmac. 68 (1980) 719-730.

[59] W.F. Stenson, E. Lobos. Sulfasalazine inhibits the synthesis of chemotactic lipids by neutrophils, J. Clin. Invest. 69(1982) 494–497.

[60] W.F. Stenson. Role of eicosanoids as mediators of inflammation in inflammatory bowel disease. Scand. J. Gastroenterol. Suppl. 172 (1990) 13–18.

[61] J.G. Williams, M.Hallett. Effect of sulphasalazine and its active metabolite, 5-amino-salicylic acid, on toxic oxygen metabolite production by neutrophils. Gut 30 (1989) 1581-1587.

[62] S.M. McKenzie, W.F. Doe, G.D. Buffinton. 5-Aminosalicylic acid prevents oxidant mediated damage of glyceraldehyde-3-phosphate dehydrogenase in colon epithelial cells. Gut 44 (1999) 180–185.

[63] P. Gionchetti, C. Guarnieri, M. Campieri, A. Belluzzi, C. Brignola, P. Iannone, M. Miglioli, L. Barbara. Scavenger effect of sulfasalazine, 5-aminosalicylic acid, and olsalazine on superoxide radical generation. Dig. Dis. Sci. 36 (1991) 174-178.

[64] N.J. Simmonds, A.D. Millar, D.R. Blake, D.S. Rampton. Antioxidant effects of aminosalicylates and potential new drugs for infammatory bowel disease: assessment in cell-free systems and inflamed human colorectal biopsies. Aliment. Pharmacol. Ther.13 (1999) 363-372.

[65] P.A. Baeuerle, D. Baltimore. NF-κB: ten years after. Cell 87 (1996) 13– 20.

[66] H. Bantel, C. Berg, M. Vieth, M. Stolte, W. Kruis, K. Schulze-Osthoff. Mesalazine Inhibits Activation of Transcription Factor NF-κB in Inflamed Mucosa of Patients With Ulcerative Colitis. Am. J. Gastroenterol. 95 (2000) 3452-3457.

[67] G. Rogler, K. Brand, D. Vogl, S. Page, R. Hofmeister, T. Andus, R. Knuechel, P.A. Baeuerle, J. Scholmerich, V. Gross. Nuclear factor κB is activated in macrophages and epithelial cells of inflamed intestinal mucosa, Gastroenterol. 115 (1998) 357-369.

[68] S.Y. Zhou, D. Fleisher, L.H. Pao, C. Li, B. Winward, E.M. Zimmermann. Intestinal metabolism and transport of 5-aminosalicylate. Drug Metab. Disp. 27 (1999) 479-485.

[69] W.J. Sandborn, S.B. Hanauer. Systematic review: the pharmacokinetic profiles of oral mesalazine formulations and mesalazine pro-drugs used in the management of ulcerative colitis. Aliment. Pharmacol. Ther. 17 (2003) 29-42.

[70] E. Sim, N. Lack, C. Wang, H. Long, I.Westwood, E. Fullam, A. Kawamura. Arylamine *N*-acetyltransferases: Structural and functional implications of polymorphisms. Toxicol. 254 (2008) 170–183.

[71] R.F. Minchin, P.E. Hannab, J.M. Dupret, C.R. Wagner, F. Rodrigues-Lima, N.J. Butcher. Arylamine *N*-acetyltransferase I. Int. J. Biochem. Cell Biol. 39 (2007) 1999–2005.

[72] H. Goebell, U. Klotz, B. Nehlsen, P. Layer. Oroileal transit of slow release 5 aminosalicylic acid. Gut 34 (1993) 669–675.

[73] P.H. Layer, H. Goebell, J. Keller, A. Dignass, U. Klotz. Delivery and fate of oral mesalamine microgranules within the human small intestine, Gastroenterol. 108 (1995) 1427–1433

[74] A.I. Qureshia, R.D. Cohen. Mesalamine delivery systems: do they really make much difference? Adv. Drug Deliv. Rev. 57 (2005) 281-302.

[75] S.L. Stanley. Amoebiasis. Lancet 361 (2003) 1025-1034

[76] J. Harries. Amoebiasis: a review. J. R. Soc. Med. 75 (1982) 190-197.

[77] H. Seneca. Amebiasis. a review II. Laboratory diagnosis, differential diagnosis and therapy. Am. J. Dig. Dis. 7 (1956) 310-322.

[78] http://en.wikipedia.org/wiki/File:Entamoeba_histolytica_life_cycle-en.svg

[79] R. Haque, D. Mondal, P. Duggal, M. Kabir, S. Roy, B.M. Farr, R.B. Sack, W.A. Petri. Entamoeba histolytica infection in children and protection from subsequent amebiasis. Infect. Immun. 74 (2006) 904-909.

[80] K.L. Chan, J.Y. Sung, R. Hsu, C.T. Liew. The association of amoebic colitis and chronic ulcerative colitis. Singapore Med J. 36 (1995) 303-305.

[81] C.D. Wells, M. Arguedas. Amebic Liver Abscess. Southern Medical Journal 97 (2004) 673-682.

[82] S.J. Powell. New developments in the therapy of Amoebiasis. Gut 11 (1970) 967-969.

[83] E.D. Everett. Metronidazole and Amoebiasis. Digestive Diseases 19 (1974) 626-636.

[84] H.B. Fung, T. Doan. Tinidazole : a nitroimidazole antiprotozoal agent. Clinical Therapeutics 27 (2005) 1859-1884.

[85] C.F. Villamil, H.A. Dolcini, J.T. Arabehety, N.M. Stapler. Treatment of Intestinal Amebiasis with paromomicyn, Am. J. Dig. Dis. 9 (1964) 426-428.

[86] J.S. Simms-Cendan. Metronidazole. Infectious Diseases Update 3 (1996) 153-156.

[87] C.D. Freeman, N.E. Klutman, K.C. Lamp. Metronidazole. A therapeutic review and update. Drugs 54 (1997) 679-708.

[88] F.P. Tally, V.L. Sutter, S.M. Finegold. Metronidazole Versus Anaerobes In Vitro Data and Initial Clinical Observations. Calif. Med. 117 (1972) 22-26.

[89] F.P. Tally, B.R. Goldin, N. Sullivan, J. Johnston, S.L. Gorbach. Antimicrobial Activity of Metronidazole in Anaerobic Bacteria. Antimicrob. Agents Chemother. 13 (1978) 460-465.

[90] H.N. Prince, E. Grunberg, E. Titsworth, W.F. Delorenzo. Effects of 1-(2-Nitro-1-Imidazolyl)-3-Methoxy-2-Propanol and 2-Methyl-5-Nitroimidazole-1-Ethanol Against Anaerobic and Aerobic Bacteria and Protozoa. Appl. Microbiol. 18 (1969) 728-730.

[91] J. Samuelson. Why Metronidazole Is Active against both Bacteria and Parasites. Antimicrob. Agents Chemother 43 (1999) 1533–1541.

[92]A. Schmid, H. Schmid. Pharmaco-Toxicological Mode of Action of Antimicrobial 5-Nitroimidazole Derivatives. J. Vet. Med. A 46 (1999) 517–522.

[93] P.K. Dutta, J. Dutta, V.S. Tripathi. Chitin and chitosan: chemistry, properties and applications. J. Sci. Ind. Res. 63 (2004) 20-31.

[94] M.N.V.R Kumar. A review of chitin and chitosan applications. React. Funct. Polym. 46 (2000) 1–27.

[95] C.L. Vernazza, G.R. Gibson, R.A. Rastall. In vitro fermentation of chitosan derivatives by mixed cultures of human faecal bacteria. Carbohydr. Polym. 60 (2005) 539–545.

[96] T. Kean, M. Thanou. Biodegradation, biodistribution and toxicity of chitosan. Adv. Drug Deliv. Rev. 62 (2010) 3–11.

[97] M. Rinaudo. Chitin and chitosan: Properties and applications. Prog. Polym. Sci. 31 (2006) 603–632.

[98] I. Fiebrig, S.E. Harding, A.J. Rowe, S.C. Hyman, S.S. Davis. Transmission electron microscopy studies on pig gastric mucin and its interactions with chitosan. Carbohydr. Polym. 28 (1995) 239-244.

[99] V. Grabovac, D. Guggi, A. Bernkop-Schnurch. Comparison of the mucoadhesive properties of various polymers. Adv. Drug Deliv. Rev. 57 (2005) 1713–1723.

[100] P. He, S.S. Davis, L. Illum. In vitro evaluation of the mucoadhesive properties of chitosan microspheres. Int. J. Pharm. 166 (1998) 75–88.

[101] N. Bhattarai, J. Gunn, M. Zhang. Chitosan-based hydrogels for controlled, localized drug delivery. Adv. Drug Deliv. Rev. 62 (2010) 83–99.

[102] J. Berger, M. Reist, J.M. Mayer, O. Felt, R. Gurny, Structure and interactions in chitosan hydrogels formed by complexation or aggregation for biomedical applications. Eur. J. Pharm. Biopharm. 57 (2004) 35–52.

[103] N. Boucard, C. Viton, A. Domard. New aspects of the formation of physical hydrogels of chitosan in a hydroalcoholic medium. Biomacromol. 6 (2005) 3227–3237.

[104] V.K. Mourya, N.N. Inamdar. Chitosan-modifications and applications: Opportunities galore. React. Funct. Polym. 68 (2008) 1013–1051.

[105] J. Vinsova, E. Vavrikova. Recent Advances in Drugs and Prodrugs Design of Chitosan. Curr. Pharm. Des. 14 (2008) 1311-1326.

[106] M.M. Thanou, A.F. Kotze, T. Scharringhausen, H.L. Lueben, A.G. de Boer, J.C. Verhoef, H.E. Junginger. Effect of degree of quaternization of *N*-trimethyl chitosan chloride for enhanced transport of hydrophilic compounds across intestinal Caco-2 cell monolayers Journal of Controlled Release 64 (2000) 15–25.

[107] A.B. Sieval, M. Thanou, A.F. Kotzé, J.C. Verhoef, J. Brussee, H.E. Junginger. Preparation and NMR characterization of highly substituted IV-trimethyl chitosan chloride. Carbohydr. Polym. 36 (1998) 157-165.

[108] V.K. Mourya, N.N. Inamdar. Chitosan-modifications and applications: Opportunities galore. React. Funct. Polym. 68 (2008) 1013–1051.

[109] R. Yamaguchi, Y. Araj, T. Itoh, S. Hirano, Preparation of partially N-succinylated-chitosan and their cross-linked gels, Carbohydr. Res. 88 (1981) 172-175.

[110] K. Kafedjiiski, A.H. Krauland, M.H. Hoffer, A. Bernkop-Schnurch. Synthesis and in vitro evaluation of a novel thiolated chitosan. Biomaterials 26 (2005) 819–826.

[111] A. Bernkop-Schnurch, D. Guggi, Y. Pinter. Thiolated chitosans: development and in vitro evaluation of a mucoadhesive, permeation enhancing oral drug delivery system. J. Controlled Release 94 (2004) 177–186.

[112] V. Dodane, V.D. Vilivalam. Pharmaceutical applications of chitosan. PSTT 6 (1998) 246-253.

[113] H. Park, G. Saravanakumar, K. Kim, I.C. Kwon. Targeted delivery of low molecular drugs using chitosan and its derivatives. Adv. Drug Deliv. Rev. 62 (2010) 28–41.

[114] A.M. De Campos, A. Sanchez, M.J. Alonso. Chitosan nanoparticles: a new vehicle for the improvement of the delivery of drugs to the ocular surface. Application to cyclosporin A. Int. J. Pharm. 224 (2001) 159–168.

[115] S. Türker, E. Onur, Y. Özer. Nasal route and drug delivery systems. Pharm. World Sci. 26 (2004) 137–142.

[116] S. Miyazaki, A. Nakayama, M. Oda, M. Takada, D. Atwood. Drug release from oral mucosal adhesive tablets of chitosan and sodium alginate. Int. J. Pharm. 118 (1995) 257-263.

[117] M. Ramdas, K.J. Dileep, Y. Anitha, W. Paul, C.P. Sharma. Alginate encapsulated bioadhesive chitosan microspheres for intestinal drug delivery. J. Biomater. Appl. 13 (1999) 290-206.

[118] C.E. Kast, C. Valenta, M. Leopold, A. Bernkop-Schnurch. Design and in vitro evaluation of a novel bioadhesive vaginal drug delivery system for clotrimazole. J Controlled Release 81 (2002) 354-374.

[119] L. Illum, I. Jabbal-Gill, M. Hinchcliffe, A.N. Fisher, S.S Davis. Chitosan as a novel nasal delivery system for vaccines. Adv Drug Deliv Rev. 23 (2001) 81-96.

[120] H. Tozaki , T. Odoriba , N. Okada , T. Fujita, A. Terabe, T. Suzuki, S. Okabe, S. Muranishi, A. Yamamoto. Chitosan capsules for colon-specific drug delivery: enhanced localization of 5-aminosalicylic acid in the large intestine accelerates healing of TNBS-induced colitis in rats. J. Controlled Release 82 (2002) 51–61.

[121] I.Orienti, T. Cerchiara, B. Luppi, F. Bigucci, G. Zuccari, V. Zecchi. Influence of different chitosan salts on the release of sodium diclofenac in colon-specific delivery. Int. J. Pharm. 238 (2002) 51-59.

[122] J. Nunthanid, K. Huanbutta, M. Luangtana-anan, P. Sriamornsak, S. Limmatvapirat, S. Puttipipatkhachorn. Development of time-, pH-, and enzyme-controlled colonic drug delivery using spray-dried chitosan acetate and hydroxypropyl methylcellulose. Eur. J. Pharm. Biopharm. 68 (2008) 253–259.

[123] Y. Xu, C. Zhan, L. Fan, L. Wang, H. Zheng. Preparation of dual crosslinked alginate-chitosan blend gel beads and in vitro controlled release in oral site-specific drug delivery system. Int. J. Pharm. 336 (2007) 329–337.

[124] K. Mladenovska, R.S. Raicki, E.I. Janevik, T. Ristoski, M.J. Pavlova, Z. Kavrakovski, M.G. Dodov, K. Goracinova Colon-specific delivery of 5-aminosalicylic acid from chitosan-Ca-alginate microparticles. Int. J. Pharm. 342 (2007) 124–136.

[125] O. Munjeri, J.H. Collett, J.T. Fell. Hydrogel beads based on amidated pectins for colon-specific drug delivery: the role of chitosan in modifying drug release. J. Controlled Release 46 (1997) 273–278.

[126] K. Aiedeh, M.O. Taha. Synthesis of Chitosan Succinate and Chitosan Phthalate and Their Evaluation as Suggested Matrices in Orally Administered, Colon-Specific Drug Delivery Systems. Arch. Pharm. Pharm. Med. Chem, 332 (1999) 103–107.

[127] M.E. Davis, M.E. Brewster. Cyclodextrin-based pharmaceutics: past, present and future. Nat. Rev. Drug Discov. 3 (2004) 1023-1035.

[128] J. Szejtli. Past, present, and future of cyclodextrin research. Pure Appl. Chem. 10 (2004) 1825–1845.

[129] N. Szerman, I. Schroh, A.L. Rossi, A.M. Rosso, N. Krymkiewicz, S.A. Ferrarotti. Cyclodextrin production by cyclodextrin glycosyltransferase from Bacillus circulans DF 9R. Biores. Technol. 98 (2007) 2886–2891

[130] E.M.M Del Valle. Cyclodextrins and their uses: a review. Process Biochem. 39 (2004) 1033–1046.

[131] F. Hirayama, K. Uekama. Cyclodextrin-based controlled drug release system. Adv. Drug Deliv. Rev. 36 (1999) 125–141.

[132] R.N. Antenucci, J.K. Palmer. Enzymic degradation of α- and β-cyclodextrins by Bacteroides of the human colon. J. Agric. Food Chem. 32 (1984) 1316-1321.

[133] B. Flourie, C. Moris, L. Achour, H. Dupas, C. Hatat, J.C. Rambaud Fate of β-Cyclodextrinin the Human Intestine. J. Nutrit. 123 (1993) 676-680

[134] A.T.H.J. De Bie, B.V. Ommen, A. Bar. Disposition of [^{14}C]α-Cyclodextrin in Germ-Free and Conventional Rats. Reg. Tox. Pharm. 39 (2004) S57–S66.

2. AIM OF THE WORK

Colon specific drug delivery has gained increased importance not only for drug delivery in treatment of local colonic diseases but also as potential site for the systemic delivery of therapeutic peptides and proteins. To achieve successful colon targeted drug delivery, a drug needs to be protected from degradation, release and/or absorption in the upper portion of the GI tract and then ensure abrupt or controlled release in the proximal colon.

The aim of this work was to develop different colon specific delivery systems by using two model drugs for the treatment of colon diseases:

- 5-ASA,
- metronidazole.

Two different types of colon drug delivery systems were chosen:

- enzyme-dependent system,
- pH-dependent system.

Different 5-ASA pH-dependent systems were developed as colon specific delivery formulations for the treatment of IBD, and their properties were studied and compared.

N-Succinyl-chitosan was chosen as carrier system and was obtained by introducing succinyl groups into chitosan NH_2-terminals of the glucosamine units. (It presents good solubility at neutral and alkaline pH, but it is insoluble at acidic pH. It also has favorable properties as drug carrier such as biocompatibility and low toxicity. Due to the presence of carboxyl groups it exhibits pH-dependent swelling behaviour).

5-ASA loaded *N*-succinyl-chitosan and chitosan were prepared.

To increase 5-ASA water solubility and stability, β-CDs were loaded into the polymers and the influence of CD on the system characteristics was studied. These systems were chemically and analytically characterized; *in vitro* swelling and release studies were performed.

5-ASA loaded N-succinyl-chitosan microparticles were also prepared and characterized.

5-ASA loaded *N*-succinylchitosan microparticles and physical mixture were also prepared and characterized; mucoadhesion studies were performed and their

effectiveness for the treatment of IBD was finally examined *in vivo* using TNBS rat model.

Macromolecular prodrugs of metronidazole and α-, β- and γ-cyclodextrin or chitosan were prepared by linking the drug with a covalent bond to the macromolecule (CD or CHT).

The strategy for the prodrugs production consisted of linking the drug through a spacer to the macromolecule. The spacers utilized were succinyl or glutaryl moieties and they were used because a free carboxylic group was necessary to couple the drug to the hydroxyl group of CD or to the amino moiety of CHT.

Three ester conjugates were prepared with metronidazole and CD:

metronidazole-succinyl-α-cyclodextrin,

metronidazole-succinyl-β-cyclodextrin,

metronidazole-succinyl-γ-cyclodextrin.

Two amide conjugates were synthesized by linking MTZ to chitosan:

metronidazole-succinyl-chitosan,

metronidazole-glutaryl-chitosan.

All the prodrugs were chemically and analytically characterized. *In vitro* stability and *ex vivo* release studies were performed to investigate their usefulness as colon delivery systems.

3. DEVELOPMENT AND CHARACTERIZATION OF FREEZE-DRIED *N*-SUCCINYL-CHITOSAN SYSTEMS FOR COLON SPECIFIC DELIVERY OF 5-ASA

(Submitted to Molecules, 2011)

Abstract

The aim of this work was to develop new formulations to achieve colon-specific delivery of 5-aminosalicylic acid (5ASA). 5ASA was loaded into three-dimensional amorphous matrices, prepared by freeze drying, using either chitosan (CH) or its *N*-Succinyl derivative (SucCH). Matrices containing β-cyclodextrins (CDs) were also prepared to study their influence on the 5ASA release. 5ASA-loaded matrices, with or without CDs, were characterized by several methods and their properties compared. Infra-Red (IR) and Differential Scanning Calorimetry (DSC) analyses were carried out to study interactions between drug, CDs, and polymer. The systems were evaluated for morphology, drug loading capacity, *ex vivo* mucoadhesive properties, swelling behaviour, and *in vitro* drug release studies. Overall results showed that SucCH is good candidate for colon targeting of 5ASA. In fact, SucCH matrix led to a low drug release in acid medium (pH=1.2, ≅ 15%) while, in alkaline medium, 5ASA was almost completely released (>90%).

3.1. Introduction

5-Aminosalicylic acid (5ASA) is an anti-inflammatory drug used for the long term therapy of inflammatory bowel disease, a group of inflammatory conditions that affect colon and small intestine and among which ulcerative colitis and Crohn's disease are the most diffuse and important [1]. 5ASA has been shown to block the production of interleukin-1 and tumour necrosis factor-α (TNF-α) [2,3]. It is also one of the most potent known free radical scavenger and antioxidant [4,5], and inhibits the activation of nuclear factor-κB (NF-κB), a central transcription regulatory factor involved in mediating the initiation and perpetuation of inflammatory processes [6].

Orally administered it is easily absorbed in the stomach and in the small intestine, but therapeutic concentrations are not reached in the distal tract. Moreover, the absorbed drug is rapidly inactivated by acetylation in gut epithelium and liver [7,8]. Its efficacy in inflammatory bowel disease depends on its presence at high concentration in the colon. To achieve a colon specific delivery and to obtain a long term maintenance therapy, it is necessary to develop new modified release

formulations. Different approaches have been evaluated to target 5ASA to the colon, such as: pH-dependent, enzyme-dependent and time-dependent systems. These formulations are designed to reduce systemic absorption and to achieve high levels of 5ASA in the colon lumen [9-14].

Chitosan (CH) has been largely studied as pharmaceutical excipient for colon specific delivery [15,16]. It is a biocompatible, atoxic and biodegradable polymer that could be used to increase the retention time of a drug delivery system in the colon due to its ability to adhere to the mucous layer [17]. CH has favourable biological properties but it rapidly dissolves in the gastric cavity. In fact, it is soluble in acidic solution below pH 6.5 and one limit for its pharmaceutical application is its insolubility at high or neutral pH [18]. To improve its solubility a chemical modification is required and *N*-Succinyl-chitosan (SucCH) was synthesized by introducing succinyl groups into chitosan *N*-terminals of the glucosamine units thus conferring it good solubility properties at both neutral and alkaline pH [19-21].

5ASA is slightly soluble in water and is light and oxygen sensitive [22]. Drug solubility is a key factor in the drug release from inert as well as swellable delivery systems where diffusion, preceded by the drug dissolution, controls the release. For poorly soluble drugs, their low dissolution rate is the actual limiting factor of drug delivery [23]. One approach to increase 5ASA solubility and stability consists in its inclusion in cyclodextrins (CDs) [22]. As well known, CDs are oligosaccharides that are largely employed in pharmaceutical formulations for their capability to form inclusion complexes with poorly soluble drugs to improve their water solubility and, therefore, their bioavailability. In the last decade, CDs have also been proposed as modulators of drug release from different polymeric delivery systems [24] that include hydrogel, gels, and erodible hydrophilic matrices as well as biodegradable microspheres.

In this research, aiming at developing new colon specific delivery systems for 5ASA, three-dimensional amorphous matrices made with CH or SucCH, were prepared and characterized by using several methods (SEM; DSC; FT-IR, swelling behaviour, and drug release). Moreover, in this first part of our research, we have particularly focused on the influence of β-CDs on the 5ASA release. Therefore,

matrices including these cyclic oligosaccharides were also prepared, characterized and their properties compared to those of the free-CDs formulations.

3.2. Experimental

3.2.1. Materials

Chitosan (CH) of average molecular weight (75,000 Da), succinic anhydride and 5-aminosalicylic acid (5ASA) were obtained from Sigma-Aldrich, (Milan, Italy). β-cyclodextrin (CD) was kindly supplied by Roquette Co. (Lestrem, France). All the products and solvents were of analytical grade. Spectra-Por® dialysis membrane (cut-off 12000-14000 Dalton, regenerated cellulose) was purchased from Spectrum Lab Inc. (CA, USA).

3.2.2. Preparation and characterization of N-Succinyl-chitosan

Chitosan was succinylated according to the method reported by Hirano et al. (1981) [25] with some modifications. Briefly 0.64 g of CH were dissolved under stirring in a 5% (v/v) aqueous acetic acid solution (50 ml), and the resulting solution was slowly diluted with 50 ml of methanol. Then 4.22 g of succinic anhydride, previously dissolved in a minimum amount of acetone (30 ml), added dropwise to the CH solution. The reaction was maintained under stirring overnight at room temperature. The obtained viscous gel was diluted with a NaOH 2 M solution, which was added dropwise until pH=10 was reached and a clear solution was formed. The solution was concentrated by a rotary evaporator (Rotavapor Büchi R110, Switzerland) and immediately dialyzed for three days against distilled water. Then, the solution was freeze-dried to obtain a white cotton-like material. The product was characterized by CHN (Fisons model EA 1108 Elemental Microanalyser), IR spectrum (Bruker Equinox 55) and DSC spectrum (Toledo model 821e).

IR (KBr mull) 3319 cm^{-1} (-NH_2 and -OH stretching), 1731 cm^{-1} (carboxylic acid C=O stretching), 1668 cm^{-1} (amide I) 1585 cm^{-1} (amide II), 1162 cm^{-1} 1072 cm^{-1} 1035 cm^{-1} (sugar structure).

CHN: found C: 36.96; H: 6.62; N: 4.30; calculated from $[C_6H_{10}O_4N\ (HCOCH_3)_{0.15}\ (H_2)_{0.17}\ (HCOC_2H_4COONa)_{0.68}]$ C: 37.91; H: 6.11; N: 4.88.

The degree of succinylation, defined as the average number of succinyl groups per repeating units of glucosamine, was calculated from the elemental analysis data and chemically determined also using 2,4,6-trinitrobenzenesulfonic method [26].

3.2.3. Preparation of chitosan or N-Succinyl-chitosan matrices

CH and SucCH were dispersed in distilled water (0.5% w/v). 5ASA or 5ASA and β-CD (4:1 molar ratio) were added to the dispersion, which was homogenized using an ultraturrax, then frozen at −15°C/−20°C and freeze-dried for 24 hours at −70°C and 60 mmHg, using a Freeze-Dryer Criotecnica, (MMCOTA, Rome, Italy).

3.2.4. Determination of 5ASA content in matrices

The amount of 5ASA loaded into the freeze-dried matrices was determined by a dissolution method. Briefly 10 mg of dried powder was dissolved in a hydroalcoholic solution (methanol-pH 1.2 buffer, 1:1, v/v for CH matrices; methanol-pH 7.4 buffer, 1:1 v/v for SucCH matrices). The mixture was vigorously shaken for 2 hours in order to dissolve the matrix into the solution. After centrifuging, the supernatant was withdrawn and the 5ASA content was analyzed by HPLC (see below). The drug loading capacity was expressed as the ratio of actual-theoretical 5ASA content.

3.2.5. Quantitative determination of 5ASA

5ASA content was quantified at 300 nm by HPLC using a chromatograph Alliance 2695 (Waters, Italy) equipped with a photodiode array detector 996 and a computer integrating apparatus (Empower 2). The column was an X bridge-Waters C18 column (60 Å, 5 μm, 4.8 x 150 mm, Waters). The mobile phase was a mixture of acetonitrile, water, and acetic acid (72:20:8, v/v), which was filtered through a 0.45 μm membrane filter before use, and was delivered at a flow rate of 1.0 ml/min. The injected sample volume was 10 μl. Sample preparation and analyses were performed at room temperature. A standard calibration curve (peak area of 5ASA versus known drug concentration) was built up by using working, standard solutions (0.5-0.005 mg/ml). Calibration graphs were plotted according to the linear regression analysis,

which gave a correlation coefficient value (R^2) of 0.9996. The 5ASA retention time (t_r) was 3.0 minutes and the minimum detectable amount was 25 μg/ml.

3.2.6. Evaluation of the polymer-drug interaction using Fourier Transform Infra-Red measurements (FTIR) and Differential Scanning Calorimetry (DSC)

FTIR measurements were carried out at room temperature using Bruker Equinox 55. About 2 mg of the samples were ground thoroughly with KBr and pellets were formed under a hydraulic pressure of 600 kg/cm^2. Spectra of 5ASA, CH, SucCH, 5ASA loaded polymer matrices were performed.

DSC studies were performed using a DSC Mettler Toledo model 821e. The samples (2-5 mg) were scanned in sealed aluminum pans under nitrogen atmosphere. DSC thermograms were scanned in the first heating run at a constant rate of 10°C/min and a temperature range of 0-325°C. DSC thermograms of pure substances and drug loaded polymer matrices were recorded.

3.2.7. Scanning electron microscopy

The surface morphology of the polymer matrices were examined using a scanning electron microscope (SEM), Hitachi S4100 (Madrid, Spain). Powder samples were dispersed on an aluminium stub with a self-adhered carbon film. The samples were made electrically conductive by coating with gold/palladium under vacuum. The SEM images were taken at an excitation voltage of 20 kV.

3.2.8. In vitro swelling studies

The swelling of freeze-dried matrices was performed in a membrane dialysis bag that contained 100 mg of each systems; the membrane bag was placed in a closed flat bottom tube with 40 ml of a buffer solution that was maintained at 37° C for 24 hours. The test was carried out in 2 different solutions: pH 1.2 and pH 7.4. To simulate the gastro-intestinal transit it was also performed with a pH gradient method by placing the membrane for 2 hours at pH 1.2 and then replacing the acidic solution with pH 7.4 buffer (mixed buffer). At specific time intervals, samples were

removed, blotted with a piece of paper for 5 s to absorb excess water on surface and then weighted.

The swelling ratio (S_W %) was calculated using the following equation:

$$[\, S_w\% = \frac{W_t - W_{t0}}{W_{t0}} \times 100\,] \qquad (1)$$

where W_t represents the weight of the system at a certain time and W_{t0} represents the original dry weight.

3.2.9. In vitro release studies

Each matrix was placed in a dialysis bag and in a closed flat bottom tube, 40 ml of pH 1.2 or pH 7.4 solutions were loaded. The release study was carried out for 24 h under magnetic stirring in a thermostatic bath at 37° C. In order to simulate the passage through the stomach and the intestine, tests were performed also using a pH gradient method as seen for the swelling studies. During the experiments, at regular time intervals, 20 ml of the medium were withdrawn and replaced with the same amount of fresh solution to ensure sink conditions. The withdrawn samples were analyzed for 5ASA content by HPLC as described before (see paragraph 3.6).

3.2.10. Mathematical modelling of release kinetics

In order to describe the drug release mechanism, the *in vitro* drug release mean data (cumulative drug release up to 60%) were fitted to the power law equation (Equation 2)

$$[\, \frac{M_t}{M_\infty} = K \times t^n\,] \qquad (2)$$

where M_t and M_∞ are the absolute amount of drug released at t and infinite time, respectively; K is a constant reflecting structural and geometric characteristic of the device, and n is the release exponent characterizing the diffusion mechanism. According to the criteria for release kinetics from swellable systems, release exponent values n=0.45, 0.45<n<0.89 and 0.89 indicate, respectively, Fickian (Case

I) diffusion, non-Fickian (anomalous) transport, and diffusion and zero-order (Case II) transport [27-29].

3.2.11. Preparation of GI tissues and mucoadhesive test

Male Wistar rats (13-weeks old) had been fasted for 24 h. The fasted conditions were set to minimize the contents in the GI tract, which disturbed the washing process for the following use. The intestine tissues (i.e. duodenum, jejunum, ileum and colon) were excised from sacrificed rats. Each section of tissues was slowly washed with a large amount of normal saline solution (0.9% NaCl w/v). The intestine tissues (duodenum, jejunum, ileum and colon) were immediately used for this study.

Swelling of samples was simulated putting the matrices in a flat bottom tube with the buffer solution and thermostated at 37° C. At scheduled time intervals buffer solution was withdrawn and mucoadhesion studies were done using different part of rat intestine tissue. The mucoadhesion studies were done using a universal tensile tester (Lloyd Instruments, LR 50K model, UK). The stainless steel plate (L-shape) was fitted by one of its side into the upper and lower jaws of the instrument so as the other surfaces of the plates were facing each other. The rat intestine tissue was stuck at the upper plate surface with the glue, while matrix was placed on the lower plate. PBS, pH 7.4, was used as a medium and 20 μL were spread on the contact surface between matrix and tissue. Then the upper jaw with tissue stuck on the plate was lowered slowly so that it just touched the matrix surface. No external force was applied. The matrix was kept in contact with the tissue for 5 min and then the upper jaw was slowly moved upward at the speed of 10 mm/min.

All the experiments were done in triplicate. The maximum detachment force (F_{MAX}), i.e. the force required for separating the system from the tissue surface was obtained directly from NimaST518.vi software (Nima Technology Ltd, Coventry, England) and the total amount of forces involved in the probe withdrawal from the tissue (work of adhesion, W_{ad}) was then calculated from the area under the force versus distance curve. These parameters were used to compare the different prepared matrices.

3.2.12. Statistical analysis of data

Data analysis was carried out with the software package R, version 2.10.1. Results are expressed as the mean ± standard deviation. Multiple comparisons of means (Tukey test) were used to substantiate statistical differences between groups, while Student's t-test was applied for comparison between two samples. Significance was tested at the 0.05 level of probability (p).

3.3. Results and Discussion

3.3.1. Preparation of N-Succinyl-chitosan

N-Succinyl-chitosan was successfully synthesized following methods reported in the literature (Scheme 1). Polymer derivatization was confirmed by FTIR analysis (Figure 1). Chitosan FTIR spectrum shows: at 2912 cm^{-1} the stretching vibration of –OH and $–NH_2$; at 1658 and 1602 cm^{-1} stretching respectively of amide I and II; $-NH_2$ bending at 1650 cm^{-1}. The absorption bands at 1159 cm^{-1} (asymmetric stretching of the C-O-C bridge), 1095 and 1039 cm^{-1} (skeletal vibration involving the C-O stretching) are characteristic of its saccharide structure [30,31]. Moreover, the FTIR spectrum of *N*-Succinyl-chitosan shows: stretching vibrations of –OH and $–NH_2$ at 3319 cm^{-1}; the C=O stretching of amide I band at 1668 cm^{-1} and the amide II band at 1585 cm^{-1}. Peaks at 1162, 1072, and 1035 cm^{-1} are typical of the sugar structure. Peaks at 1731 and 1417 cm^{-1} denote the presence of carboxyl groups thus confirming chitosan derivatization and *N*-Succinyl-chitosan formation. In particular, the peak at 1731 cm^{-1} is the stretching band of C=O and the peak at 1417 cm^{-1} belongs to –COOH symmetric stretching vibration [32].

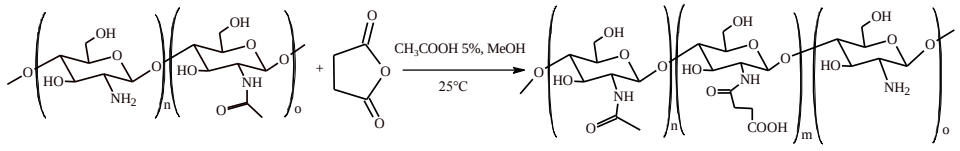

Scheme 1. Synthesis of *N*-Succinyl-chitosan.

The degree of succinylation, defined as the average number of succinyl groups per repeating units of glucosamine, was 68%.

3.3.2. Preparation of chitosan or N-Succinyl-chitosan matrices

The rational of this work was to exploit the promising bioadhesive properties of CH or SucCH freeze-dried matrix and to evaluate their possible combination with the excellent biopharmaceutical properties of CDs. Anionic succinyl groups of SucCH can interact electrostatically with remaining cationic amino groups on the C_2 position of SucCH to form intra- and inter-molecular polyelectrolyte complexes capable of controlling drug release. Moreover, the incorporation of CDs into these polyionic polymer matrices may allow interaction between the polymer and the hydrophilic outer surface of the CDs as well as interaction between 5ASA and CDs, with a consequent greater degree of drug release control.

Freeze-drying was used to prepare CH or SucCH matrices including either 5ASA or 5ASA and CDs. This procedure gave rise to highly fluffy cotton-like powders. The found drug loading capacity was high for all the samples, as shown in Table 1, but no statistical differences could be found between matrices with or without β-CDs.

Table 1. 5ASA loading capacity %.

Systems	5ASA/CH	5ASA/SucCH	5ASA/CD/CH	5ASA/CD/SucCH
Loading Capacity %	89±8	92±7	94±9	95±5

3.3.3. Evaluation of the polymer-drug interaction using Fourier Transform Infra-Red measurements (FTIR) and Differential Scanning Calorimetry (DSC)

The FTIR spectra of pure compounds and obtained matrices are shown in Figure 1. In the FTIR spectrum of pure 5ASA, the assignments of the observed absorption bands are as follows: -COOH stretching (hydrogen bonded) associated with the hydroxyl groups at 3008 cm^{-1}, C=O stretching of the -COOH at 1650 cm^{-1},-NH_2 bending at 1622 cm^{-1}, C-O stretching at 1137 cm^{-1} and in plane C-O-H bending at 1190–1267 cm^{-1} [13]. Band at 1456 cm^{-1} belongs to the –OH bending, while C-N stretching appears at 1357 cm^{-1} and bands at 1490 and 1382 cm^{-1} refer to C=C phenyl group stretching.

Both CH and 5ASA characteristic peaks are observed in the FTIR spectrum of 5ASA loaded chitosan system (5ASA/CH), which indicates that the drug was filled in the polymeric network. The absorption band at 1658 and 1602 cm^{-1} of C-H (amide I and II respectively) shifted to 1660 and 1589 cm^{-1}. Bands at 1157, 1097 and 1051 cm^{-1} are characteristic absorption bands of the chitosan (sugar structure), while those at 1496, 1459, and 1380 cm^{-1} are typical of 5ASA.

5ASA/SucCH system presents typical bands of 5ASA and SucCH, confirming the presence of both molecules in the system. SucCH bands: 1722, 1656, 1577, 1411, 1114, 1074, and 1039 cm^{-1}; 5ASA bands: 1502, 1452 and 1396 cm^{-1}. CD-containing matrices do not show any significant difference.

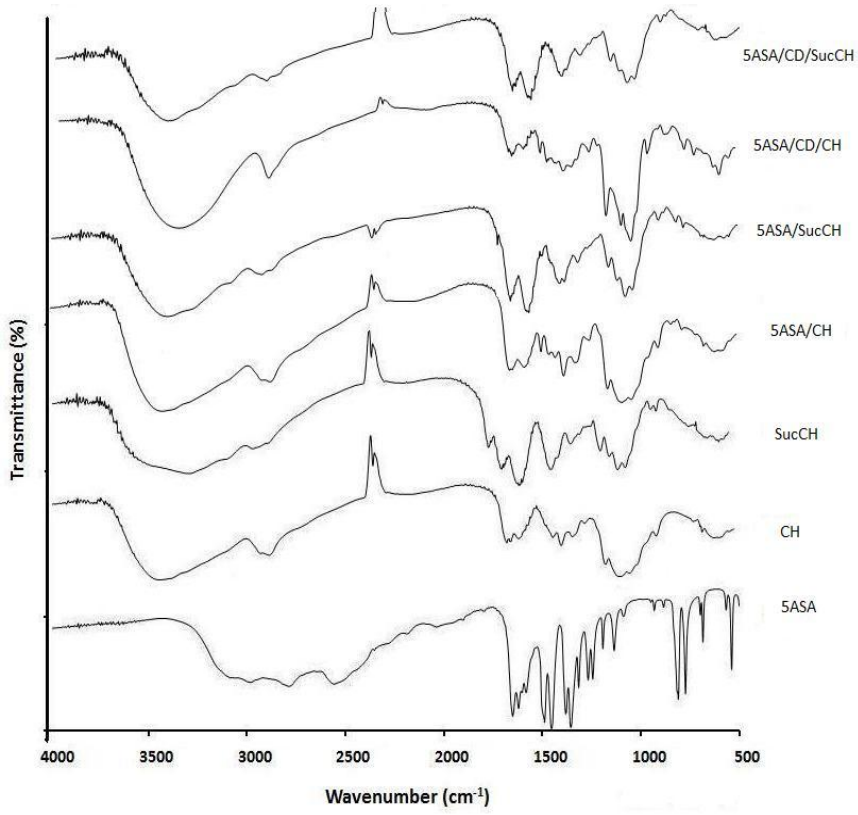

Figure 1. FTIR spectra of 5-ASA (5ASA), chitosan (CH), *N*-Succinyl-chitosan (SucCH), 5-ASA and chitosan (5ASA/CH), 5-ASA and *N*-Succinyl-chitosan (5ASA/SucCH), 5-ASA/β-cyclodextrin/chitosan (5ASA/CD/CH), 5-ASA/β-cyclodextrin/*N*-Succinyl-chitosan (5ASA/CD/SucCH) freeze-dried matrices.

Shift of the peaks and reduced intensity of the bands in the 5ASA/polymer systems confirmed the loading of the drug into the polymers as well as interactions between the two components.

In the calorimetric study, thermal curve of the pure drug exhibits an endothermic peak at 277 °C and an enthalpy of 24 mW mg^{-1}, corresponding to its melting point (Figure 2). The CH and SucCH thermograms show typical polysaccharide behaviour with two degradation steps: a wide endotherm around 100 °C and an exotherm at 315°C that is less evident in SucCH. The first peak in the polymer thermograms corresponds to water evaporation, while the second one refers to polymer degradation.

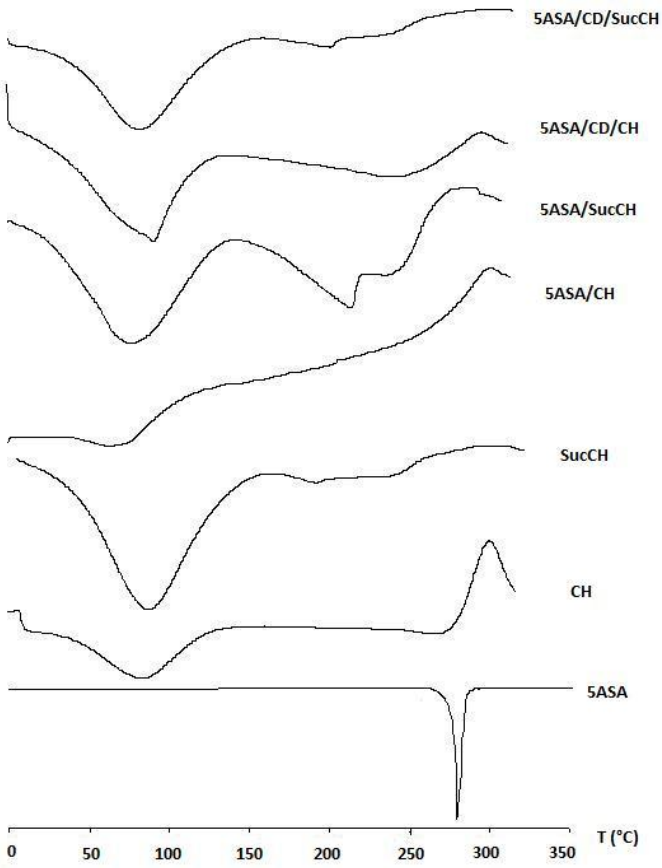

Figure 2. DSC curves of 5-ASA (5ASA), chitosan (CH), *N*-Succinyl-chitosan (SucCH), 5-ASA and chitosan (5ASA/CH), 5-ASA and *N*-Succinyl-chitosan (5ASA/SucCH), 5-ASA/β-cyclodextrin/chitosan (5ASA/CD/CH), 5-ASA/β-cyclodextrin/*N*-Succinyl-chitosan (5ASA/CD/SucCH) freeze-dried matrices.

In thermograms of 5ASA containing matrices, with and without CDs, 5ASA fusion peak disappears indicating the presence of solid-state interactions between the drug and both polymers. In addition, the thermogram of 5ASA/SucCH shows esotherm-endotherm peaks around 210°C, which denotes an interaction between anionic succinyl groups of the polymer and cationic amino groups of 5ASA. These signals are not present in the termograms of the pure SucCH as well as in that of 5ASA/CD/SucCH matrix, where an inclusion complex between 5ASA and β-CD could have formed during the freeze-drying procedure.

3.3.4. Scanning electron microscopy (SEM)

SEM images of CH and SucCH matrices are reported in Figure 3. No differences in morphology between matrices prepared with and without CD were observed. All the prepared polymer systems showed a three-dimensional structure. The surface pattern of CH matrix was slightly rougher and tightly packed in (Fig. 3a), whereas SucCH matrix appeared highly porous with small, flat, and folded sheets, with a large surface area (Fig. 3b). This three-dimensional structure might be due to interactions between the carboxyl and amino groups of SucCH.

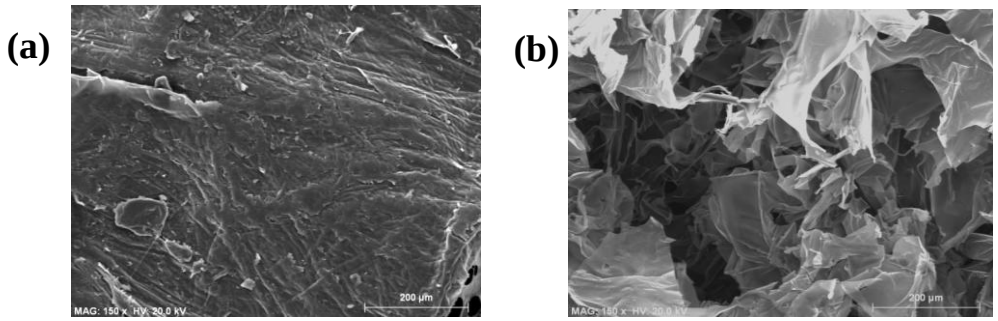

Figure 3. SEM photographs of (a) 5ASA/CH, (b) 5ASA/SucCH systems.

3.3.5. In vitro swelling studies

Swelling degree is a characteristic of hydrogels that controls drug loading as well as drug release. Swelling of the studied matrices was studied as weight evolution of the freeze-dried systems and was assayed at pH 1.2 (Figure 4a), pH 7.4 (Figure 4b), and also in a mixed buffered medium (pH 1.2 for 2 hours and pH 7.4 until 24 hours; Figure 4c). Swelling degree is represented as swelling ratio (S_w). Swelling behaviour of the samples was in accordance with their physico-chemical properties. In fact, CH, a cationic polymer, easily swelled and jelled at pH 1.2 but it did not at pH 7.4. When swelling experiments were performed in the mixed buffer, CH swelled only during the first two hours, in the acid medium, where it reached a maximum S_w that did not vary further (Figure 4c). When CDs were mixed with 5ASA and chitosan (5ASA/CD/CH), the swelling ratio decreased using acid and mixed buffers because of the presence of the hydrophilic but no-swellable CDs. On the contrary, CDs did not affect the CH swelling in alkaline medium where the system behaved as an inert matrix.

SucCH had an opposite behaviour: it showed low swelling activity in acidic medium at pH 1.2 (Figure 4a), while it swelled and jelled at pH 7.4 (Figure 4b). This is due to the SucCH modification: succinyl groups (and consequently –COOH moiety) are predominant in this polymer and their ionization at alkaline pH made the matrix to swell. Swelling studies in mixed buffer confirmed SucCH behaviour in acid and alkaline media: the system started to swell only when the buffer medium was changed from acid to alkaline (Figure 4c). Also in this case, the presence of CDs (5ASA/CD/SucCH) decreased the polymer swelling at pH 7.4 and in mixed buffer, while at pH 1.2 no differences were observed.

Therefore, obtained results point out that influence of β-CDs on CH and SucCH swelling is also dependent on the medium pH. Indeed, when the polymers can easily interact with the aqueous medium, β-CDs reduce the polymer swelling probably as a consequence of a preferential water uptake by the hydrophilic CDs. On the contrary, no influence at all can be found when the polymer does not interact with the aqueous medium.

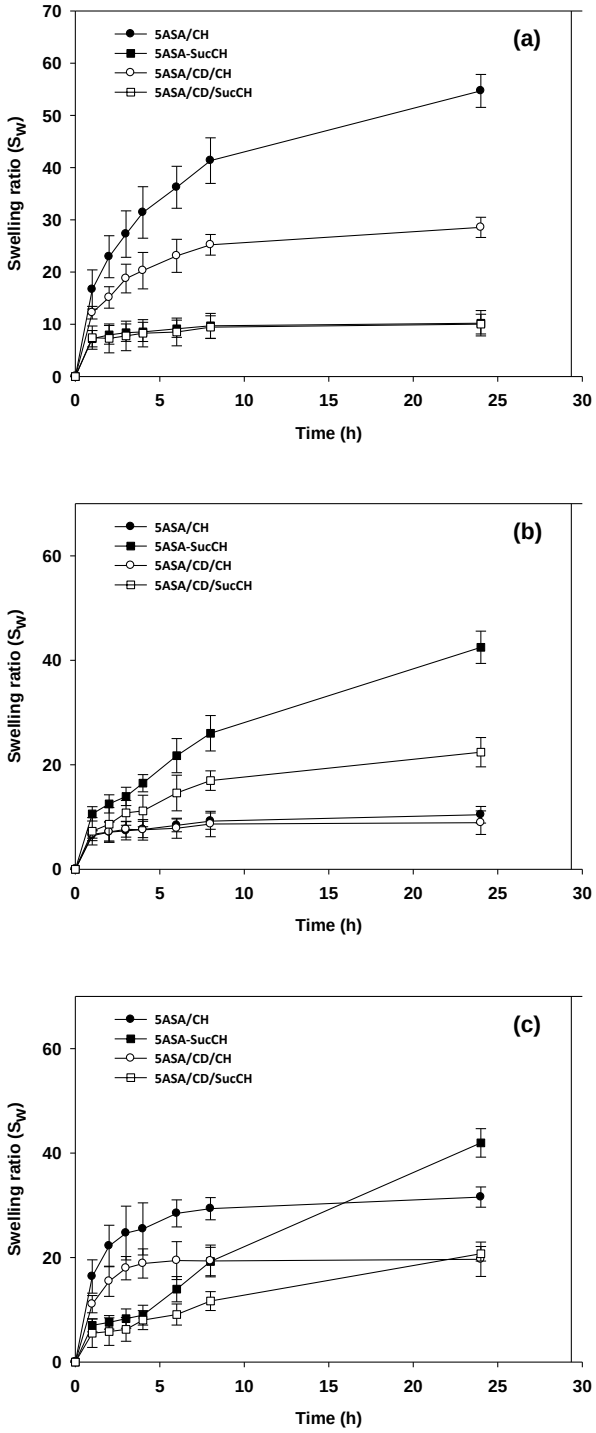

Figure 4. Swelling ratio (S_w) of 5ASA freeze-dried systems at (a): pH 1.2, (b): pH 7.4, and (c): mixed medium (2 h at pH 1.2 and up to 24 h at pH 7.4). Error bars represent standard deviation, *n* =3.

3.3.6. In vitro release studies

As for the swelling experiments, *in vitro* release studies were carried out for 24 hours at pH 1.2, 7.4, and in mixed buffer. Release of 5ASA from matrices containing only the drug appears to be substantially determined by the swelling kinetics (Figures 5a, b and c). As soon as the matrices swelled and the water could penetrate into, the drug was solubilised and released from the system. When the systems were not able to interact with the aqueous medium, only a small amount of 5ASA was released.

Therefore, at pH 1.2, drug release from 5ASA/CH was quite fast and, after 6 hours, 82% drug release was obtained (Figure 5a). On the contrary, in alkaline buffer the process was slower and only 35% drug release was obtained at the end of the experiments (Figure 5a). An opposite behaviour was shown by the SucCH matrix: drug release was fast and higher than 90% at pH 7.4 while the release rate decreased at pH 1.2.

Interesting results were obtained when CD containing matrices were tested. In fact, a faster drug release was obtained from the "inert" matrices, while the presence of the CDs led to a slightly slow release rate in the presence of the swollen CH (pH=1.2) and SucCH (pH=7.4). According to literature, in the "inert" matrices the increased drug release rate is mostly probably due to the ability of CDs to form an inclusion complex with 5ASA with a consequent enhanced drug solubility that improves drug delivery [23-24]. When CDs are dispersed in the swollen matrices, on the contrary, the complexing capability of the CDs is less effective in the release rate promotion probably because of a limited diffusivity of the formed 5ASA/CD complex through the swollen polymer [23,33].

Drug release in the mixed buffer was always quite fast in the first six hours although the 5ASA release profile from SucCH was slower than from all the other samples. In fact, drug release rate from CH was very fast in the first 4 hours (50% released drug) but then it slowed down and only 70% total drug amount was released at the end of the experiments. On the contrary, SucCH led to a slow but constant drug release rate during the first 8 hours and, at the end of the experiments, 92% 5ASA release was obtained. The highest drug release after 24 hours was obtained from the SucCH and the CD-containing CH matrices. Consequently, β-CDs in the cationic polymer CH

were able to improve 5ASA release in the alkaline conditions. However, SucCH alone was capable of better controlling drug release that in acidic medium was lower (≅ 15%) than all the other formulations that released more than 49% of 5ASA (Fig. 5c). Therefore, results from the release experiments showed that SucCH is a potential candidate for targeting 5ASA to colon.

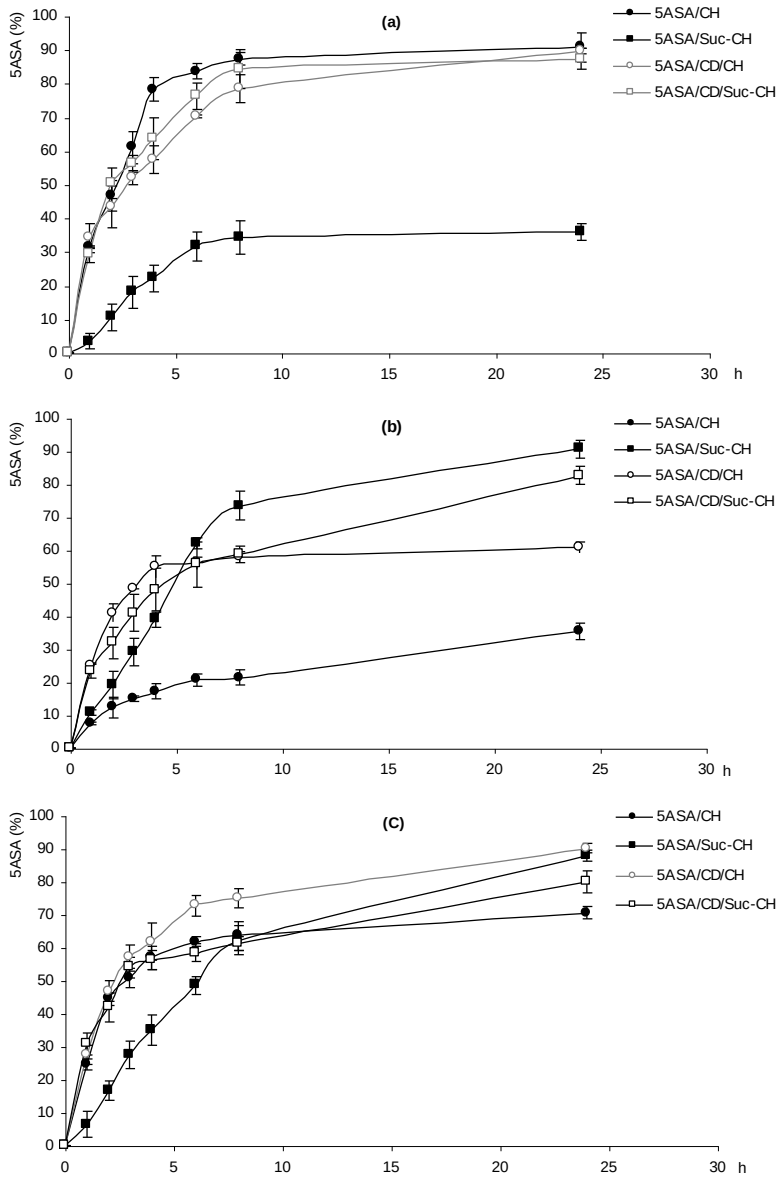

Figure 5. Drug release (%) from 5ASA or 5ASA/CD from chitosan or *N*-Succinyl-chitosan freeze-dried systems at: (a) pH 1.2; (b) pH 7.4 and (c) in mixed medium (2 h at pH 1.2 and up to 24 h at pH 7.4). Error bars represent standard deviation, *n* =3.

3.3.7. Mathematical modelling of release kinetics

To deduce the mechanism of drug release from the matrices, the release data were fitted to general power law equation (2) [27], generally used to describe drug release from swellable matrices, and results related to experiments in the mixed buffer are shown in Table 2. As can be seen from the obtained correlations coefficient values ($R \geq 0.99$), the release data fit well to the empirical equation. The n exponent obtained from the release studies ranged from 0.69 to 0.91 (Table 2), thus indicating a non-Fickian (anomalous) transport ($0.45 < n < 0.89$) for all the tested samples [27-30].

Mechanism of drug release from hydrophilic and erodible matrices is rather complex as a consequence of the several physical process involved especially when CDs are present together with a poor soluble drug. In fact, the involved processes regard: penetration of water into the matrix with consequent swelling and solubilization /erosion of the matrix, dissolution of both the drug and CDs in the swollen matrix, CD/drug complex formation, and counterdiffusion of drug, CD, and complex in the swollen layer [34]. Therefore, all these process are responsible of an anomalous non-Fickian diffusion mechanism.

Table 2. Regression analysis and correlation coefficient values for release data from different systems according to Ritger-Peppas kinetic equation.

Systems	n	k	R^2
5ASA/CH	0.72±0.05	0.38±0.11	0.9954
5ASA/SucCH	0.91±0.03	0.12±0.01	0.9920
5ASA/CD/CH	0.69±0.05	0.30±0.15	0.9948
5ASA/CD/SucCH	0.70±0.04	0.35±0.09	0.9958

3.3.8. Mucoadhesion study

Mucoadhesion is becoming an important strategy to improve the highly variable residence time experienced by drugs and dosage forms at various sites in the gastro-intestinal tract and consequently to reduce variability and improve efficacy. In the treatment of inflammatory bowel disease, the intimate contact with the colonic

mucosa should improve local therapy. The interaction between mucus and hydrophilic polymers is a result of physical entanglement and secondary bonding, mainly H-bonding and van der Waals attraction. These forces are related to the chemical groups of the polymeric chain, and in particular hydroxyl, carboxyl, amine, ester and amide groups generally contribute to good adhesion properties. Moreover, the polymer swelling ability, increasing molecule mobility, facilitates interpenetration and interaction with the mucus layer. Chitosan shows hydroxyl, amide, and amine groups able to give hydrogen bonds and its linear molecules express good chain flexibility and thus a good physical entanglement [35]. Furthermore, it exhibits strong mucoadhesive properties due to the formation of hydrogen and ionic bonds between the positively charged amino groups of chitosan and the negatively charged sialic acid residues of mucin glycoprotein. It is known that negatively charged polymers bearing –COOH group (e.g., Carbomers) interact with mucus by hydrogen and van der Waals bonds, created between their carboxylic groups and the sialic acid residues of mucin glycoprotein [36]. SucCH contains carboxylic group, hydroxyl, and amino groups and, therefore, good mucoadhesive ability can be hypothesized due to ionic, hydrogen and van der Waals bonds.

In this study *ex vivo* mucoadhesive properties of the studied systems were evaluated using different part of rat intestine. The maximum detachment force (F_{MAX}), i.e. the force required for separating the sample from the tissue surface, and the total amount of forces involved in the probe withdrawal from the tissue (work of adhesion, W_{ad}) on different GI mucosa are shown in Table 3.

All the tested systems showed good mucoadhesion for the colon: W_{ad} mean value was higher for SucCH but no statistical differences could be found in the mucoadhesive properties of the matrices both with and without CDs. Although the polymer ability to swell is a prerequisite for mucoadhesion, since it concerns wetting uncoiling and spreading of the polymer over the mucus [37], results of table 3 show that the CH systems were as mucoadhesive as SucCH in the last portion of the GI tract.

However, also these results highlight the highest potential of the SucCH matrix as delivery system for targeting 5ASA to colon.

Table 3. ***Ex vivo*** **mucoadhesive performance of 5ASA freeze-dried systems. Effect of GI mucosa on maximum detachment force and (F_{MAX}) and work of adhesion (W_{ad}).**

Systems		Duodenum	jejunum	ileum	colon
5ASA/CH	F_{MAX} (mN)	2.2±0.5	3.3±0.3	3.3±0.4	3.8±0.5
	W_{ad}(mN mm)	0.9±0.2	1.3±0.2	1.3±0.1	1.5±0.2
5ASA/SucCH	F_{MAX} (mN)	2.7±0.3	2.4±0.2	2.7±0.3	4.0±0.5
	W_{ad}(mN mm)	1.1±0.3	0.9±0.2	1.1±0.2	1.5±0.3
5ASA/CD/CH	F_{MAX} (mN)	2.0±0.4	3.2±0.4	3.5±0.5	3.6±0.5
	W_{ad}(mN mm)	0.8±0.2	1.1±0.2	1.4±0.3	1.5±0.2
5ASA/CD/SucCH	F_{MAX} (mN)	2.9±0.4	2.3±0.3	2.8±0.4	3.9±0.5
	W_{ad}(mN mm)	1.1±0.2	0.9±0.1	1. ±0.3	1.5±0.4

3.4. Conclusions

Overall obtained results showed that SucCH matrix might be a good candidate for colon specific delivery of 5ASA. Indeed, SucCH matrix was able to better control drug release, which was quite low in acidic medium and almost complete in alkaline environment, in comparison with CH and CD-containing polymeric matrices. CDs showed a dual effect on drug release, which was always reduced from the swollen polymeric matrices. On the contrary, CDs improved drug release from the inert polymers. Further studies are in progress to evaluate new drug delivery systems for 5ASA by using SucCH.

Acknowledgments

This work was partially supported by MIUR grants (PRIN 2008, Prot. N. 2008HTJLN2_002; Azioni Integrate Italia-Spagna 2009). Sardegna Ricerche Scientific Park (Pula, CA, Italy) is acknowledged for free access to facilities of the Nanobiotechnology. Dr Maria Letizia Manca was financed by Regione Autonoma

della Sardegna under the Master and Back Program, Reference code: PR1-MAB-A2008-63.

3.5. References

[1] E.S. Bruce. Therapy of Inflammatory Bowel Disease. Gastroenterology 118 (2000) S68-S82.

[2] Y.R. Mahida, C.E.D. Lamming, A. Gallagher, A.B. Hawthorne, C. Hawkey. 5-Aminosalicylic acid is a potent inhibitor of interleukin 1β production in organ culture of colonic biopsy specimens from patients with inflammatory bowel disease. Gut 32 (1991) 50-54.

[3]E.Y. Bissonette, J.A. Enciso, A.D. Befus. Inhibitory Effects of Sulfasalazine and Its Metabolites on Histamine Release and TNF-α Production by Mast Cells. J. Immunol.156 (1996) 219-223.

[4]J.G. Williams, M.B. Hallett. Effect of sulphasalazine and its active metabolite, 5-amino-salicylic acid, on toxic oxygen metabolite production by neutrophils. Gut 30 (1989) 1581-1587.

[5]S.M. McKenzie, W.F. Doe, G.D. Buffinton. 5-Aminosalicylic acid prevents oxidant mediated damage of glyceraldehyde-3-phosphate dehydrogenase in colon epithelial cells. Gut 44 (1999) 180–185.

[6]H. Bantel, C. Berg, M. Vieth, M. Stolte, W. Kruis, K. Schulze-Osthoff. Mesalazine Inhibits Activation of Transcription Factor NF-κB in Inflamed Mucosa of Patients With Ulcerative Colitis. Am. J. Gastroenterol. 12 (2000) 3452-3457.

[7] S.Y. Zhou, D. Fleisher, L.H. Pao, C. Li, B. Winward, E.M. Zimmermann. Intestinal metabolism and transport of 5-aminosalycilate. Drug Metabol. Disp 27 (1998) 479-485.

[8] W.J. Sandborn, S.B. Hanauer. Systematic review: the pharmacokinetic profiles of oral mesalazine formulations and mesalazine pro-drugs used in the management of ulcerative colitis. Aliment. Pharmacol. Ther. 17 (2003) 29-42.

[9] D. Soodabeh, H. Jalal, K. Abbas. Release of 5-aminosalicylic acid from acrylic type polymeric prodrugs designed for colon-specific drug delivery. J. Control. Rel. 58 (1999) 279–287.

[10]V.R. Sinha, R. Kumria. Polysaccharides in colon-specific drug delivery. Int. J. Pharm. 224 (2001) 19-38.

[11] H. Tozaki, T. Odoriba, N. Okada, T. Fujita, A. Terabe, T. Suzuki, S. Okabe, S. Muranishi, S. Yamamoto. Chitosan capsules for colon-specific drug delivery: enhanced

localization of 5-aminosalicylic acid in the large intestine accelerates healing of TNBS-induced colitis in rats. J. Control. Rel 82. (2002) 51–61.

[12] M. Zou, H. Okamoto, G. Cheng, X. Hao, J. Sun, F. Cui, K. Danjo. Synthesis and properties of polysaccharide prodrugs of 5-aminosalicylic acid as potential colon-specific delivery systems. Eur. J. Pharm. Biopharm. 59 (2005) 155–160.

[13] J. Nunthanid, K. Huanbutta, M. Luangtana-anan, P. Sriamornsak, S. Limmatvapirat, S. Puttipipatkhachorn. Development of time-, pH-, and enzyme-controlled colonic drug delivery using spray-dried chitosan acetate and hydroxypropyl methylcellulose. Eur. J. Pharm. Biopharm. 68 (2008) 253–259.

[14] R. Cassano, S. Trombino, A. Cilea, T. Ferrarelli, R. Muzzalupo, N. Picci. L-lysine pro-prodrug containing trans-ferulic acid for 5-amino salicylic acid colon delivery: Synthesis, characterization and in vitro antioxidant activity evaluation. Chem. Pharm. Bull. 58 (2010) 103-105.

[15]R. Hejazi, M. Amiji. Chitosan-based gastrointestinal delivery systems. J. Control. Rel. 89 (2003) 151–165.

[16] J.H. Park, G. Saravanakumar, K. Kim, I.C. Kwon. Targeted delivery of low molecular drugs using chitosan and its derivatives. Adv. Drug Deliv. Rev. 62 (2010) 28-41.

[17] I.A. Sogias, C.A. Williams, V.V. Khutoryanskiy. Why is Chitosan Mucoadhesive? Biomacromolecules 9 (2008) 1837–1842.

[18] M.N:V. Ravi Kumar. A review of chitin and chitosan applications. React. Func. Polym. 46 (2000) 1-27.

[19] R. Yamaguchi, Y. Araj, T. Itoh, S. Hirano. Preparation of partially *N*-succinylated chitosans and their cross-linked gels. Carbohydr. Res. 88 (1981) 172-175.

[20] Y. Kato, H. Onishi, Y. Machida. *N*-succinyl-chitosan as drug carrier: water insoluble and water soluble conjugates. Biomaterials 25 (2004) 907-915.

[21] Y. Chengyun, C. Dawei, G. Jiwei, H. Haiyang, Z. Xiuli, Q. Mingxi. Preparation of *N*-Succinyl-chitosan and their physical-chemical properties as novel excipient. Pharm. Soc. Japan 126 (2006) 789-793.

[22] N. Zerrouk, J.M. Gines Dorado, P. Arnaud, C. Chemtob. Physical characteristics of inclusion compounds of 5-ASA in α and β cyclodextrin. Int. J. Pharm. 171 (1998) 19–29.

[23] M.E. Sangalli, L. Zema, A. Maroni, A. Foppoli, F. Giordano, A. Gazzaniga. Influence of betacyclodextrin on the release of poorly soluble drugs from inert and hydrophilic heterogeneous polymeric matrices. Biomaterials 22 (2001) 2647-2651.

[24] A. Miro, A. Rondinone, A. Nappi, F. Ungaro, F. Quaglia, M.I La Rotonda. Modulation of release rate and barrier transport of Diclofenac incorporated in hydrophilic matrices: Role

of cyclodextrins and implications in oral drug delivery. Eur. J. Pharm. Biopharm. 72 (2009) 76-82.

[25] S. Hirano, T. Moriyasu, N-(Carboxyacyl)chitosans, Carbohydrate Research 92 (1981) 323–327

[26] S.L. Snyder, P.Z. Sobocinski. An improved 2,4,6-trinitrobenzenesulfonic acid method for the determination of amines. Anal. Biochem. 64 (1975) 284-288.

[27] P.L Ritger, N.A. Peppas. A simple equation for description of solute release II. Fickian and anomalous release from swellable devices. J. Control. Rel. 5 (1987) 37–42.

[28] N.A. Peppas. Analysis of Fickian and non-Fickian drug release from polymers. Pharm. Acta Helv. 60 (1985) 110–111.

[29] X. Zhang, Z. Wu, X. Gao, S. Shu, H. Zhang, Z. Wang, C. Li. Chitosan bearing pendant cyclodextrin as a carrier for controlled protein release. Carbohydr. Polym. 2 (2009) 394-401.

[30] Y. Shigemasa, H. Matsura, H. Sashiwa, H. Saimoto. Evaluation of different absorbance ratios from IR spectroscopy for analyzing the degree of deacetylation in chitin. Int. J. Biol. Macromol. 18 (1996) 237-242.

[31] Z. Aiping, C. Tian, Y. Lanhua, W. Hao. Synthesis and characterization of *N*-succinyl-chitosan and its self-assembly of nanospheres. Carbohydr. Polym. 66 (2006) 274–279.

[32] Y. Dai, P. Li, J. Zhang, A. Wang, Q. Wei. A Novel pH Sensitive *N*-Succinyl Chitosan/Alginate Hydrogel Bead for Nifedipine Delivery. Biopharm. Drug Dispos. 29 (2008) 173–184.

[33] D.C. Bibby, N:M. Davies, I.G. Tucker. Mechanisms by which cyclodextrins modify drug release from polymeric drug delivery systems. Int. J. Pharm. 197 (2000) 1-11.

[34] B. Cappello, G. De Rosa, L. Giannini, M.I. La Rotonda, G. Mensitieri, A. Miro, F. Quaglia, R. Russo. Cyclodextrin-containing poly(ethyleneoxide) tablets for the delivery of poorly soluble drugs: potential as buccal delivery system Int. J. Pharm. 619 (2006) 63-70.

[35] F. Bigucci, B. Luppi, T. Cerchiara, M. Sorrenti, G. Bettinetti, L. Rodriguez, V. Zecchi. Chitosan/pectin polyelectrolyte complexes: Selection of suitable preparative conditions for colon-specific delivery of vancomycin. Eur. J. Pharm. Sci. 35 (2008) 435–441.

[36] D. Dodou, P. Breedveld, P.A. Wieringa. Mucoadhesives in the gastrointestinal tract: revisiting the literature for novel applications. Eur. J. Pharm. Biopharm. 60 (2005) 1–16.

[37] N. Thirawong, J. Nunthanid, S. Puttipipatkhachorn, P. Sriamornsak. Mucoadhesive properties of various pectins on gastrointestinal mucosa: An in vitro evaluation using texture analyzer. Eur. J. Pharm. Biopharm. 2007, 67, 132–140.

4. pH-SENSITIVE 5-ASA LOADED *N*-SUCCINYL-CHITOSAN SYSTEMS FOR COLON SPECIFIC DELIVERY: PREPARATION, CHARACTERIZATION AND IN VITRO EVALUATION

Abstract

The objective of this study was to prepare two different systems for the delivery of 5-aminosalicylic acid (5-ASA) to the colon. *N*-Succinyl-chitosan (SucCH) was chosen as carrier system because of its excellent pharmaceutical properties. It was prepared by introducing succinic group into chitosan *N*-terminals of the glucosamine units. Due to the presence of carboxyl groups it exhibits pH-dependent swelling behavior and good mucoadhesivness. 5-ASA loaded SucCH microparticles and freeze-dried systems were prepared using spray-drying and freeze-drying techniques respectively. FTIR, DSC, X-ray diffraction studies were carried out to characterize the systems and to evaluate drug-polymer interactions. Morphology studies, size distribution, zeta potential, swelling properties and drug release were also performed in order to understand the potential of the systems to be effective to deliver the drug to the site of action. By imaging with SEM, acceptable spherical non porous microparticles were obtained. *In vitro* swelling and drug release studies were in accordance with the polymer properties, showing the highest swelling ratio and drug release at pH=7.4 (colonic pH).

4.1. Introduction

Ulcerative colitis and Crohn's disease are chronic, immunologically mediated disorders that are collectively referred to as inflammatory bowel disease (IBD). Although their exact etiologies remain uncertain, results from research indicate that IBD are heterogeneous diseases characterized by various genetic abnormalities that lead to overly aggressive T-cell responses to a subset of commensal enteric bacteria [1]. Ulcerative colitis is limited to the colon, although Crohn's disease can involve any part of the gastrointestinal tract from the mouth to the anus, it most commonly affects the small intestine and/or the colon. Standard treatment for ulcerative colitis and Crohn's disease depends on extent of involvement and disease severity [2]. 5-Aminosalicylic acid (5-ASA) is an anti-inflammatory drug commonly used in the treatment of IBD. It is effective for use in mild to moderate disease and as maintenance therapy [3]. The precise mechanism of action of the drug is not known, but is likely due to a combination of anti-inflammatory properties. It is able to block

the production of interleukin-1 (IL-1) and tumor necrosis factor-α (TNF-α) [4,5]. 5-ASA is a potent inhibitor of the cyclooxygenase pathway, inhibiting the production of prostaglandin E2 in inflamed intestinal specimens [6] and it is also one of the most potent known free radical scavengers and antioxidants [7,9]. Moreover 5-ASA has been shown to inhibits of activation of nuclear factor-κB (NF-κB), a central transcription regulatory factor involved in mediating the initiation and perpetuation of inflammatory processes [10,11]. When pure 5-ASA is taken orally, however, the stomach and upper small intestine absorb most of the drug before it reaches the colon [12]. Therefore, to be effective as an oral agent for IBD and reach the site of action at therapeutic levels, 5-ASA has to escape absorption by the stomach and upper intestines. For this purpose different approaches have been developed and studied. The most important systems can be divided into three groups: time-dependent, enzyme-dependent and pH-dependent systems [13,14]. Time-dependent systems are based on the principle of delaying the release of the drug until it enters to the colon. Enzyme-dependent systems take advantage of the colonic microflora that has a large amount of specific enzymes that are not present in the rest of GI tract. They make the drug to be released specifically in the colon by breaking covalent bonds between a drug and its carrier (prodrugs) or by eroding biopolymers [15]. pH-dependent systems exploit the generally accepted view that the pH of the human GI tract increases progressively from the stomach (pH 1-2) to small intestine (pH 5-6) and colon (pH 7-8).

pH-sensitive hydrogels have attracted increasing attention due to their unique properties. Swelling of such hydrogels in the stomach is minimal and thus the drug release is also minimal. Due to increase in pH, the swelling degree increases as the hydrogels pass down the intestinal tract. The use of natural polymers in the design of pH sensitive hydrogels has received much attention due to their excellent biocompatibility and biodegradability. Among them chitosan and its derivative are very promising [16]. *N*-Succinyl-chitosan (SucCH) is a new chitosan derivate that could be obtained by introducing succinyl groups into chitosan *N*-terminals of the glucosamine units [17-19]. It exhibits good solubility properties at neutral and basic pH. It is reported to have favorable drug carrier properties such as biocompatibility, low toxicity, long-term retention in the body and pH-dependent swelling behaviour.

The presence of carboxyl groups and other hydrophilic moiety makes the polymer mucoadhesive; these groups adhere to the mucosal tissue via hydrogen bonding between carboxyl groups of the polymer and hydroxyl groups of the oligosaccharides present in the glycoproteins of the intestinal mucosa [20].
In a previous work 5-ASA loaded SucCH freeze-dried systems were prepared [21], in this study with the aim to increase the drug loading and evaluate the influence of particle size on the delivery system propeties, 5-ASA loaded SucCH microparticles (MP) and freeze-dried system (FD) were prepared using spray-drying and freeze-drying technique respectively. Physicochemical characterizations, including microparticle size, morphology, zeta potential, drug loading were performed. Swelling and drug release studies from both the systems were carried out at different pH values.

4.2. Materials and Methods

4.2.1. Materials

Chitosan (CH) of medium molecular weight, succinic anhydride and 5-ASA were obtained from Aldrich, (Milan, Italy). Spectra-por® dialysis membrane (MWCO 12000-14000 Dalton, regenerated cellulose) was purchased from Spectrum Lab (Inc, USA). All the products and solvents were of analytical grade.

4.2.2. Preparation of N-Succinyl-chitosan

Chitosan medium molecular weight was succinylated according to the method reported in a previous work [21].

4.2.3. Preparation of 5-ASA/N-Succinyl-chitosan freeze-dried system (FD)

5-ASA/SucCH system was prepared at 1:1 molar ratio. The appropriate amount of *N*-Succinyl-chitosan were weighted and solubilized in 70 ml of distilled water, when it was completely solubilized 5-ASA was added to the solution. The dispersion was homogenized using an ultraturrax, then frozen at −80°C and freeze-dried for 24 hours at −50°C and 60 mmHg, using a Freeze-Dryer Criotecnica, (MM Cota, Rome, Italy).

4.2.4. Preparation of microparticles (MP)

5-ASA loaded SucCH microparticles (MP) were prepared using spray-drying method. Briefly 400 mg of 5-ASA was dispersed in 100 ml of distilled water and then 500 mg of SucCH was added and let solubilize under magnetic stirring. The mixture was infused into a spray dryer nozzle unit of Minispray Dryer (Büchi B-290, Switzerland). The conditions of the spray-drying process were: nozzle diameter 0.7 mm, aspiration: 80%, inlet temperature: 150°C, outlet temperature: 100°C. Blank SucCH microparticles were prepared using the same conditions as for the drug-loaded particles. Microparticles were collected and stored at 25°C, 60% Hr.

4.2.5. Characterization of MP and FD

4.2.5.1. Evaluation of the polymers-drug interaction using Fourier transform infra-red measurements (FTIR)

FTIR measurements were taken at an ambient temperature using Bruker Equinox 55 (Germany). About 2 mg of the samples were ground thoroughly with KBr and pellets were formed under a hydraulic pressuse of 600 kg/cm^2. 5-ASA, chitosan, SucCH, MP and FD spectra were performed.

4.2.5.2. Evaluation of the polymers-drug interaction and physical state of 5-ASA using differential scanning calorimetry (DSC) and X-ray diffraction studies

DSC studies were performed using a DSC Mettler Toledo model 821e (Switzerland). The samples (2-5 mg) were scanned in sealed aluminium pans under nitrogen atmosphere. DSC thermograms were scanned in the first heating run at a constant rate of 10°C/min and a temperature range of 0-325°C. DSC thermograms of pure substances, drug loaded SucCH MP and FD were recorded.

X-ray diffractogram pattern for 5-ASA alone was recorded with Bragg–Brentano geometry on a Bruker AXS D5005 (DRXP, Germany) in the 2θ range from 5° to 45°, in steps of 0.02° at 6 s per step.

4.2.5.3. Scanning electron microscopy (SEM)

Shape and surface morphology of the empty and 5-ASA loaded SucCH microparticles were examined using a scanning electron microscope (SEM, S-4100

Hitachi, Madrid, Spain). The samples were mounted on an aluminum stub using double-sided tape. The samples were made electrically conductive by coating under vacuum with gold-palladium. The SEM picture was taken at an excitation voltage of 20 kV.

4.2.5.4. Particle size analysis

Measurement of the particle size of MP was carried out with Analysette 22 Micro tec plus (Fritsch, Germany) after suspending the particles in distilled water and sonicating the suspension for 10 min in ultrasonic bath. The average particle size was expressed as the volume surface diameter, d_{vs} (μm).

4.2.5.5. Zeta potential

Suspension of microparticles in distilled water previously sonicated for 10 min in ultrasonic bath was used to determine the zeta potential of MP. The zeta potential of the particles was recorded using Malvern Zeta Sizer apparatus (model Zen 3600, Malvern, UK). Each sample was analysed at least six times to obtain an average value and a standard deviation. Samples of blank SucCH microparticles and FD were also submitted to this study.

4.2.5.6. Content of 5-ASA in the systems

The actual content of 5-ASA in MP and FD was determined by dissolving an exactly weighed amount of the systems at pH 7.4 with magnetic stirring at room temperature for 30 hours. 5-ASA concentration was assayed by HPLC, using a Perkin Elmer® Series 200 equipped with a UV detector Waters 484® (λ=300 nm). The mobile phase consisted of Acetic Acid solution 0.1 M: Acetonitrile (80:20) and was filtered through a 0.45 μm membrane filter before use. The mobile phase was eluted at a flow rate of 0.5 ml/min. The column was a Kromasil® C-18, 5.0 μm (150 cm x 4.6 mm) [22].

4.2.6. In vitro swelling

Swelling studies were performed in a membrane dialysis bag that contained 100 mg of each systems; the membrane bag was placed in a closed flat bottom tube with 200

ml of a buffer solution that was maintained at 37°C up to 24 hours. It was carried out in three different solutions with different pH values in order to simulate the gastro-intestinal tract: stomach (pH=2), small intestine (pH=5.5) and large intestine (pH=7.4). At specific time intervals, samples were removed from the swelling medium and blotted with a piece of paper for 5 s to absorb excess water on surface and were weighted.

The Swelling ratio (S_w) was calculated using the following equation:

$$\left[S_w(\%) \equiv \frac{W_t - W_{t_0}}{W_{t_0}} \times 100 \right] \quad (1)$$

where S_w represents the swelling ratio, W_t and W_{t0} represent weights of the sample at a certain time and the original dry weight, respectively.

4.2.7. Drug release studies

Drug release studies were carried out into a diffusion cell like the Franz cell. Three different solutions were utilized as seen in the in vitro swelling studies (pH=2, 5.5 and 7.4). In the receptor compartment 6 ml of the respective solution were placed. In the donor compartment 5 mg of MP (or FD) were placed and 300 µl of the same solution were added; the two compartment were separated by a Millipore® membrane with pore of 0.45 µm. Drug release studies were carried out under magnetic stirring at 37°C up to 24 hours. At appropriate time intervals 200 µl of the solution from the receptor compartment were withdrawn and the same amount was replaced with the appropriate solution to maintain sink condition. The amount of 5-ASA released was assayed by HPLC as described before.

The mean release profiles (cumulative drug release up to 90%) were fitting according to the power law equation (Eq. (2)) in order to describe the drug release mechanism.

$$\left[\frac{M_t}{M_\infty} = Kt^n \right] \quad (2)$$

Where M_t and M_∞ are the absolute amount of drug released at t and infinite time, respectively; K is a constant reflecting structural and geometric characteristic of the device, and n is the release exponent characterizing the diffusion mechanism. According to the criteria for release kinetics from swellable film systems, release

exponent values n=0.45, 0.45<n<0.89 and 0.89 indicate, respectively, Fickian (case I) diffusion, non-Fickian (anomalous) transport, and diffusion and zero-order (case II) transport [23,24].

4.2.8. Statistical analysis

Data analysis was carried out with the software package R, version 2.10.1. Results are expressed as the mean ± standard deviation (S.D.). Multiple comparisons of means (Tukey test) were used to substantiate statistical differences between groups, while Student's t-test was used for comparison between two samples. Significance was tested at the 0.05 level of probability (p).

4.3. Results and discussion.

4.3.1 Preparation of N-Succinyl-chitosan

N-Succinyl-chitosan was successfully synthesized according to the methods reported in literature (Scheme 1).

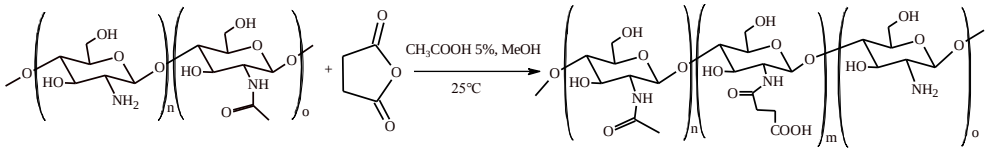

Scheme 1. *N*-Succinyl-chitosan preparation

IR, DSC and X-ray diffraction studies revealed the derivatization of chitosan.

FTIR spectra of chitosan and SucCH are shown in Figure 1. CH spectrum is characterized by a broad absorption around 1660 cm^{-1} (Amide I, C=O stretching mode), 1610 cm^{-1} (amide II, N-H deformation mode) and 1650 cm^{-1} (-NH_2 bending of non-acetylated NH_2 groups). Characteristic for its saccharide structure are absorption bands at 1161 cm^{-1} (asymmetric stretching vibration of the C-O-C bridge), 1101 cm^{-1} and 1058 cm^{-1} (skeletal vibration involving C-O stretching) [25,26].

SucCH spectrum presents amide I and II band at 1668 and 1585 cm^{-1} respectively and the characteristics peaks of sugar structure at 1162, 1072 and 1035 cm^{-1}. The new bands at 1731 and 1417 cm^{-1}, which corresponds to the carboxyl group confirm the derivatization of the amino group [20].

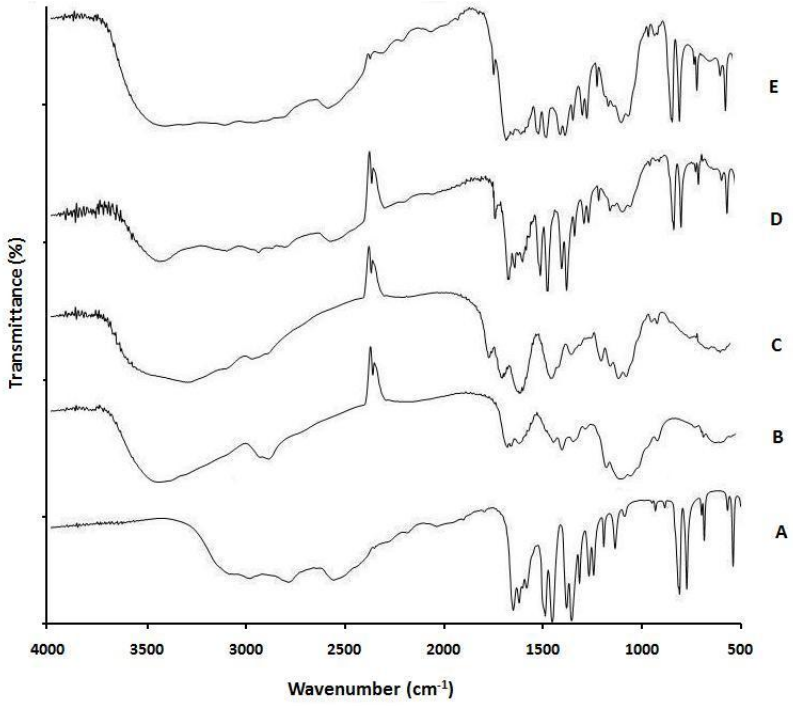

Figure 1. FTIR spectra of 5-ASA (A), CH (B), SucCH (C), FD (D) and MP (E).

DSC thermograms of chitosan and SucCH are shown in Figure 2. In general, the thermal properties of chitosan and its derivatives are similar to those of cellulose. They do not melt but degrade at elevated temperatures [27]. The spectra of chitosan shows a broad endothermic peak around 78°C and sharp exothermic peak at 306.3°C (Figure 2B). The former endothermic peak may be due to the water that the chitosan contains, while the latter may be attributed to the decomposition of chitosan. The endothermic peak of SucCH (Figure 2C) around 79°C may be due to the loss of water and moisture content in the polymer. The small broad exothermic peak at 310°C corresponds to its thermal decomposition. The results indicated that the structure of chitosan chains has been changed due to the introduction of succinyl group and the reduced ability of crystallization [28].

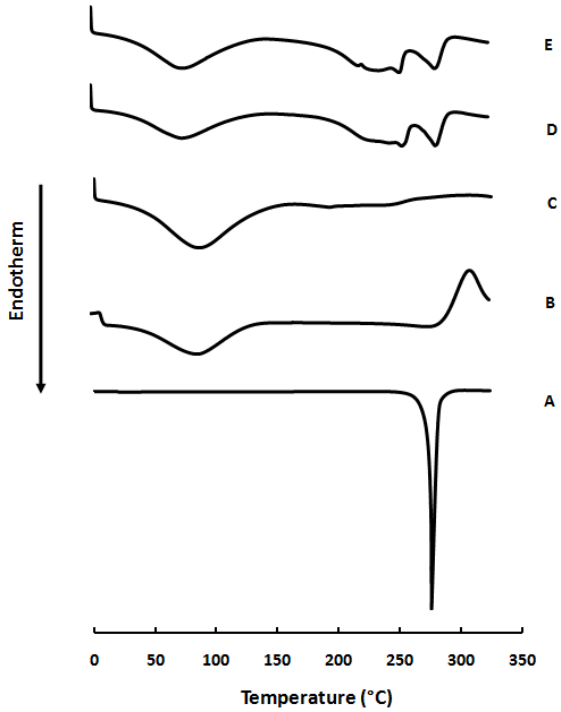

Figure 2. DSC thermograms of 5-ASA (A), CH (B), SucCH (C), FD (D) and MP (E).

X-ray diffraction spectra of chitosan and its derivative (Figure 3) show that chitosan exhibits two reflection fall at 2θ = 11.0° and 2θ = 19.56°. Samuels et al. [29] reported that the reflection fall at 2θ = 11.0° was assigned to crystal form I and the strongest reflection appears at 2θ = 19.56° which corresponds to crystal forms II. However, with the *N*-Succinyl substitution, there are two less intense broad peaks at around 2θ = 12.02° and 18.86°. This result indicates that crystal forms have been destroyed in SucCH macromolecules and suggests that intermolecular hydrogen bindings (H-bonds) in SucCH are greatly decreased in comparison with that of chitosan. As a result, its solubility is higher than that of chitosan, it can be disperse into distilled water and obtain a transparent and stable system [30].

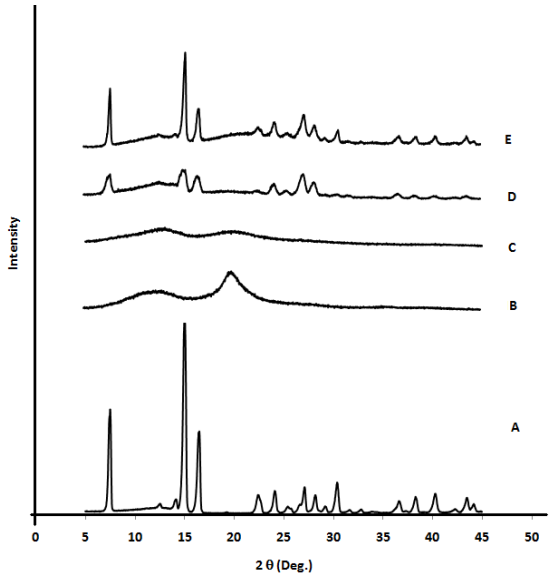

Figure 3. X-ray diffractograms of: 5-ASA (A), CH (B), SucCH (C), FD (D) and MP (E).

4.3.2. Polymers–drug interaction analysis using FTIR Spectroscopy

According to the characteristic spectra of the polymer and 5-ASA separately, in the freeze-dried system and in the microparticles, an attempt was made to detect the eventual existence and type of interactions between the polymers and the drug.

Chitosan and SucCH spectra have been previously discussed. Considering 5-ASA (Figure 1A), the characteristic IR band at 1652 cm^{-1} corresponds to the C=O stretching of the –COOH group, -NH_2 bending is assigned to the peak at 1622 cm^{-1}, bands at 1456 belong to the –OH bending, while C-N stretching to the peak at 1357 cm^{-1}. The bands in a range of 2000–3000 cm^{-1} correspond to stretching vibrations of the hydrogen bonds in the 5-ASA molecule [31]. Freeze-dried system's FTIR spectrum presents typical bands of 5-ASA and SucCH, confirming the presence of both the molecules in the system, however due to the presence of interactions between the two molecule some bands are shifted; -COOH stretching bands of SucCH is present at 1720 cm^{-1} and bands at 1130, 1085 and 1053 cm^{-1} are the characteristics of the sugar structure. 5-ASA bands are the following: 1654 cm^{-1} (-COOH stretching); 1641 cm^{-1} (-NH_2 bending), 1456 (-OH bending) and 1357 cm^{-1} (C-N stretching).

The microparticle spectrum shows typical 5-ASA bands and typical SucCH bands as seen for the freeze-dried system.

4.3.3. Evaluation of the polymers-drug interaction and physical state of 5-ASA using differential scanning calorimetry (DSC) and X-ray diffraction studies

Thermogram of 5-ASA is characterized by a sharp endothermic peak at 277°C (Figure 2A) and an enthalpy of 24 mW mg^{-1}, which corresponds to its melting point. In FD and MP (Figure 2D and 2E, respectively) this endothermic peak exists at 281°C with a broader shape and smaller enthalpy (1.41 and 1.17 mW mg^{-1} respectively). The shift of drug melting peaks might be a result of a heat-induced drug-polymer interaction during DSC measurements [32]. Also the endothermic peak of SucCH is present at 67.1 and 67.5°C respectively. The appearance of a new peak at around 254 and 252°C denotes an interaction between anionic succinyl group of SucCH and cationic amino group of 5-ASA.

These results were confirmed by X-ray diffractogram studies.

The diffractogram of 5-ASA alone is shown in Figure 3A and results of several peaks of different intensities between $2\theta = 6°$ and 45°. The diffractograms of the two formulations are shown in Figure 3D and 3F, respectively and they present the typical XRD peaks of both systems. When the drug was loaded into SucCH polymer in the form of microparticles or physical mixture the intensity of each peak markedly decreased. That means that both of two molecules are present but there are some interaction between them that affect the cristallinity of 5-ASA and decrease the intensity of the peaks.

4.3.4. Particle size analysis, zeta potential and 5-ASA content

The formulation and preparation process resulted in production of negatively charged particles with a d_{vs} of 5.1±2.2 μm. Zeta potentials of blank SucCH microparticles and 5-ASA loaded SucCH microparticles were -44.2±3.9 mV and -20.7±4.9 mV, respectively; while SucCH freeze-dried system zeta potential was -11.3±3.9 mV. No remarkable difference was found in particle size and distribution between blank- and drug-loaded microparticles, indicating that the loading of 5-ASA in the microparticles substantially did not influence their size.

The amount of 5-ASA present in FD and MP were 50% and 49.2%, respectively. The results are shown in Table 1.

Table 1. Content and examined parameters of 5-ASA loaded systems

System	*5-ASA content (%)*	*EE (%)*	*Yield (%)*	*Particle size (μm)*	*Zeta pot. (mV)*
Microparticles	49.3±2.1	50.1±1.6	55.2±0.5	5.1±2.2	−44.2±3.9
Freeze-dried	50.0±2.3	93.75±3.2	93.75±2.8	-	−11.3±3.91

4.3.5. Morphological analysis.

By imaging with SEM, an acceptable spherical morphology was observed. The surface appeared mostly smooth with some roughness. The absence of ideal spherical morphology can be probably attributed to the drying process that causes certain invaginations in the particles. The particles tend to agglomerate, probably due to the specific localization of the polymers and existence of attractive electrostatic forces.

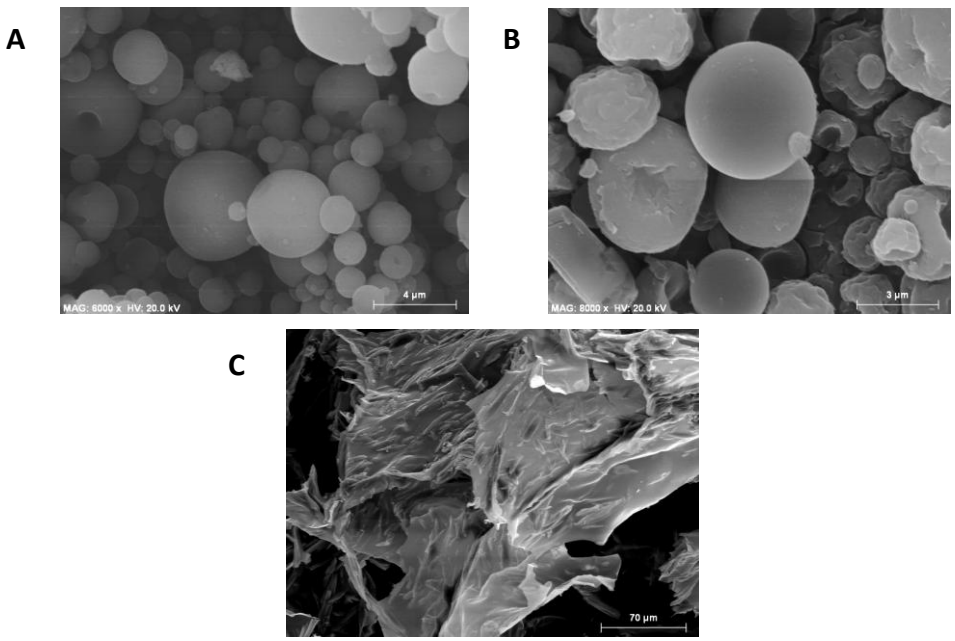

Figure 4. SEM pictures of blank SucCH microparticles (A) MP (B) and FD (C).

Figure 4A depicts the surface topography of unloaded *N*-Succinyl-chitosan microparticles while Figure 4B shows 5-ASA loaded SucCH microparticles.
In Figure 4C freeze-dried system is presented, it shows a filamentous and rough powder proper to a polymeric system like SucCH.

4.3.6. In vitro swelling

The swelling studies of FD and MP were performed at different pH values and are shown in Figure 5. The two systems showed the highest swelling at pH=7.4, while the swelling in acidic pH was considerably smaller as evidenced from the shown data. In FD (Figure 5a) there were no differences between pH=2.0 and 5.5 swelling with an index never reaching the 10%. On the contrary at pH=7.4 the FD sample constantly increased up to 25% at 24 hours showing a tendency to increase.

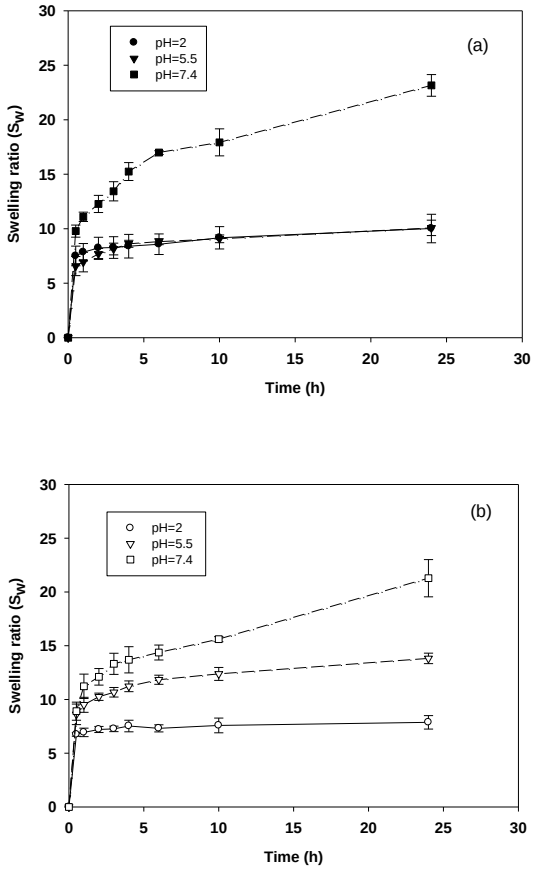

Figure 5. In vitro swelling studies of FD (a) and MP (b) in different dissolution mediums. Error bars represent standard deviation, *n* =3.

This property is due to the presence of carboxyl groups, which in acidic conditions are undissociate. At alkaline pH the carboxyl groups are negatively charged and their affinity for the water increases making them to swell and solubilize at this pH value.

The swelling ratio of the microparticles was different at the three pH values and it increased as the pH increased (Figure 5b). As expected the highest ratio was at pH=7.4 as discussed before and it followed the same trend of FD, reaching 21% of swelling after 24 hours. The swelling ratio at pH=2 never surpassed the 8%. At pH=5.5 it was a little bit higher then that one of the freeze-dried system probably due to the larger specific surface area of the microparticles that let the water enter in a easier way. From the shown data it can be concluded that the swelling index depended on the presence of carboxyl groups of SucCH and their different affinity for the alkaline or acid pH values.

4.3.7. Drug release studies

As previously mentioned, 5-ASA formulations have to pass preferentially unmodified through the stomach and small intestine to reach the large intestine, where the drug should be released to exerts its action. For this reason drug release studies were performed in three different solutions: pH=2.0, 5.5 and pH=7.4. Drug release studies were carried out up to 24 hours because the colonic transit time goes from 20 to 30 hours [33].

In Figure 6a, 5-ASA release profiles from FD are shown; drug release was faster at pH=7.4 than at pH=2.0 and 5.5. Indeed after 6 hours, 5-ASA release at pH=2.0 and 5.5 did not overpass 10%, while 30% of drug was released at pH=7.4, where after 24 hours more than 75% of the loaded 5-ASA was released.

Drug release studies from microparticles are shown in Figure 6b. As seen for the freeze-dried system the released drug percentage increased with the pH medium. In condition simulating gastric content (pH=2.0), 5-ASA release during the first 2 hours (stomach transit time) was less than 10%, while at pH=7.4 the drug release rate was 30% showing a different affinity of the polymer for the two solutions. After 4 hours (small intestine transit time) the percentage of drug released at pH=5.5 and

7.4 was respectively 25% and 51%, that is more than double of drug released at pH=7.4 in comparison to pH=5.5.

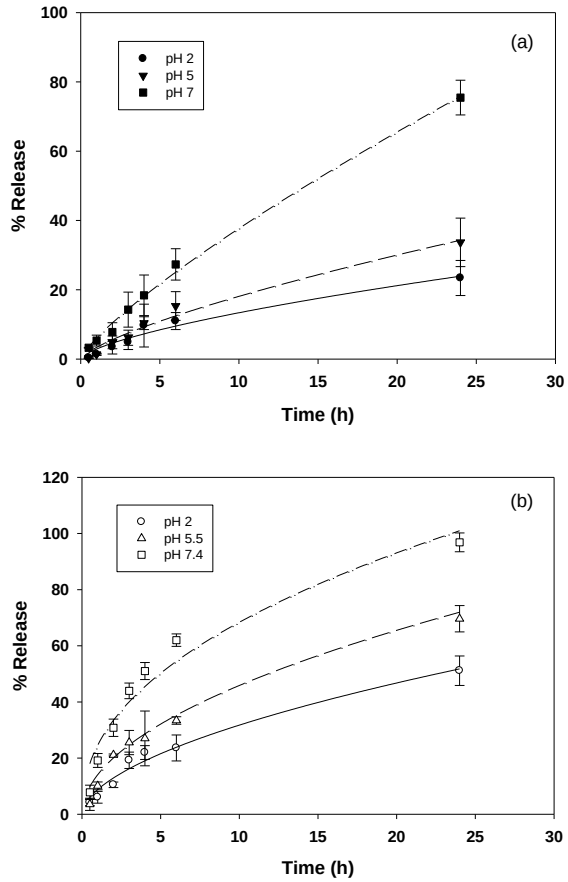

Figure 6. In vitro 5-ASA release studies from FD (a) and MP (b) in different dissolution mediums. Error bars represent standard deviation, *n* =3.

At increasing pH the affinity of the SucCH to the buffer solution increases. It is due to the chitosan modification: the number of succinyl groups (and consequently -COOH moiety) present in SucCH is higher than the amino groups ($-NH_2$). The carboxylic group can be deprotonated at alkaline pH but not at acidic pH and it had a higher affinity for pH=7.4 solution. However, under acidic conditions, the carboxyl moieties are either partially ionized (at pH=5.5) or predominantly unionized (at pH=2.2). The uncharged carboxylic acid groups are considerably less hydrophilic compared to their charged conjugate-bases, i.e. the carboxylate anions. Therefore the drug was probably released due to combined mechanisms of swelling, jelling, drug

diffusion in the gel layer and solubilization of the systems. The polymer firstly let the solvent enter into the matrix, swelled maintaining its three dimensional structure; then at pH=7.4 it slowly solubilized releasing the loaded drug.

Moreover, drug release from FD is slower than that one from microparticle due to the different specific surface area. The larger specific surface area speeds up the microparticle swelling and helps the entrance of the solvent in the polymer matrix causing a faster drug release.

To investigate more precisely the mechanism of drug release results were analysed according to Ritger–Peppas equation (Eq. (2)). The fitting results are presented in Table 2. As can be seen from the obtained correlations coefficient values ($R \geq 0.975$), the release data fit well to the empirical Eq. (2). In all cases, n values were between 0.45 and 0.89 (Table 2) (from 0.44 to 0.80). Therefore drug release is characteristic for an anomalous transport, which can be regarded as an indicator of for the superposition of both Fickian diffusion (diffusion controlled drug release) and case-II transport (swelling controlled drug release).

Table 2. Comparison of estimate parameters from curve fitting of drug dissolution in pH media to power law expression.

Microparticles	K (h^{-1})	n	R^2
pH=2	8.76±0.99	0.56±0.04	0.988
pH=5.5	14.63±2.02	0.51±0.05	0.977
pH=7.4	24.53±3.02	0.44±0.05	0.975

Freeze-dried system	K (h^{-1})	n	R^2
pH=2	2.89±0.59	0.66±0.07	0.980
pH=5.5	3.37±0.62	0.73±0.06	0.987
pH=7.4	5.99±0.47	0.80±0.03	0.998

4.4. Conclusion

In conclusion the 5-ASA loaded SucCH microparticles and freeze-dried system were prepared as new formulations for the controlled and delivered release of 5-aminosalicylic acid. SucCH was chosen as carrier due to its favorable pharmaceutical properties. DSC, FTIR, X-ray diffraction studies were useful to show the derivatization of chitosan and to confirm the effective loading of the drug into the polymer. Results from physical characterization (morphology, particle size, zeta potential) and drug loading of the prepared microparticles and freeze-dried system are in favour of their localization and prolonged presence time in colon. In vitro swelling behaviour and release studies showed the usefulness of both formulations for the 5-ASA delivery, showing that both systems released the drug preferentially at colonic pH (pH=7.4). Therefore, these systems might be good candidates for further research aimed to evaluate their effects on the inflammatory response in an experimental chronic model of induced colitis in Wistar rats.

4.5. References

[1] R.B. Sartor. Mechanisms of disease: pathogenesis of Crohn's disease and ulcerative colitis. Nat. Clin. Pract. Gastroenterol. Hepatol. 3 (2006) 390-407.

[2] B.E. Sands. Therapy of Inflammatory Bowel Disease. Gastroenterol. 118 (2000) S68-S82.

[3] A.I. Qureshi, R.D. Cohen. Mesalamine delivery systems: do they really make much difference? Adv. Drug Deliv. Rev. 57 (2005) 281– 302.

[4] D. Rachmilewitz, F. Karmeli, L.W. Schwartz, P.L. Simon. Effect of aminophenols (5-ASA and 4-ASA) on colonic interleukin-1 generation. Gut 33 (1992) 929–932.

[5] Y.R. Mahida, C.E. Lamming, A. Gallagher, A.B. Hawthorne, C.J. Hawkey. 5-Aminosalicylic acid is a potent inhibitor of interleukin 1β production in organ culture of colonic biopsy specimens from patients with inflammatory bowel disease. Gut 32 (1991) 50-54.

[6] J.R.S. Hoult, P.K. Moore. Effects of sulfasalazine and its metabolites on prostaglandin synthesis, inactivation and actions on smooth muscle. Br. J. Pharmac. 68 (1980) 719-730.

[7] J.G. Williams, M.Hallett. Effect of sulphasalazine and its active metabolite, 5-amino-salicylic acid, on toxic oxygen metabolite production by neutrophils. Gut 30 (1989) 1581-1587.

[8] S.M. McKenzie, W.F. Doe, G.D. Buffinton. 5-Aminosalicylic acid prevents oxidant mediated damage of glyceraldehyde-3-phosphate dehydrogenase in colon epithelial cells. Gut 44 (1999) 180–185.

[9] P. Gionchetti, C. Guarnieri, M. Campieri, A. Belluzzi, C. Brignola, P. Iannone, M. Miglioli, L. Barbara. Scavenger Effect of Sulfasalazine, 5-Aminosalicylic acid, and Olsalazine on Superoxide Radical Generation. Dig. Dis. Sci. 36 (1991) 174-178.

[10] H. Bantel, C. Berg, M. Vieth, M. Stolte, W. Kruis, K. Schulze-Osthoff. Mesalazine Inhibits Activation of Transcription Factor NF-κB in Inflamed Mucosa of Patients With Ulcerative Colitis. Am. J. Gastroenterol. 95 (2000) 3452-3457.

[11] G. Rogler, K. Brand, D. Vogl, S. Page, R. Hofmeister, T. Andus, R. Knuechel, P.A. Baeuerle, J. Scholmerich, V. Gross. Nuclear factor κB is activated in macrophages and epithelial cells of inflamed intestinal mucosa, Gastroenterol. 115 (1998) 357-369.

[12] S.Y. Zhou, D. Fleisher, L.H. Pao, C. Li, B. Winward, E.M. Zimmermann. Intestinal metabolism and transport of 5-aminosalicylate. Drug Metab. Disp. 27 (1998) 479-485.

[13] P. Kumar, B. Mishra. Colon Targeted Drug Delivery Systems -An Overview. Curr. Drug Deliv. 5 (2008) 186-198.

[14] M.K. Chourasia, S.K. Jain. Pharmaceutical approaches to colon targeted drug delivery systems. J. Pharm. Phamaceut. Sci. 6 (2003) 33-66.

[15] V.R. Sinha, R. Kumria. Microbially triggered drug delivery to the colon. Eur. J. Pharm. Sci. 18 (2003) 3–18.

[16] Y. Dai, P. Li, J. Zhang, A. Wang, Q. Wei. A Novel pH Sensitive *N*-Succinyl Chitosan/Alginate Hydrogel Bead for Nifedipine Delivery. Biopharm. Drug Dispos. 29 (2008) 173–184.

[17] C. Yan, D. Chen, J. Gu, H. Hu, X. Zhao, M. Qiao. Preparation of *N*-Succinyl-chitosan and their physical-chemical properties as novel excipient. Pharm. Soc. Jap. 126 (2006) 789-793.

[18] S. Hirano, T. Moriyasu. *N*-(Carboxyacyl)chitosans. Carbohydr. Res. 92 (1981) 323–327.

[19] R. Yamaguchi, Y. Araj, T. Itoh, S. Hirano. Preparation of partially N-succinylated chitosan and their cross-linked gels. Carbohydr. Res. 88 (1981) 172-175.

[20] M.R. Rekha, Chandra P. Sharma. pH sensitive Succinyl Chitosan Microparticles: A Preliminary Investigation Towards Oral Insulin Delivery. Trends Biomater. Artif. Organs 21 (2008) 107-115.

[21] C. Mura et al. Development and characterization of freeze-dried *N*-Succinyl-chitosan systems for colon-specific delivery of 5-ASA submitted to Molecules, 2011.

[22] F.N. Hussain, R.A. Ajjan, M. Moustafa, J.C. Anderson, S.A. Riley. Simple method for the determination of 5-aminosalicylic and *N*-acetyl-5-aminosalicylic acid in rectal tissue biopsies. J. Chrom. B 716 (1998) 257–266.

[23] N.A. Peppas. Analysis of Fickian and non-Fickian drug release from polymers. Pharm. Acta Helv. 60 (1985) 110–111.

[24] P.L. Ritger, N.A. Peppas. A simple equation for description of solute release II. Fickian and anomalous release from swellable devices. J. Controlled Release 5 (1987) 37–42.

[25] Y. Shigemasa, H. Matsura, H. Sashiwa, H. Saimoto. Evaluation of different absorbance ratios from IR spectroscopy for analyzing the degree of deacetylation in chitin. Int. J. Biol. Macromol. 18 (1996) 237-242.

[26] Y. Dong, C. Xu, J. Wang, H. Wang, Y. Wu, Y. Ruan. Determination of degree of substitution for N-acetylated chitosan using IR spectra. Science in China, series B, 44 (2001) 216-224.

[27] C.Y. Choi**,** S.B. Kim**,** P.K. Pak**,** D.I. Yoo**,** Y.S. Chung**.** Effect of *N*-acylation on structure and properties of chitosan fibers. Carbohydr. Polym. 68 (2007) 122-127.

[28] C. Zhang, Q. Ping, H. Zhang, J. Shen. Synthesis and characterization of water-soluble O-succinyl-chitosan. Eur. Polym. J. 39 (2003) 1629–1634.

[29] R.J. Samuels. Solid state characterization of the structure of chitosan films. J. Polym. Sci. Polym. Phys. 19 (1981) 1081–1105.

[30] Z. Aiping, C. Tian, Y. Lanhua, W. Hao, L. Ping. Synthesis and characterization of *N*-succinyl-chitosan and its self-assembly of nanospheres, Carbohydr. Polym. 66 (2006) 274–279.

[31] K. Mladenovska, O. Cruaud, P. Richomme, E. Belamie, R.S. Raicki, M.-C. Venier-Julienne, E. Popovski, J.P. Benoit, K. Goracinova. 5-ASA loaded chitosan–Ca–alginate microparticles: Preparation and physicochemical characterization. Int. J. Pharm. 345 (2007) 59-69.

[32] J. Nunthanid, K. Huanbutta, M. Luangtana-anan, P. Sriamornsak, S. Limmatvapirat, S. Puttipipatkhachorn. Development of time-, pH-, and enzyme-controlled colonic drug delivery using spray-dried chitosan acetate and hydroxypropyl methylcellulose. Eur. J. Pharm. and Biopharm. 68 (2008) 253-259.

[33] R. Kumar, M.B. Patil, S.R. Patil, M.S. Paschapur. Polysaccharide based colon specific drug delivery: a review. Int. J. Pharm. Tech. Res. 1 (2009) 334-346.

5. *N*-SUCCINYL-CHITOSAN SYSTEMS FOR 5-AMINOSALICYLIC ACID COLON DELIVERY: *IN VIVO* STUDY WITH TNBS-INDUCED COLITIS MODEL IN RATS

Abstract

5-Aminosalicylic acid (5-ASA) loaded *N*-Succinyl-chitosan (SucCH) microparticle and freeze-dried system were prepared as potential delivery systems to the colon. Physicochemical characterization and in vitro release and swelling studies were previously assessed and showed that the two formulations appeared to be good candidates to deliver the drug to the colon. In this work the effectiveness of these two systems in the treatment of inflammatory bowel disease was evaluated. In vitro mucoadhesive studies showed excellent mucoadhesive properties of both the systems to the inflamed colonic mucosa. Experimental colitis was induced by rectal instillation of 2,4,6-trinitrobenzene sulfonic acid (TNBS) into male Wistar rats. Colon/body weight ratio, clinical activity score system, mieloperoxydase activity and histological evaluation were determined as inflammatory indices. The two formulations were compared with drug suspension and SucCH suspension. The results showed that the loading of 5-ASA into SucCH polymer markedly improved efficacy in the healing of induced colitis in rats.

5.1. Introduction

Colon-targeting drug delivery systems have applications in several therapeutic areas [1-4]. These include topical treatment of colon diseases and systemic delivery of therapeutic peptide and proteins (that are normally degraded in the upper gastrointestinal tract). Additionally, colonic delivery of drugs may be extremely useful when a delay in drug absorption is required from a therapeutic point of view, e.g. in case of diurnal asthma, angina pectoris and arthritis. One of the important therapeutic applications of colon targeting delivery systems is the treatment of large intestine disorders, such as irritable bowel syndrome, ulcerative colitis, Crohn's disease, colon cancer and amebiasis. Chron's disease and ulcerative colitis are two related but distinct chronic inflammatory disorders of the gastrointestinal tract, commonly denoted as inflammatory bowel disease (IBD). The exact causes remain uncertain but thus far, IBD is thought to be the result of an appropriate and ongoing activation of the mucosal immune system driven by the normal luminal flora in a genetically susceptible host [5,6]. This paradigm has emerged, to a great extent,

from studies in animal models of mucosal inflammation [7]. Several animal models of intestinal inflammation have been developed and can be divided into four categories: spontaneous colitis, inducible colitis, genetically engineered and adoptive transfer models [8]. Among them trinitrobenzene sulfonic acid (TNBS)-induced colitis have been widely used [9-11]. TNBS is thought to be hapten, because it is presumed to bind endogenous proteins in the colonic mucosa and to induce a local immunologic response through macrophage and T cell activation [12]. 5-Aminosalycilic acid (5-ASA) is an anti-inflammatory drug largely used to treat inflammatory bowel disease [13]. 5-ASA oral administration is limited due to its rapid absorption in the upper part of the gastrointestinal (GI) tract [14] and there is a little localization of the drug in the site of action (colon). The efficacy of treatment depends on providing the therapeutical concentration of the drug at the site of inflammation. For this reason three methods have been widely used for 5-ASA targeting: a prodrug concept, enteric coating and/or prolonged release of the drug through semipermeable membrane [15]. Controlled release preparation are specifically designed to minimize systemic absorption and to achieve optimum delivery of the biologically active 5-ASA to the distal small intestine and the colon. Thus relatively high concentrations of free 5-ASA can be achieved in the intestinal lumen without producing systemic exposure and subsequent toxicity.

Chitosan and some of its various synthetic derivatives have recently attracted great interest for colon delivery. Chitosan (CH) is a polycationic polysaccharide derived from naturally occurring chitin by alkaline deacetylation. Chemically, it is formed by β-(1-4)-linked D-glucosamine (deacetylated unit) and *N*-acetyl-D-glucosamine (acetylated unit) [16]. It has favorable biological properties but it rapidly dissolves in the gastric cavity. To overcome its solubility at acidic pH, enteric coated chitosan capsules and microparticles were prepared [17,18], pH-sensitive based chitosan hydrogels systems [19] and chitosan polyelectrolyte complexes [20] as well as chitosan salts [21] and derivative [22] have been developed for drug the targeting to the colon.

N-Succinyl-chitosan (SucCH) is a derivative of chitosan that could be obtained by introducing succinyl groups into *N*-terminals of chitosan glucosamine units [23-25]. It is reported to have favorable drug carrier properties such as biocompatibility and

low toxicity [26]. Due to the presence of carboxyl groups it exhibits pH dependent swelling behavior and it is insoluble at acidic pH value. It possesses mucoadhesive properties because of its hydrophilicity leading to hydrogen bond formation, swelling characteristics, and sufficient chain flexibility. Moreover, it is a negatively charged polymer and it adheres more easily to the inflamed tissues due to the presence in the ulcerative tissues of a high number of positively charged proteins [27]. All these advantages endowed this material with huge potential for the application as site-specific or controlled-release drug delivery systems.

Recently we have developed 5-ASA loaded *N*-Succinyl-chitosan microparticles and freeze-dried systems as a targeted colon delivery system against IBD [28]. Physicochemical characterizations, including FTIR, DSC, X-ray diffraction studies, zeta potential, drug loading and microparticles size were performed. In vitro swelling and release studies were also carried out and the obtained results from in vitro characterization showed that the two systems could be suitable candidate for colon delivery of 5-ASA.

In the present studies the therapeutic efficiency of these drug carrier system was evaluated using experimental TNBS colitis rat model. Initially *ex vivo* mucoadhesion studies were performed. To demonstrate the efficiency of the systems, rats were also treated with 5-ASA suspension, as well as SucCH suspension. The efficacy of all formulations was determined by the colon/body weight ratio, clinical activity score system, myeloperoxidase activity and histological evaluation.

5.2. Materials and Methods

5.2.1. Materials

Chitosan of medium molecular weight, succinic anhydride and 5-ASA were obtained from Sigma-Aldrich, (Milan, Italy). 2,4,6-trinitrobenzenesulfonic acid (TNBS), hexadecyltrimethylammonium bromide (HTAB), 3,3',5,5'-tetramethylbenzidine (TMB), hydrogen peroxide 30% and peroxidase from horseradish were purchased form Sigma-Aldrich (Spain). Spectra-por® dialysis membrane (MWCO 12000-14000 Dalton, regenerated cellulose) was purchased

from Spectrum Lab (Inc, USA). All the products and solvents were of analytical grade.

5.2.2. Preparation of N-Succinyl-chitosan and 5-ASA loaded SucCH systems

Chitosan medium molecular weight was succinylated according to the method reported by Hirano et al. [25] with some modifications.

5-ASA/SucCH system (FD) was prepared at 1:1 molar ratio using freeze-drying technique (Freeze-dryer Criotecnica, MM Cota, Rome, Italy).

5-ASA loaded SucCH microparticles (MP) were obtained using spray-drying method, (Minispray Dryer, Büchi B-290, Switzerland) at 1:1.25 ratio (5-ASA:SucCH). The conditions of the spray-drying process were: nozzle diameter 0.7 mm, aspiration: 80%, inlet temperature: 150°C, outlet temperature: 100°C. Blank SucCH microparticles were prepared using the same conditions as for the drug-loaded particles.

5.2.3. Physiscochemical Characterization of MP and FD

FTIR, DSC and X-ray diffractogram spectra were performed for 5-ASA, chitosan, SucCH, FD and MP.

FTIR measurements were taken at an ambient temperature using Bruker Equinox 55 (Germany). About 2 mg of the samples were ground thoroughly with KBr and pellets were formed under a hydraulic pressuse of 600 kg/cm^2.

DSC studies were performed using a DSC Mettler Toledo model 821e (Switzerland). The samples (2-5 mg) were scanned in sealed aluminium pans under nitrogen atmosphere. DSC thermograms were scanned in the first heating run at a constant rate of 10°C/min and a temperature range of 0-325°C.

X-ray diffractograms pattern were recorded with Bragg–Brentano geometry on a Bruker AXS D5005 (DRXP, Germany) in the 2θ range from 5° to 45° in steps of 0.02° at 6 s per step.

Shape and surface morphology of the empty and 5-ASA loaded SucCH microparticles were examined using a scanning electron microscope (SEM, S-4100 Hitachi, Madrid, Spain).

Measurement of the particle size and diameter of the microparticles was carried out with Analysette 22 Micro tec plus (Fritsch, Germany) after suspending the particles in distilled water and sonicating the suspension for 10 min in ultrasonic bath. The average particle size was expressed as the volume surface diameter, d_{vs} (μm).

The zeta potential of the systems was recorded using Malvern Zeta Sizer apparatus (model Zen 3600, Malvern, UK). Each sample was analysed at least six times to obtain an average value and a standard deviation. Samples of blank SucCH microparticles were also submitted to this study.

5-ASA content in the two systems was assayed by HPLC as it was described previously [28].

5.2.4. In vitro swelling and drug release studies

Swelling and drug release studies were carried out in three different solutions in order to simulate the gastro-intestinal tract pH values: stomach (pH=2), small intestine (pH=5.5) and large intestine (pH=7.4). The *in vitro* release studies were performed under sink conditions and the amount of 5-ASA released was assayed by HPLC as described elsewhere [28].

5.2.5. Preparation of GI tissues and mucoadhesive test

Wistar rats (13-week old) had been fasted for 24 h. The fasted conditions were set to minimize the contents in the GI tract, which disturbed the washing process for the following use. The tissues (i.e. duodenum and colon) were excised from rats that were sacrificed. Each section of tissues was then slowly washed with a large amount of normal saline solution. Then, the tissues (duodenum, healthy colon and inflamed colon) were immediately used for this study. Inflamed colon was obtained by inducing the model of chronic inflammation in the rat colon as described below. Samples were placed in a closed flat bottom tube with 1 ml of buffer and in a thermostated bath at 37.0° C. pH=5.5 solution was used for the mucoadhesion in the duodenum and pH=7.4 was used for the mucoadhesion in the colon. At scheduled time intervals the mucoadhesion studies were done using different part of rat intestine tissue. At 120 min the mucoadhesion using duodenum tissue was studied and at 150 min using colon. The mucoadhesion study was done using a universal

tensile tester (Lloyd Instruments, LR 50K model, UK). The stainless steel plate (L-shape) was fitted by one of its side into the upper and lower jaws of the instrument so as the other surfaces of the plates were facing each other. The rat tissue was stuck at the upper plate surface with the glue, while the sample was placed on the lower plate. Then the upper jaw with tissue stuck on the plate was lowered slowly so that it just touched the sample surface. No external force was applied. The sample was kept in contact with the tissue for 5 minutes and then the upper jaw was slowly moved upward at the speed of 3 mm/min. All the experiments were done in triplicate. The maximum detachment force (F_{max}), i.e. the force required for separating the sample from the tissue surface was obtained directly from NimaST518.vi software (Nima Technology Ltd., Coventry, England) and the total amount of forces involved in the probe withdrawal from the tissue (work of adhesion, W_{ad}) was then calculated from the area under the force versus distance curve. These parameters were used to compare the different formulations tested.

5.2.6. Induction of colonic inflammation

These studies were carried out on Wistar male rats aged 8–12 weeks and weighing 230–250 g. Animals were housed in an air-conditioned room at 22±3 °C, 55±5% humidity, 12 h light/dark cycles and allowed free access to water and laboratory chow for the duration of the studies. To induce the model of chronic inflammation in the rat colon, the method described by Morris et al. [29] was followed with some slight modifications. Briefly, rats were arbitrarily separated into treatment groups, fasted for 48 h with free access to water and then anaesthetized with isoflurane. A graduated rubber canula was inserted rectally into the colon such that the tip was 8 cm proximal to the anus. 0.5 ml of a solution of TNBS (81 mg/kg body weight) dissolved in 50% ethanol v/v was instilled into the lumen of the colon through the rubber probe (total volume 0.5 ml solution). A control group received 0.5 ml 50% ethanol v/v administered as before. The induction and development of inflammation were monitored every day during 13 days. Rats (in groups of 5) were sacrificed with an overdose of anesthesia the days 3,5,7,9 and 13 after TNBS administration. The development of inflammation was evaluated in respect to colon /body weight ratio, clinical activity score, myeloperoxidase activity and histological changes.

5.2.7. Treatment studies design

Rats were divided into 4 groups: to group one was administered SucCH suspension, group two received 5-ASA suspension, group three received 5-ASA loaded freeze-dried system (FD) and finally to group four microparticles (MP) was administered. A dose of 120 mg/kg/day of 5-ASA calculated from the dose from humans (70 kg) [30] were administered by oral gavage once a day for three days in the period of the most intensive inflammation (days 3,4 and 5 after TNBS administration).

5.2.8. Assesment of colonic injury and inflammation

The rats were killed with an overdose of anesthesia then the abdomen was opened and the distal colon was removed. The samples of inflamed tissue were excised to measure the ratios of distal colon weight to body weight (C/B ratio), the criteria for scoring the gross morphologic damage (clinical activity score system), the myeloperoxidase activities and histological evaluation.

5.2.8.1. Determination of colon/body weight ratio

The rats were killed with an overdose of anesthesia, then the abdomen was opened and the distal colon was rapidly excised and opened longitudinally along the mesenteric edge. The colon was washed with 0.9% (w/v) saline and placed with the mucosal surface upward over a glass plate chilled with ice and then weighted. The ratio of the 8 cm segment distal colon weight was calculated as an index of colonic tissue edema.

5.2.8.2. Clinical activity score system

Colitis activity was quantified with a clinical score assessing weight loss, stool consistency and rectal bleeding [31,32]. No weight loss was counted as 0 point, 1–5% as 1 point, 5–10% as 2 points, 10–20% as 3 points and >20% as 4 points. For stool consistency, 0 point was given for well-formed pellets, 2 points for pasty and semiformed stools that did not stick to the anus and 4 points were given for liquid stools that stick to the anus. Bleeding was scored as 0 point for no blood, 2 points for positive finding and 4 points for gross bleeding. The sum of these scores was

forming the clinical score ranging from 0 (healthy) to 12 (maximal activity of colitis).

5.2.8.3. Myeloperoxidase activity

The measurement of the myeloperoxidase activity was performed to quantify the severity of the colitis. It is a peroxidase enzyme reliable index of inflammation caused by infiltration of activated neutrophils into the inflamed tissue. Activity was analyzed according to De Young et al. [33,34]. Briefly, colon specimen was added to 750 μl of HTAB buffer (0.5% in 80 mM phosphate buffer pH=5.4) on ice and homogenized. The homogenate was centrifuged (Heraeus Fresco 17 Centrifuge, Thermo Electron Corporation, Spain) at -4°C and at 10000 rpm for 15 min (Eppendorf AG 22331, Germany). Myeloperoxidase activity in the supernatant was measured spectrophotometrically. Supernatant (25 μl) was incubated with 75 μl of phosphate buffers pH=7.4 and 10 μl of phosphate buffer pH=5.4 and 0.026% hydrogen peroxide (10 μl) at 37°C for 5 minutes. Then 20 μl of TMB 18 mM (dissolved in 8% DMF) were added to the previous mixture and incubated for 10 minutes. Finally the reaction was stopped by the adding of 15 μl of sodium acetate 1.5 M (pH=3.0) and the absorbance was measured at 620 nm.

5.2.8.4. Histological evaluation

Two tissue samples (3 cm samples distal and proximal) were excised from each colon and maintained in formaldehyde (10% v/v) for microscopic studies. These tissue samples were processed routinely and embedded in paraffin. Longitudinal sections (5 μm) were stained with haemotoxylin and eosin. Microscopic assessment by light microscope was performed blind on coded slices.

5.2.9. *Statistical analysis*

Data analysis was carried out with the software package R, version 2.10.1. Results are expressed as the mean ± standard deviation (S.D.). Multiple comparisons of means (Tukey test) were used to substantiate statistical differences between groups, while Student's t-test was used for comparison between two samples. Significance was tested at the 0.05 level of probability (p).

5.3. Results and discussion.

5-ASA loaded microparticles and freeze-dried system were prepared according to the previously stated formulations and subjected to further characterization [28].

5.3.1. Physiscochemical characterization of the systems

N-Succinyl-chitosan was successfully synthesized according to the methods reported in literature. FTIR, DSC and X-ray diffractograms spectra revealed the derivatization of chitosan and confirmed the loading of the drug into 5-ASA/SucCH systems, denoting that some interaction between the polymer and the drug are present.

Negatively charged particles with a d_{vs} of 5.1±2.2 μm were prepared. No remarkable differences was found in particle size and distribution between blank- and drug-loaded microparticles, indicating that 5-ASA loading in the microparticles substantially did not influence their size.

Zeta potentials of blank SucCH microparticles and 5-ASA loaded SucCH microparticles and freeze-dried system were -44.2±3.94 mV, -20.7±4.89 mV and -11.3±3.91 mV, respectively.

By imaging with SEM, an acceptable spherical morphology was observed. The surface appeared mostly smooth with some roughness.

The amount of 5-ASA present in 5-ASA/SucCH freeze-dried system and microparticles were 50% and 49.2% respectively.

5.3.2. In vitro swelling and drug release studies

As shown previously, the two systems showed the highest swelling at pH=7.4, while the swelling at acidic pH was considerably smaller as a consequence of the physico-chemical properties of the SucCH [28].

The *in vitro* release studies were in accordance with the swelling studies. They showed that drug release rate from freeze-dried system and microparticles increased with the increase of pH. The maximum drug release percentage was reached at pH=7.4, as expected. Drug release from FD was slower than that from microparticles due to the different specific surface area. The higher specific surface area speeded up the microparticles swelling and helped the solvent penetration into

the polymer matrix causing a faster drug release. As results show, FD and MP could be useful for the preparation of new 5-ASA formulation.

5.3.3. Mucoadhesion studies

Mucoadhesive polymers are used to immobilize a drug delivery device on a specific site for targeted release and optimal drug delivery due to intimacy and duration of contact. It has been proposed that the interaction between the mucus and mucoadhesive polymers is a result of physical entanglement and secondary bonding, mainly H-bonding and van der Waals attraction. These forces are related to the chemical structure of the polymers and chemical groups of mucoadhesive polymers that contribute to mucoadhesion include hydroxyl, carboxyl, amine, and amide groups in the structure. Polymer characteristics that are necessary for mucoadhesion are: strong H-bonding groups, strong anionic charges, high molecular weight, sufficient chain flexibility, and surface energy properties favoring spreading onto mucus [35].

N-Succinyl-chitosan presents all of these properties, and therefore it could be a good mucoadhesive polymer. The in vitro mucoadhesive properties of 5-ASA loaded SucCH systems were studied using rat's stomach, duodenum, healthy and inflamed colon (induced by TNBS administration as seen before). The maximum detachment force (F_{max}), i.e. the force required for separating the system from the tissue surface and the total amount of forces involved in the probe withdrawal from the tissue (work of adhesion, W_{ad}) of both formulations on different GI mucosa are shown in Figure 1.

Large intestinal mucosa showed a stronger mucoadhesion than small intestinal mucosa. This is probably due to the fact that there is a difference in the functional histology of epithelia of small and large intestinal mucosa. The absence of villi in large intestine, at the tissue level, may be a benefit for the mucoadhesion as the adhesion between the sample and mucosa or epithelia can occur easily. Moreover, at cellular level, the ratio of goblet cells in large intestine is higher than in other parts of GI tract resulting in higher mucin level, and thus in higher mucoadhesion onto the large intestinal mucosa [35].

Mucoadhesion of the two systems to the inflamed colonic mucosa resulted higher than healthy mucosa; it has been previously suggested by other authors that a possible cause for the affinity of negatively charged systems to the ulcerated mucosa of the rat was the high concentration of positively charged proteins in the inflamed regions [27].

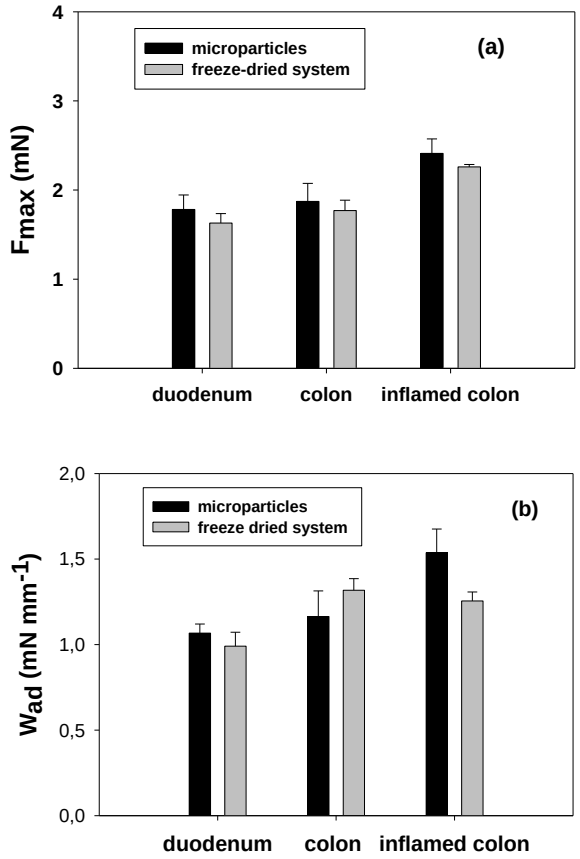

Fig. 1. ***Ex vivo*** **mucoadhesive performance of 5-ASA systems. Effect of GI mucosa on (a) maximum detachment force (F_{max}) and (b) work of adhesion (W_{ad}). Error bars represent standard deviation, *n* =3.**

No significant mucoadhesion differences between microparticles and freeze-dried systems were observed.

5.3.4. Induction of colonic inflammation.

TNBS was chosen as a model of inflammatory bowel disease; IBD can be induced by the administration of an enema containing the contact sensitizing allergen trinitrobenzene sulfonic acid (TNBS) in ethanol 50%. The main advantages of this model were: simplicity, reproducibility and time and dose related development of inflammation [36,37].

First of all, to select an optimal schedule to induce the inflammation by TNBS, we examined the development of the inflammation process at different days after intracolonic administration of TNBS in comparison to the control group that received ethanol 50% (v/v).

The development of the inflammation was monitored daily; rats suffered from diarrhea and weight-lost and during the first days of TNBS administration, rats suffered from rectal bleeding. Figures 2A and B show respectively opened colon of control rats that received ethanol 50% (v/v) and of rats after induction of colitis with TNBS, killed on day 9. The group of animals sacrificed 9^{th} day after colonic administration of TNBS showed necrotic changes and presented thick and rigid bowel.

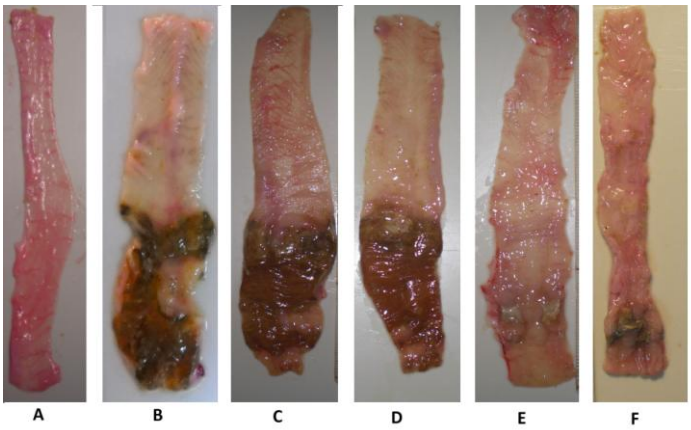

Figure 2. Photographs of the colon of rat after the induction of colitis with TNBS sacrificed on day 9: A control (ethanol receiving group), B (untreated TNBS group), C (SucCH treated group 1) D (5-ASA treated group 2) E (freeze-dried system treated group 3) and F (microparticles treated group 4)

Figures 3, 4 and 5 show respectively colon/body (C/B) weight ratio, clinical activity score system, and myeloperoxidase (MPO) activity in TNBS induced colitis on days 3, 5, 7, 9 and 13. All of the three experiments had a maximum at day 9 after the administration of TNBS, and recovered on the day 13.

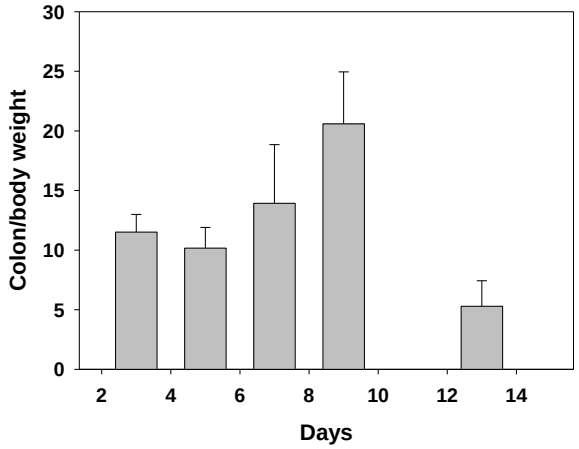

Figure 3. Index of colonic tissue edema (colon/body weight ratio) of animals with TNBS induced colitis . Each bar is an average value±S.D. of five animals.

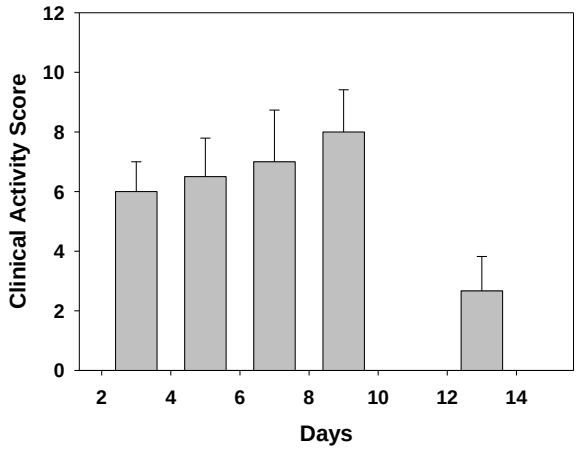

Figure 4. Clinical activity score system of animals with TNBS induced colitis. Each bar is an average value±S.D. of five animals

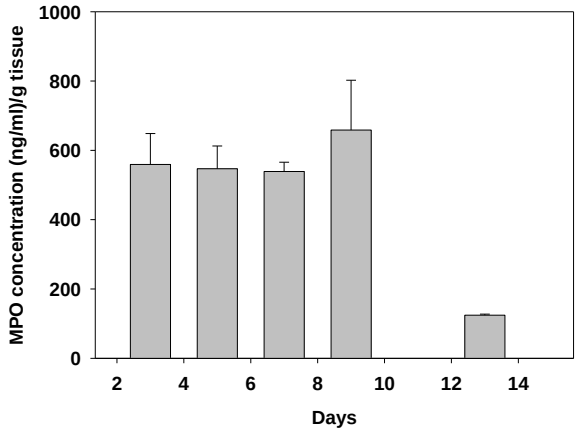

Figure 5. Myeloperoxidase activity of animals with TNBS induced colitis. Each bar is an average value±S.D. of five animals

5.3.5. Treatment studies design

Afterward, the effectiveness of 5-ASA for the treatment of the inflammation was evaluated by administrating 5-ASA formulations daily on days 3, 4 and 5. Rats were killed on day 9 because it was the day of maximal inflammation, as seen before. C/B ratio, clinical activity score and myeloperoxidase activity were compared with induced TNBS colitis untreated rats.

In Figure 2 (C,D,E and F) opened colons of groups 1, 2, 3 and 4 are presented, respectively, and compared to the untreated TNBS induced colitis rat on day 9 and control rats that received just ethanol 50% (v/v). Colons from groups 1 (Fig. 2C) and 2 (Fig. 2D) are very similar to the untreated TNBS ones with the presence of necrotic zone and thick and rigid bowel. Colons from groups 3 (Fig. 2E) and 4 (Fig. 2F) present just a little necrotic tissue and it mostly appear healthy and more similar to the control group that received ethanol 50% (v/v).

After FD and MP administration, rats from group 3 and 4 started to gain weight and have normal stool without the presence of bleeding; on the contrary after 5-ASA or SucCH administration rats from group 1 and 2 continued to lose weight and had diarrhea during all the experiment long.

The effects of 5-ASA, SucCH and the two 5-ASA formulations on the C/B ratio and clinical activity score and myeloperoxidase activity after oral administration are shown in Figures 6, 7 and 8, respectively. The colon body weight ratio markedly

decreased in rats of group 3 and 4 compared to the control that received only intracolonic TNBS (untreated rats). On the other hand no marked effect was observed on the C/B ratio of the rats of group 1 and 2 (Fig. 6). It confirms that 5-ASA alone when taken orally is almost completely absorbed before it reaches the site of action, and that it is necessary to load the drug into a new formulation that prevents its absorption and carry the drug to the large intestine. SucCH did not have any therapeutic effect for IBD.

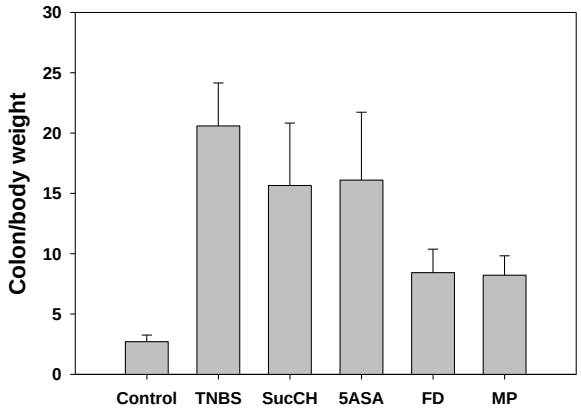

Figure 6. Colon/body weight ratio of animals with TNBS induced colitis after treatment with SucCH suspension (SucCH) group 1, 5-ASA suspension (5ASA) group 2, 5-ASA/SucCHT freeze-dried system (FD) group 3, 5-ASA/SucCH microparticles (M) group 4 and compared with induced TNBS colitis untreated rats (TNBS) and healthy (ethanol receiving rats, Control). Each bar is an average value±S.D. of five animals.

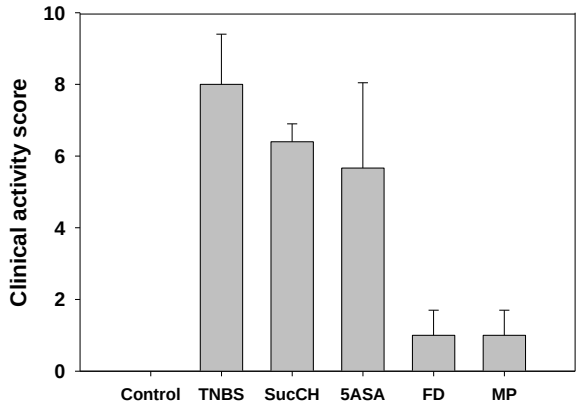

Figure 7. Clinical activity score of animals with TNBS induced colitis after treatment with SucCH suspension (SucCH) group 1, 5-ASA suspension (5ASA) group 2, 5-ASA/SucCH freeze-dried system (FD) group 3, 5-ASA/SucCH microparticles (M) group 4 and compared with induced TNBS colitis untreated rats (TNBS) and healthy (ethanol receiving rats, Control). Each bar is an average value±S.D. of five animals.

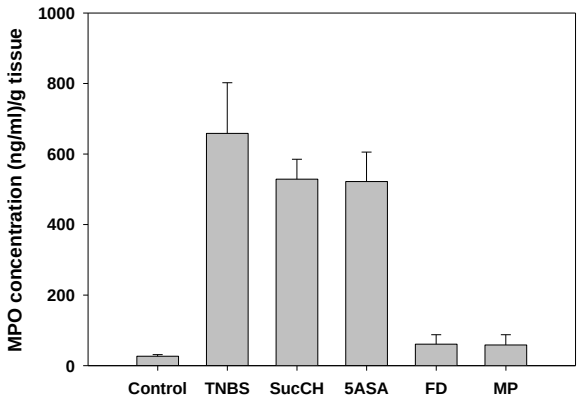

Figure 8. Myeloperoxidase activity of TNBS induced colitis at rats after treatment of SucCH suspension (SucCH) group 1, 5-ASA suspension (5ASA) group 2, 5-ASA/SucCH freeze-dried system (FD) group 3, 5-ASA/SucCH microparticles (M) group 4 and compared with induced TNBS colitis untreated rats (TNBS) and healthy (ethanol receiving rats, Control). Each bar is an average value±S.D. of five animals.

Similar results were also observed in the experiments of clinical activity score systems and MPO activity (Fig. 7 and 8, respectively). Myeloperoxidase activity markedly decreased after oral administration of FD and MP in the animal groups 3 and 4, showing and confirming that the inflammation decreased after the oral administration of the two formulations.

5.3.6. Histological evaluation.

Histological examination was made for the 50% ethanol receiving rats (healthy control), untreated TNBS induced colitis rats and treated group 1, 2, 3, and 4 rats. All the samples were taken from rats sacrificed on the 9th day after administration of TNBS.

The control group shows normal colon structure: healthy mucosa with both enterocytes and goblet cells and between them connective tissue (lamina propria, Figure 10A), muscularis mucosae and normal submucosa and muscularis externa.

Untreated animals showed necrosis, loss of the necrotic mucosa and substitution with granulation tissue. A strong inflammatory process was present in the lamina propria, submucosa and muscularis externa. As can be seen in figure 10B process of ulceration with fibrinoid necrosis of the mucosal surface and granulation tissue below the necrotic tissue were observed.

Animals treated with SucCH suspension showed necrosis, loss of the mucosa, intense transmural inflammation and granulation tissue appearance. Histologiacal findings indicated also the presence of ulceration with fibrinoid material on the surface of the mucosa and granulation tissue that involves the whole submucosa. (Figure 10C). Moreover the muscularis propria presented cronic inflammation and fibrosis.

Animals treated with 5-ASA suspension presented superficial erosion, thinning of the mucosa accompanied by thickening of the muscularis mucosae, and a cronic inflammatory process that affects the mucosa and submucosa with early development of lymphoid follicles. A few parts with normal mucosa structure but presence of strong follicular hyperplasia in the muscularis externa and parts with necrosis, loss of mucosa and substitution with granulation tissue and inflammation process were also observed (Figure 10D).

Animals treated with FD showed substantially normal mucosal structure with slight presence of chronic inflammation in the muscularis propria (Figure 10E)

Animals treated with MP showed normal mucosa structure (Figure 10F).

Histological findings indicated that untreated TNBS group showed presence of strong inflammation accompanied with necrosis and loss of the mucosa. Similar results were also obtained with SucCH suspension receiving group and 5-ASA suspension receiving group. Indeed histological findings FD and MP showed decreasing of inflammation followed by intensive regeneration and normal mucosal structure.

Histological evaluation provides additional information in addition to these obtained by the clinical activity score, colon/body weight ratio, and myeloperoxydase activity, thus confirming the usefulness of the two 5-ASA/SucCH systems in the treatment of inflammatory bowel disease.

A

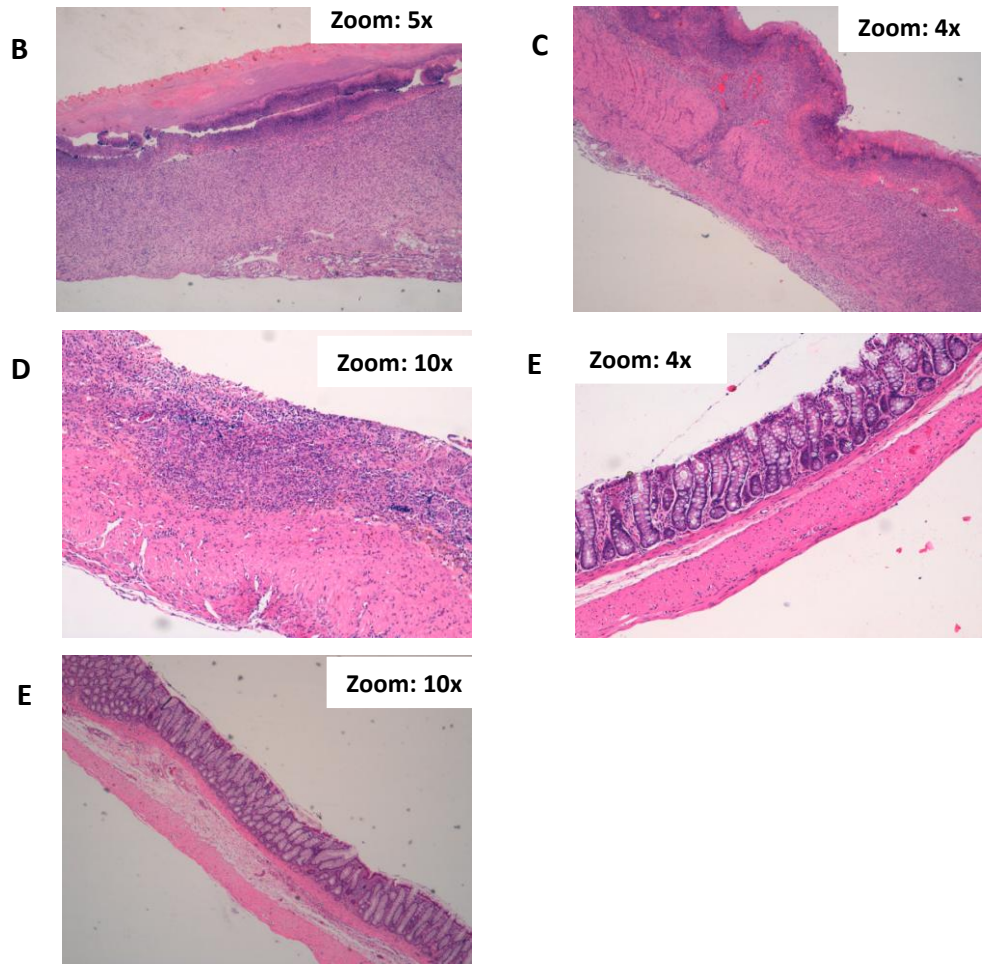

Figure 10. Histology of a representative colon specimen of a rat after the induction of colitis with TNBS sacrificed on day 9: A control (ethanol receiving group), B (untreated TNBS group), C (SucCH treated group 1), D (5-ASA treated group 2), E (freeze-dried system treated group 3) and F (microparticles treated group 4).

5.4. Conclusion

Two new systems for the controlled and delivered release of 5-aminosalicylic acid were prepared and their efficacy in the treatment of IBD was evaluated with TNBS colitis rat model. In our previous work, 5-ASA loaded microparticles and freeze-dried system were subjected to physicochemical characterization and in vitro swelling and release studies. Physical properties of the evaluated systems were in favor of drug accumulation in the site of action. In this work, mucoadhesive studies showed that the mucoadhesive properties of the two formulations extended the residence of the systems in the targeted inflamed area. The TNBS model confirmed

that both formulations could serve as new drug delivery systems for 5-ASA. Colon/body weight ratio, clinical activity score systems, myeloperoxidase activity, and histology evaluation showed that the animals treated with the two formulations had an improvement in the pathology.

5-ASA loaded SucCH MP and FD compared with 5-ASA and SucCH suspension markedly improved efficacy of 5-ASA in the healing of induced colitis in rats.

In conclusion, we demonstrated that 5-ASA can be specifically delivered to the site of action and that the described systems may be useful for the treatment of inflammatory bowel disease.

5.5. References

[1] P. Kumar, B. Mishra. Colon Targeted Drug Delivery Systems -An Overview. Curr. Drug Deliv. 5 (2008) 186-198.

[2] M.K. Chourasia, S.K. Jain, Pharmaceutical approaches to colon targeted drug delivery systems. J. Pharm. Phamaceut. Sci. 6 (2003) 33-66.

[3] L. Yang, J.S. Chu, J.A. Fix. Colon-specific drug delivery: new approaches and in vitro/in vivo evaluation. Int. J. Pharm. 235 (2002) 1–15.

[4] V.R. Sinha, R. Kumria. Polysaccharides in colon-specific drug delivery. Int. J. Pharm. 224 (2001) 19–38.

[5] R.B. Sartor. Mechanisms of disease: pathogenesis of Crohn's disease and ulcerative colitis. Nat. Clin. Pract. Gastroenterol. Hepatol. 3 (2006) 390-407.

[6] D.C. Baumgart, S.R. Carding. Inflammatory bowel disease: cause and immunobiology. Lancet 369 (2007) 1627–40.

[7] M.E.A. Borm, G. Bouma. Animal models of inflammatory bowel disease. Drug Discovery Today 4 (2004) 437-443.

[8] T. Hibi, H. Ogata, A. Sakuraba. Animal models of inflammatory bowel disease. J. Gastroenterol. 37 (2002) 409–417.

[9] Y. Jung, H. Kim, H. Kim, H. Kong, B. Choi, Y. Yang, Y. Kim. Evaluation of 5-aminosalicyltaurine as a colon-specific prodrug of 5-aminosalicylic acid for treatment of experimental colitis. Eur. J. Pharm. Sci. 28 (2006) 26–33.

[10] M.S. Crcarevska, M.G. Dodov, G. Petrusevska, I. Gjorgoski, K. Goracinova. Bioefficacy of budesonide loaded crosslinked polyeletrolyte microparticles in rat model of induced colitis. J. Drug Target. 17 (2009) 788-802.

[11] H. Tozaki, T. Odoriba, N. Okada, T. Fujita, A. Terabe, T. Suzuki, S. Okabe, S. Muranishi, A. Yamamoto. Chitosan capsules for colon-specific drug delivery: enhanced

localization of 5-aminosalicylic acid in the large intestine accelerates healing of TNBS-induced colitis in rats. J. Controlled Release 82 (2002) 51–61.

[12] K. Ishiguro, T. Ando, O. Maeda, O. Watanabe, H. Goto. Novel mouse model of colitis characterized by hapten protein visualization. BioTechniques 49 (2010) 641–648.

[13] B.E. Sands. Therapy of Inflammatory Bowel Disease. Gastroenterol. 118 (2000) S68-S82.

[14] S.Y. Zhou, D. Fleisher, L.H. Pao, C. Li, B. Winward, E.M. Zimmermann. Intestinal metabolism and transport of 5-aminosalicylate. Drug Metab. Disp. 27 (1998) 479-485.

[15] A.I. Qureshi, R.D. Cohen. Mesalamine delivery systems: do they really make much difference? Adv. Drug Deliv. Rev. 57 (2005) 281– 302.

[16] M.N.V.R Kumar. A review of chitin and chitosan applications. React. Funct. Polym. 46 (2000) 1–27.

[17] H. Tozaki, J. Komoike, C. Tada, T. Maruyama, A. Terabe, T. Suzuki, A. Yamamoto, S. Muranishi. Chitosan Capsules for Colon-Specific Drug Delivery: Improvement of Insulin Absorption from the Rat Colon. J. Pharm. Sci. 86 (1997) 1016-1021.

[18] M.L. Lamosa, C. Lopez, J.L. Jato, M.J. Alonso. Design of microencapsulated chitosan microspheres for colonic drug delivery. J. Controlled Release 52 (1998) 109–118.

[19] S.K. Jain, A. Jain, Y. Gupta, M. Ahirwar. Design and Development of Hydrogel Beads for Targeted Drug Delivery to the Colon. AAPS Pharm. Sci. Tech. 8 (2007) E1-E8.

[20] F. Bigucci, B. Luppi, T. Cerchiara, M. Sorrenti, G. Bettinetti, L. Rodriguez, V. Zecchi. Chitosan/pectin polyelectrolyte complexes: Selection of suitable preparative conditions for colon-specific delivery of vancomycin. Eur. J. Pharm. Sci. 35 (2008) 435–441.

[21] I. Orienti, T. Cerchiara, B. Luppi, F. Bigucci, G. Zuccari, V. Zecchi. Influence of different chitosan salts on the release of sodium diclofenac in colon-specific delivery. Int. J. Pharm. 238 (2002) 51–59.

[22] K. Aiedeh, M.O. Taha. Synthesis of Chitosan Succinate and Chitosan Phthalate and Their Evaluation as Suggested Matrices in Orally Administered, Colon-Specific Drug Delivery Systems. Arch. Pharm. Pharm. Med. Chem. 332 (1999) 103–107.

[23] Y. Chengyun, C. Dawei, G. Jiwei, H. Haiyang, Z. Xiuli, Q. Mingxi. Preparation of *N*-Succinyl-chitosan and their physical-chemical properties as novel excipient. Pharm. Soc. Jap. 126 (2006) 789-793.

[24] S. Hirano, T. Moriyasu. *N*-(Carboxyacyl)chitosans. Carbohydr. Res. 92 (1981) 323–327.

[25] R. Yamaguchi, Y. Araj, T. Itoh, S. Hirano. Preparation of partially *N*-succinylated-chitosan and their cross-linked gels. Carbohydr. Rese. 88 (1981) 172-175.

[26] M.R. Rekha, C.P. Sharma. pH sensitive Succinyl Chitosan microparticles: a preliminary investigation towards oral insulin delivery. Trends in Biomater. Artif. Organs 21 (2008) 107-115.

[27] T.T. Jubeh, Y. Barenholz, A. Rubinstein. Differential Adhesion of Normal and Inflamed Rat Colonic Mucosa by Charged Liposomes. Pharm. Res. 21 (2004) 447-453.

[28] C. Mura et al. pH-sensitive 5-ASA loaded *N*-Succinyl-Chitosan systems for colon specific delivery: Preparation, characterization and in vitro evaluation. Manuscript in preparation, 2011.

[29] G.P. Morris, P.L. Beck, M.S. Herridge, W.T. Depew, M.R. Scewczuk, J.L. Wallace. Hapten-induced model of chronic inflammation and ulceration in the rat colon. Gastroenterol. 96 (1989) 795–803.

[30] W.J. Sandborn, S.B. Hanauer. Systematic review: the pharmacokinetic profiles of oral mesalazine formulations and mesalazine pro-drugs used in the management of ulcerative colitis. Aliment. Pharmacol. Ther. 17 (2003) 29–42.

[31] G. Hartmann, C. Bidlingmaier, B. Siegmund, S. Albrich, J. Schulze, K. Tschoep, A. Eigler, H.A. Lehr, S. Endres. Specific type IV phopsphodiesterase inhibitor rolipram mitigates experimental colitis in mice. J. Pharm. Exp. Ther. 292 (2000) 22–30.

[32] A. Lamprecht, N. Ubrich, H. Yamamoto, U. Schafer, H. Takeuchi, P. Maincent, Y. Kawashima, C.M. Lehr. Biodegradable nanoparticles for targeted drug delivery in treatment of inflammatory bowel disease. J. Pharm. Exp. Ther. 299 (2001) 775–781.

[33] L.M. De Young, J.B. Kheifets, S.J. Ballaron, J.M. Young. Edema and cell infiltration in the phorbol ester-treated mouse ear are temporally separate and can be differentially modulated by pharmacologic agents. Inflamm. Res. 26 (1989) 335-341.

[34] H. Sato, Y. Nakayama, C. Yamashita, H. Uno. Anti-Inflammatory Effects of Tacalcitol (1,24(R)(OH)2D3, TV-02) in the Skin of TPA-Treated Hairless Mice. J. Dermatol. 31 (2004) 200-217.

[35] N. Thirawong, J. Nunthanid, S. Puttipipatkhachorn, P. Sriamornsak. Mucoadhesive properties of various pectins on gastrointestinal mucosa: An in vitro evaluation using texture analyzer. Eur. J. Pharm. Biopharm. 67 (2007) 132–140.

[36] H. Tozaki, T. Fujita, J. Komoike, S. Kim, H. Terashima, S. Muranishi, S. Okabe, A. Yamamoto. Colon-specific delivery of budesonide with azopolymer-coated pellets: therapeutic effects of budesonide with a novel dosage form against 2,4,6,-trinitrobenzensulphonic acid-induced colitis in rats. J. Pharm. Pharmacol. 51 (1999) 257–261.

[37] H. Tozaki, T. Odoriba, N. Okada, T. Fujita, A. Terabe, T. Suzuki, S. Okabe, S. Muranishi, A. Yamamoto. Chitosan capsules for colon specific drug delivery: enhanced

localization of 5-aminosalicylic acid in the large intestine accelerates healing of TNBS-induced colitis in rats. J. Controlled Release 82 (2002) 51–61.

6. METRONIDAZOLE PRODRUGS: SYNTHESIS, PHYSICOCHEMICAL PROPERTIES, STABILITY, AND *EX VIVO* RELEASE STUDIES

(Submitted to European Journal of Medicinal Chemistry)

Abstract

The aim of the present study was to develop a colon targeted delivery system for metronidazole using polymeric prodrug formulation. Two chitosan amide conjugates of metronidazole were prepared by using two different spacers to covalently link the drug to the amino group of the chitosan glucosamine units. Glutaric and succinic hemiesters of metronidazole were thus prepared and then coupled to chitosan to obtain metronidazole-glutaryl- and metronidazole-succinyl-chitosan conjugates. Polymeric prodrugs were characterized by solid state NMR method, namely carbon 13 cross polarization magic angle spinning (^{13}C NMR CPMAS). Prodrug stability study was carried out in acid (pH=1.2) and in alkaline (pH=7.4) buffers in a thermostatic bath at 37°C. Drug release from the two prodrugs was studied by incubating each of them with 10% w/v cecal and colonic content of rats. Obtained results showed that both prodrugs were adequately stable in acid environment, while the succinyl conjugate was more stable than the glutaryl one in alkaline buffer. Both the prodrugs released the drug in cecal and colonic content, showing that the two systems could serve as colon specific delivery systems of metronidazole.

6.1. Introduction

The oral route has always been considered the most convenient way for drug administration. This is supported by several advantages that oral administration shows in comparison with other routes. In particular, high patient acceptance and a high degree of flexibility in dosage form design as well as on dosing. However, oral administration leads to drug absorption along the gastrointestinal tract (GIT) according to the physicochemical properties of the administered drug. This is a drawback when drugs show a preferential site of absorption or when an appropriate concentration is required in a specific portion of the GIT such as the colon is. In these conditions, formulation of a delivery systems capable of reaching the specific site of drug activity is required.

During last decades, the colon has received a great deal of attention in the delivery of drugs for the treatment of local diseases associated with this portion of the GIT but also for its potential for the delivery of proteins and therapeutic peptides

sensitive to the enzymes in both the stomach and small intestine. The proximal or ascendant colon is considered as the optimum site for colon-target delivery of drugs [1]. A variety of approaches have been used to deliver drugs locally to colon. They include: pH dependent, time dependent or enzyme dependent systems [2-4].

Recently, prodrugs in which a drug is covalently bound to a carrier have been proposed as a source of colon targeting [5-7]. Prodrugs usually improve drug physicochemical properties in order to increase the drug concentration at the action site, to prolong the effect, decrease toxicity and undesirable side effects. The prodrug should be stable in the stomach and in the small intestine, non-toxic, biodegradable, and biocompatible. It can be a small molecule (aminoacid, carbohydrate) or a macromolecule (polymers) [8]. The prodrug takes advantage of some specific colon characteristics that make the drug to be released specifically in the last part of the GIT. It is well known that the colon has a large and specific enzyme concentration, which is not present in the rest of the GIT [9,10]. Then a prodrug, which passes unmodified the stomach and the upper intestine, can reach the colon where the drug can be released by the action of the colonic enzymes.

Chitosan (CHT) is a natural and cationic high molecular weight polysaccharide. It is composed of randomly distributed β-(1-4)-linked D-glucosamine (deacetylated unit) and *N*-acetyl-D-glucosamine (acetylated unit). CHT is produced commercially by deacetylation of chitin (60-100%), which is the structural element in the exoskeleton of crustaceans (crabs, shrimp, etc.) and cell walls of fungi. It has favourable biological properties such as biodegradability and biocompatibility. For this reason it has attracted a lot of attention in the pharmaceutical and medical fields [11-17] and several chitosan-based gastrointestinal delivery systems have been prepared [18-23]. CHT is not absorbed in the upper part of the GIT, but it is selectively degraded by some enzymes of the colonic microflora [24-26]. These characteristics make the CHT a suitable carrier for the preparation of a polymeric prodrug [8, 26], generally obtained by linking the drug to CHT through a spacer [15]. Therefore, the prodrug can be prepared by linking the drug to the CHT through an amide bond formed with the amino group on position 2 of the glucosamine units.

In this work, as a model drug, metronidazole (MTZ) was used. MTZ is a nitroimidazole derivative particularly used in the treatment of anaerobic bacteria and Protozoa infections. MTZ is the drug of choice for the treatment of Amoebiasis, an infection of the large intestine caused by *Entamoeba histolytica* [27,28].

The parasite reaches preferentially the colon and causes haemorrhage and ulceration. Therefore, MTZ must be released in the colon to assure its effective activity against the parasite but, after oral administration, it is completely and promptly absorbed. As a result, only a minimal amount of the drug reaches the colon (< 10%) [29,30] and considerable side effects are also induced [31,32].

The aim of this study was to develop a colon targeted delivery system for MTZ using polymeric prodrug formulation. To this purpose, two amide conjugates of CHT and MTZ were synthesized using a succinyl and glutaryl spacer respectively. Different spacers were used to evaluate the influence of the pro-moiety on the physicochemical properties of the prodrugs as well as on their rate of bioconversion to MTZ. Firstly, metronidazole hemiesters (hemisuccinate and hemiglutarate) were synthesized and then coupled with the amino group of the CHT glucosamine units to obtain the amide conjugates.

The hemiester intermediates were characterized by spectroscopic and analytical methods (^{1}H and ^{13}C NMR, IR, and CHNO) while the prodrugs were mainly characterized by solid state NMR (^{13}C NMR CPMAS). *In vitro* prodrug stability and *ex vivo* evaluation of drug release were also carried out.

6.2. Experimental

6.2.1. General Methods

Metronidazole, succinic and glutaric anhydride, 4-dimethylaminopyridine, 1-ethyl-3-(3-dimethylaminopropyl)carbodiimide hydrochloride, chitosan of medium molecular weight and Ultrafree-MC microcentrifuge filters (pore size 30000 Dalton, PLTK cellulosic membrane) were obtained from Aldrich (Milan, Italy). Spectra-Por® dialysis membrane (MWCO 12000-14000 Dalton, regenerated cellulose) was purchased from Spectrum Labs, Inc. (USA). Solvents for HPLC were obtained from Merck (Milan, Italy). All the products and solvents were of analytical grade.

Male Sprague-Dawley rats, weighing 250-275 g were purchased from Charles River (Calco, Italy) and were housed in a temperature- and humidity-controlled room with a 12-h light/dark cycle (light from 7:00 am to 7:00 pm). Animal used in this study were maintained in facilities fully accredited by the American Association for the Accreditation of Laboratory Animal Care and all experimentation was conducted in accordance with the guidelines of the Institutional Care and Use Committee of NIDA, NIH, and of the Guide for Care and Use of Laboratory Animals (National Res. Council, 1996) and the Council of the European Communities (86/809/EEC).

High-resolution liquid ^{1}H NMR experiments were recorded at 25 °C on a Varian Unity Inova spectrometer operating at 300 MHz in DMSO-d_6 using tetramethylsilane (TMS) as internal standard reference. The experiments were carried out with the sample contained in a 5 mm tube using 7 μs pulse (90°), 2 s repetition time, and spectral with of 4 kHz. Solid state NMR spectra were collected using a Varian Unity Inova spectrometer with a 9.39 T wide-bore Oxford magnet. ^{13}C Cross Polarization Magic Angle Spinning (CPMAS) spectra were collected with a probe configured for 4 mm Si_3N_4 rotors. The contact times for cross polarization was 0.5, 1 and 2 ms and recycle time of 2 s. ^{13}C chemical shifts were referenced externally to hexamethylbenzene (CH_3 = 17.4 ppm).

Melting points were carried out in a Köfler apparatus. FTIR spectra were recorded on a Perkin Elmer System 2000 spectrophotometer using KBr mulls. CHNS analyses were carried out on a Fisons model EA 1108 Elemental Microanalyser. Eppendorf centrifuge was used for centrifugation. Thin layer chromatography (TLC) was performed on plates precoated with silica gel 60 F254 (Merck). The amount of MTZ released was assayed by HPLC at 320 nm, using a HP 1100 LC equipped with a Photodiode Array detector 996. The mobile phase consisted of citrate buffer (pH=2.6) : acetonitrile (80:20 v/v) and was filtered through a 0.45 μm membrane filter before use. The mobile phase was eluted at a flow rate of 1 ml/min. The column was a Hypersil ODS 5.0 μm (4.6 x 200 mm, HP). Retention times of MTZ, metronidazole hemisuccinate and hemiglutarate were 4.5, 6.5 and 9.0 min, respectively. Their concentrations in samples were calculated from the calibration curve constructed at the concentration range of 0.02-0.002 mg/ml (correlation coefficients, R^2 between 0.999 and 0.994).

6.*2.2. Chemistry*

6.2.2.1. General procedure for preparation of metronidazole hemiesters (**2-3**)

Hemiesters **2** (MTZ-SUC) and **3** (MTZ-GLU) were obtained according to literature procedures with slight modifications [33]. Briefly, MTZ (11.7 mmol) and succinic or glutaric anhydride (13.7 mmol) were dissolved in 80 ml of acetonitrile. The obtained solutions were stirred at room temperature respectively for 72 or 120 hours in presence of 4-dimethylaminopyridine (DMAP) as catalyst. The reaction was monitored by TLC. The solvent was evaporated in a rotary evaporator to give a residue that was washed three times with 25 ml of hot water (60 °C) and let to crystallize as a white solid powder. The precipitate was filtered off and dried in a P_2O_5 desiccator under vacuum to give the hemiesters (**2-3**).

4-[2-(2-methyl-5-nitro-1H-imidazol-1-yl)ethoxy]-4-oxobutanoic acid (**2**).

Yield: 90%, m.p.: 109 °C. IR (nujol) cm^{-1}: 1746 cm^{-1} (ester, C=O), 1716 cm^{-1} (carboxylic acid C=O), 1538 cm^{-1} (C=N), 1457 and 1377 cm^{-1} (NO_2). ^{1}H NMR (DMSO-d_6) δ (ppm) 2.42 (t, 2H, J=3.3 Hz, H_9), 2.44 (t, 2H, J=3.3 Hz, H_8), 2.46 (s, 3H, H_7), 4.37 (t, 2H, J=5.1 Hz, H_4), 4.57 (t, 2H, J=5.1 Hz, H_5), 8.02 (s, 1H, H_2). ^{13}C NMR (DMSO-d_6) δ (ppm) 14.1 (C_7), 28.8 (C_8), 28.9 (C_9), 44.9 (C_4), 62.5 (C_5), 133.2 (C_2), 138.7-135.4 (C_3) 151.8 (C_1), 172.05 (C_6), 173.52 (C_{10}). CHN: calculated from ($C_{10}H_{13}N_3O_6$) C: 44.28; H: 4.83; N: 15.49; found C: 44.45; H: 4.84; N: 15.44.

5-[2-(2-methyl-5-nitro-1H-imidazol-1-yl)ethoxy]-5-oxopentanoic acid (**3**).

Yield: 60%, m.p.: 102 °C.). IR (nujol) cm^{-1}: 1738 cm^{-1} (ester, C=O), 1719 cm^{-1} (carboxylic acid C=O), 1538 cm^{-1} (C=N), 1470 and 1380 cm^{-1} (NO_2). ^{1}H NMR (DMSO-d_6) δ (ppm) 1.77 (m, 2H, J=7.2 Hz, H_9), 2.31 (t, 2H, J=7.5 Hz, H_8), 2.39 (t, 2H, J=7.5 Hz, H_{10}), 2.57 (s, 3H, H_7), 4.49 (t, 2H, J=4.8 Hz, H_4), 4.69 (t, 2H, J=4.8 Hz, H^5), 8.14 (s, 1H, H_2), 12.22 (s, 1 H, OH). ^{13}C NMR (DMSO-d_6) δ (ppm) 14.0 (C_7), 19.8 (C_9), 32.5 (C_8), 32.6 (C_{10}) 44.8 (C_4), 62.2 (C_5), 133.1 (C_2), 138.6 (C_3) 151.6 (C_1), 172.2 (C_6), 174.0 (C_{11}). CHN: calculated from ($C_{11}H_{15}N_3O_6$) C: 46.32; H: 5.30; N: 14.73; found C: 46.46; H: 5.28; N: 14.74.

6.2.2.2. General procedure for preparation of metronidazole-spacer-chitosan conjugates (**4**, **5**)

Metronidazole-succinyl-chitosan (MTZ-SUC-CHT, **4**) and metronidazole-glutaryl-chitosan (MTZ-GLU-CHT, **5**) amide conjugates were prepared by coupling CHT with carboxyl groups of the hemiesters **2** or **3**. Each hemiester (**2** or **3**, 1 mmol) were dissolved in 10 ml of acetonitrile and 1-ethyl-3-(3-dimethlaminopropyl) carbodiimide hydrochloride (EDAC, 1.25 mmol) was added. The reaction mixture was stirred at room temperature for 2 hours to activate the carboxyl group of **2** or **3**, then a CHT solution (1 mmol in 15 ml of 5% acetic acid) was slowly added. The reaction was left under stirring at room temperature for 5 days. Part of the solvent was then removed under vacuum and the residue was dialyzed against distilled water for 48 hours. Finally the amide conjugates **4** and **5** were obtained as slightly yellow cotton-like powders by freeze-drying the dialyzed solution.

2-(2-methyl-5-nitro-1H-imidazol-1-yl)ethyl]-4-(2-chitosan)-4-oxobutanoate (**4**).

Yield: 50%. IR (KBr mull) cm^{-1}: 3423 cm^{-1} (NH_2 and OH), 1731 cm^{-1} (ester C=O), 1651 cm^{-1} (amide I) 1558 cm^{-1} (amide II), 1155 cm^{-1}, 1067 cm^{-1}, 897 cm^{-1} (chitosan sugar structure). ^{13}C CPMAS NMR (ppm): 15.8 (C_8-CHT), 31.5-22.5 (C_7-, C_8-, C_9-MTZ-SUC), 49.0 (C_2-CHT), 52,1 (C_6-CHT), 68.2 (C_3-, C_5-CHT), 73.2 (C_4-CHT), 95.5 (C_1-CHT), 165.0-175.0 (C_7-CHT, C_6-, C_{10}-MTZ-SUC).

2-(2-methyl-5-nitro-1H-imidazol-1-yl)ethyl]-5-(2-chitosan)-5-oxopentanoate (**5**)

Yield: 45%). IR (KBr mull) cm^{-1}: 3423 cm^{-1} (NH_2 and OH), 1731 cm^{-1} (ester C=O), 1651 cm^{-1} (amide I) 1557 cm^{-1} (amide II), 1157 cm^{-1}, 1067 cm^{-1}, 897 cm^{-1} (chitosan sugar structure). ^{13}C CPMAS NMR (ppm): 15.8 (C_8-CHT), 35.0-20.0 (C_7-, C_8-, C_9-, C_{10}-MTZ-GLU), 49.6 (C_2-CHT), 52,7 (C_6-CHT), 68.0 (C_3-, C_5-CHT), 72.8 (C_4-CHT), 94.5 (C_1-CHT), 166.5 (C_7-CHT), 173.5 (C_6-, C_{11}-MTZ-GLU).

6.2.3. Determination of drug content in conjugates

Drug content was determined following alkaline hydrolysis of the conjugates.

Each conjugate (10 mg) was added to 10 ml borate buffer (pH=9.5) [34] and stirred at 50 °C for 48 hours. An aliquot of the solution (0.4 ml) was then placed in an

Ultrafree-MC centrifugal filter tube with Ultrafiltration membrane (30000 Dalton) to separate the MTZ solution from the polymer. MTZ content in the purified solutions was assayed by HPLC as reported above.

6.2.4. Stability studies

The conjugate stability was checked in two different media: acid (pH=1.2) and alkaline (pH=7.4) buffers [34] in a thermostatic bath at 37 °C. 10 mg of each conjugate were placed in a membrane dialysis bag; which was closed and transferred into a flask containing 40 ml of the buffer solution. The external solution was continuously stirred and the system was maintained at 37 °C for 24 hours. At appropriate time intervals, 1 ml solution was removed from the external solution and replaced with the same buffer. 20 μL of the withdrawn solution was assayed by HPLC as reported above to determine the percentage of the released drug.

6.2.5. Drug release studies

Rats were anaesthetized by chloral hydrate (300 mg/Kg ip), the abdomen was opened and the cecum and colon were traced, legated at both ends, dissected and immediately transferred into pH=7.4 buffer. Part of the cecal and colonic bags was immediately used for the experiment (content **A**) while another part of the cecal and colonic bags was frozen and stored at -80 °C (content **B**).

The cecal or colonic bags were opened and their contents were individually weighted, pooled, and then suspended in the buffer to give 10% w/v dilution. The release studies were performed by incubating each conjugate or hemiester with a 10% w/v cecal and colonic content of rats. These studies were carried out using both cecum and colon contents **A** and **B**. 5 mg of each conjugate were added to 5 ml of the 10% w/v suspension of cecal and colonic contents (**A** or **B)** and the mixture was stirred and incubated at 37 °C under N_2 flow to maintain the anaerobic condition as the cecum and the colon are naturally anaerobic. At appropriate time intervals, 0.5 ml of the suspension were withdrawn, diluted to 1 ml with buffer and centrifuged at 5000 rpm for 3 minutes. To 0.2 ml portion of the supernatant, 0.8 ml of methanol

were added to precipitate the protein, vortexed for 2 minutes and centrifuged at 10260 rpm for 5 minutes.

The concentration of MTZ was determined in 20 μL of the supernatant by HPLC as described above. Each experiment was carried out in triplicate.

6.2.6. Statistical analysis

Data analysis was carried out with the software package R, version 2.10.1. Results are expressed as the mean ± standard deviation (S.D.). Multiple comparisons of means (Tukey test) were used to substantiate statistical differences between groups, while Student's t-test was used for comparison between two samples. Significance was tested at the 0.05 level of probability (p).

6.3. Results and discussion

6.3.1. Chemistry

In this work, two MTZ-spacer-CHT amide conjugates were studied as potential colon specific prodrugs of MTZ. Preparation of the conjugates was achieved as shown in Scheme 1 and 2.

The first step (Scheme 1) consisted in the synthesis of the metronidazole hemisuccinate (**2**) and hemiglutarate (**3**). This process was performed to introduce a carboxyl, essential group for coupling the drug to the CHT [33].

Then, in a second step (Scheme 2) activation of the hemiester carboxyl group was achieved by coupling it with the water soluble 1-ethyl-3-(3-dimethylaminopropyl)carbodiimide hydrochloride (EDAC) [35].

EDAC was chosen because CHT is insoluble in all the organic solvents and it just dissolves in water only at acidic pH. Moreover, it is stable in water and mostly used to form an amide bond for peptide synthesis. After the activation of the carboxyl group, a solution of CHT in 5% acetic acid was added and the mixture was stirred for 5 days to obtain the respective MTZ-spacer-CHT conjugate **4** and **5**.

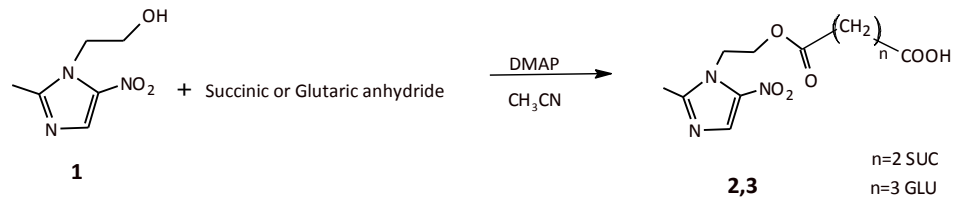

Scheme 1. Synthesis of metronidazole hemiesters 2 and 3

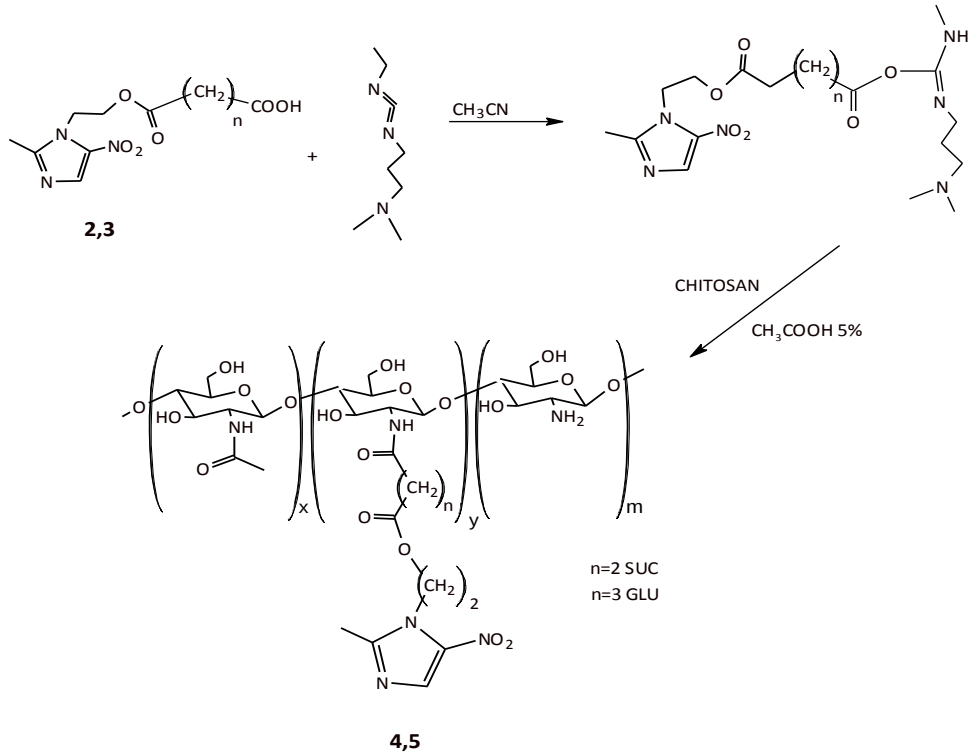

Scheme 2. Synthesis of metronidazole-spacer-chitosan conjugates (4 - 5)

The hemiester intermediates and the conjugates were spectroscopically and analytically characterized to confirm their structures.

Main information on the interaction between metronidazole hemiesters and chitosan were obtained from analysis with solid state NMR method, namely carbon 13 cross polarization magic angle spinning (^{13}C NMR CPMAS). In figure 1, as an example, the ^{13}C CPMAS spectra for the commercial CHT (a), MTZ-GLU (b) and MTZ-GLU-CHT(c) are reported since following discussion will focus only on these

compounds while assignments for products **2** and **4** are shown in the experimental section.

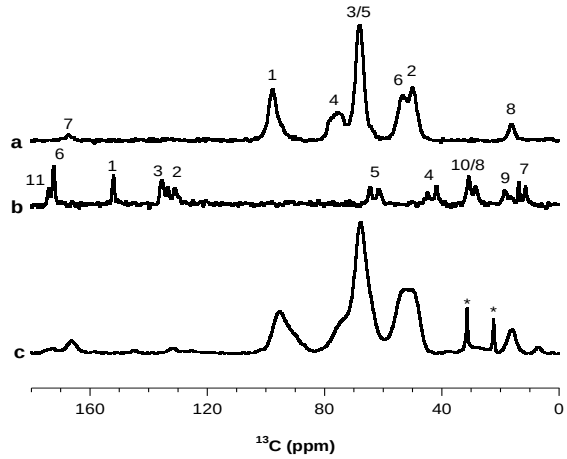

Figure 1. ^{13}C CPMAS NMR spectra for (a) CHT, cntct 2ms; (b) MTZ-GLU, cntct 2ms; (c) MTZ-GLU-CHT, cntct 0.5ms; *experimental artefacts [41].

For the sake of clarity, in the figure 2, glucosamine, acetylglucosamine repetitive units (~ 15%), and MTZ-GLU structure are also sketched with the used labeling of C atoms. The attribution of CHT carbons was made by comparison with literature data [36].

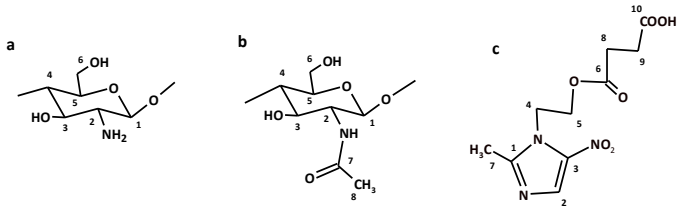

Figure 2. Schematic representation of glucosamine (a), acetylglucosamine (b), and hemiester MTZ-GLU 3 (c) with the used labeling of C atoms.

At 97.6 ppm, the resonance of anomeric carbon C1 of the glucosamine unit is observed. At 167.3 ppm and 16.4 ppm, weak resonances, respectively due to the carbonyl C7 and to methyl C8 of the N-acetylglucosamine units, are noticed. These signals, C7 and C8, are visible despite the fact that the N-acetylglucosamine is only 15% of the polymeric molecule, because the cross-polarization (CP) efficiency

depends strongly on the internuclear distance of the two involved nuclei as well as on their mobility, and also because usually the signal intensity does not provide quantitative information [37,38]. Thus, C6 resonates at 53.3 ppm while the nearby resonance at 49.6 ppm is due to C2. At 68.1 ppm, a set of overlapped resonances is due both to C3 and C5. In the frequency range 73-78 ppm, the resonance due to C4 is split in different peaks. Splittings in the order of 1-2 ppm, observed in carbon resonances, may be ascribed either to differences in the polymeric chain packing or to different internal torsion angles. In this case, the observed splittings are possibly due to both effects. In fact, the resonance of C4 is sensitive to the ω torsion angle while it is also well known that CHT exhibits polymorphism [39]. The ^{13}C NMR CPMAS spectrum for MTZ-GLU is reported in figure 1b. The attribution of the carbon resonance was made by comparison with the ^{13}C NMR spectrum in liquid state.

Table 1. ^{13}C CPMAS chemical shifts of CHT, ^{13}C NMR and ^{13}C CPMAS NMR chemical shifts of MTZ-GLU (3)

Carbon CHT (see fig. 2b)	^{13}C CPMAS NMR (ppm)	Carbon MTZ-GLU (see fig. 2c)	^{13}C NMR (ppm)	^{13}C CPMAS NMR (ppm)
1	97.6	**1**	151.6	152.0
2	49.6	**2**	133.1	131.4
3/5	68.1	**3**	138.6	135.6/134.1
4	75.5	**4**	44.8	44.9/41.7
6	53.3	**5**	62.2	64.4/61.2
7	167.3	**6**	172.2	172.1
8	16.4	**7**	14.0	13.7/11.6
		8	32.5	31.1/28.5
		9	19.8	19/16.8
		10	32.6	31.1/28.5
		11	174.0	174.2

Table 1 shows the ^{13}C CPMAS NMR signals assigned to CHT and MTZ-GLU as well as the ^{13}C NMR chemical shifts for MTZ-GLU in the liquid state. In the ^{13}C CPMAS NMR of the MTZ-GLU, seven out of eleven carbon resonances show evidence of fine structure in the form of splitting. This suggests the presence of two

environments for these carbon sites and reflects the existence of two conformations. In the liquid state, this cannot be observed because rapid motions remove dipolar and quadrupolar couplings as well as average anisotropic value so that most of the information contained in these spin interaction is lost [40].

Table 2. ^{13}C CPMAS NMR chemical shifts and respective attributions to MTZ-GLU-CHT carbons.

Carbon MTZ-GLU-CHT (ppm) (see fig. 1c)	Attributions
173.5	C6/11 MTZ-GLU
166.5	C7 CHT
144.9	C1 MTZ-GLU
131.9	C2/3 MTZ-GLU
94.5	C1 CHT
49.6	C2 CHT
68.0	C3/5 CHT
72.8	C4 CHT
52.7	C6 CHT
35.0-20.0	C7/8/9/10 MTZ-GLU
15.8	C8 CHT

The ^{13}C CPMAS NMR spectrum of the sample MTZ-GLU-CHT is shown in figure 1c. As can be seen, the presence of CHT is clear, but the signals are broad in comparison to the pure polymer (~1 ppm). This is the consequence of the MTZ-GLU that is bounded to CHT thus creating a structural disorder in the polymer [41]. The evidence of MTZ-GLU conjugation to chitosan is given by the spectrum that also demonstrates the resonance of the MTZ-GLU carbons: at 173.5 ppm, resonance corresponding to the C6 and C11 carbonyl are observed while the broad signals at 131.9 ppm are due to the C2/3. As can be seen in the figure 1c, in the range between 20-35 ppm, below the two sharp spikes (marked with an asterisk since they are experimental artifacts, i.e. rotor frequency lines) [42], weak overlapped signals are present, which can be probably due to the chemical shift of carbons C7, C8, C9 and C10 of the MTZ-GLU. In table 2 chemical shifts and their corresponding attributions to MTZ-GLU-CHT carbons are reported.

Therefore, these analyses confirmed that MTZ was linked to the amino group of the CHT glucosamine units through a succinyl or glutaryl spacer, which was linked to the drug and to the polymer by an ester and an amide bond, respectively. Both these bonds are susceptible to hydrolysis by amidase and esterase enzymes present in the colonic microflora, thus causing the drug release in the colon.

The drug loading was studied by HPLC determination after alkaline hydrolysis of the prodrugs **4** and **5**. Obtained results indicated that 10 mg of the MTZ-SUC-CHT prodrug contained 1.5 ± 0,01 mg of MTZ, while 10 mg of MTZ-GLU-CHT prodrug contained 1.05 ± 0.06 mg of MTZ. Therefore, a loading efficiency of 17.65 and 11.75% respectively was achieved.

6.3.2. Stability studies

Colon-targeting prodrugs have to survive passage through stomach and small intestine as an intact form to reach the colon, where they have to be degraded by the enzymes of the colonic microflora. Therefore, to have information on the prodrug behaviour in acidic and alkaline environment, the prodrug stability was studied *in vitro* in acid and basic buffers. In fact, on the basis of their chemical structures, both ester and amide bond of the prodrugs are susceptible to hydrolysis. Therefore, following incubation in different buffer solutions, the drug and the hemiesters could be released. In order to evaluate the stability of the prodrugs, the amount of MTZ and hemiesters released from the prodrugs **4** and **5** were quantified during 24 hours experiments. In particular, the *in vitro* stability study was carried out at pH=1.2 and pH=7.4. Results are shown in Figure 3.

As can be seen, the prodrug **4** was adequately stable at both acidic (Fig. 3a) and basic pH (Fig. 3b). Indeed, a similar small amount of hemiester **2** and MTZ (≅20%) was released after 8 hours, thus showing no difference between ester and amide bond stability in both tested media.

On the contrary, the prodrug **5** showed a different behaviour: it was adequately stable (as the prodrug **4**) at acid pH (Fig. 3a) for the first two hours but its stability decreased at pH 7.4 (Fig. 3b). After 6 hours (when the conjugate is supposed to

reach the colon), more than 40% of hemiester **3** and only less than 16% of MTZ were released (Fig. 3b).

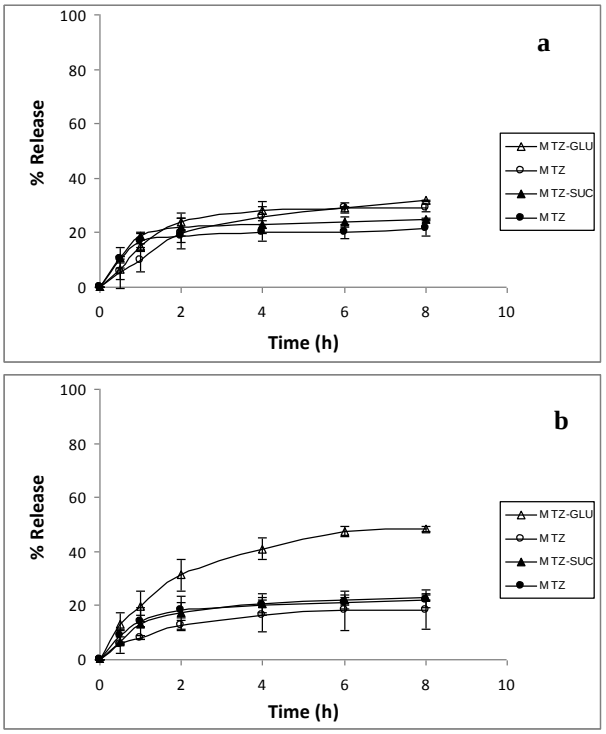

Figure 3. Stability studies of prodrugs 4 and 5 in acid (pH=1.2) and alkaline (pH=7.4) buffers at 37°C: a) buffer at pH 1.2; b) buffer at pH 7.4. Error bars represent standard deviation, *n* =3.

Therefore, in this case the hydrolysis rate of the ester and amide bonds was different: results clearly show that the amide bond was hydrolysed faster than the ester one when the spacer was the glutaryl moiety. Hence, outcomes of this stability study show that length of the spacer affects the amide bond stability especially in alkaline environment. Indeed, comparison of results obtained with succinyl and glutaryl moieties indicates that the longer the spacer chain the higher the hydrolysis rate of the prodrug in alkaline buffer.

6.3.3. Drug release studies

In order to verify the actual capability of the prodrugs **4** and **5** to release the drug into the target area [43], an *ex vivo* release study was carried out using cecum and

colon contents **A** (immediately used) and **B** (previously frozen and stored at -80 °C). Figure 4 shows comparison of the results obtained from prodrugs **4** and **5** in the release experiments with both cecum and colon contents **A**.

As can be seen, in the presence of both cecum and colon contents, the prodrug **4** released very small amount of both MTZ and hemiester **2**, especially in colon. In fact, the amount of MTZ and **2** increased only up to about 15% (cecum) and 5% (colon) in the first 30 minutes of the experiments to decrease and disappear after 4 and 2 hours in cecum and colon, respectively. However, it is well known that MTZ is metabolized in the colon: *N*-(2-hydroxyethyl)-oxamic acid [44] and acetamide [45] are formed when the drug is reduced as a result of the colonic anaerobic bacteria activity.

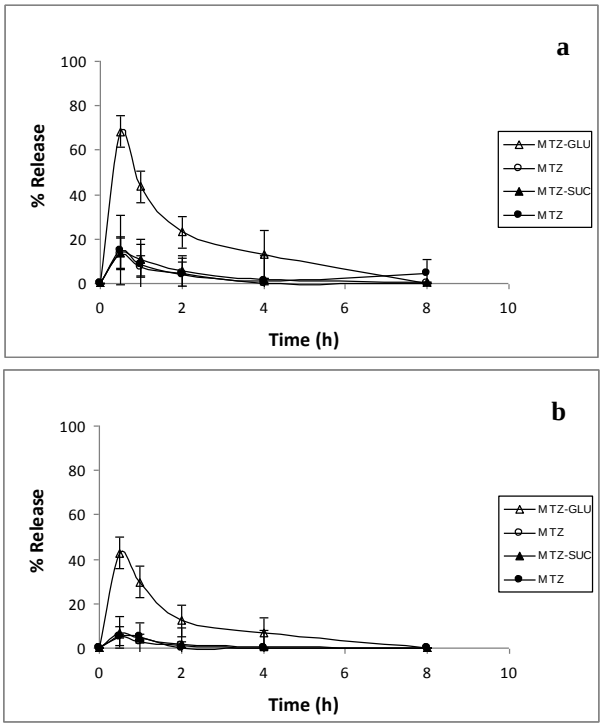

Figure 4. Cumulative release of 1 (MTZ), 2 (MTZ-SUC) and 3 (MTZ-GLU) from prodrugs 4 and 5 during incubation with fresh contents A of cecum (a) and colon (b) at 37°C. Error bars represent standard deviation, *n* =3.

Therefore, these results could be the consequence of a very fast metabolic process that involves the released MTZ in the last portions of the GIT content. Incubation of

prodrug **5** with both cecum and colon content **A** led to a similar release profile but, in this case, the maximum amount of released hemiester **3** was much greater than MTZ (≅ 68% in cecum and ≅ 42% in colon). This result could be due to a slower hydrolysis process of this hemiester in the presence of both cecum (Fig. 4a) and colon (Fig. 4b) content **A.**

Different results were obtained when the release study was carried out in cecum and colon content **B** (Fig. 5).

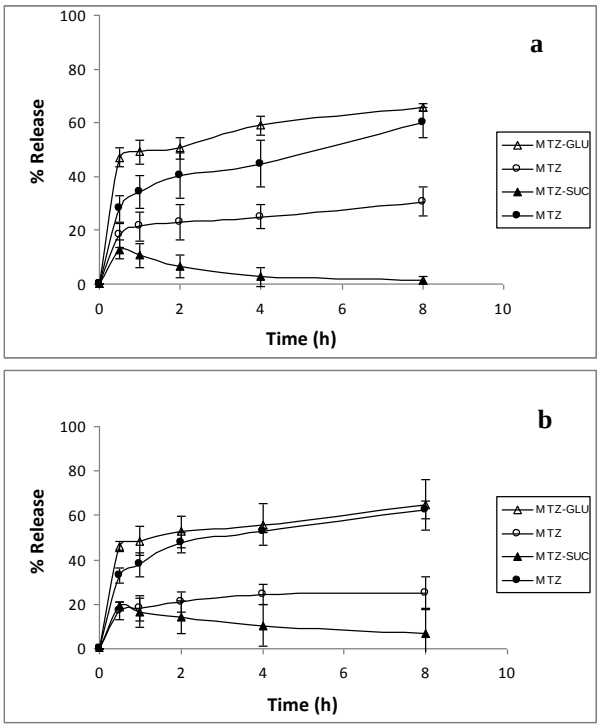

Figure 5. Cumulative release of 1 (MTZ), 2 (MTZ-SUC) and 3 (MTZ-GLU) from prodrugs 4 and 5 during incubation with frozen contents B of cecum (a) and colon (b) at 37°C. Error bars represent standard deviation, *n* =3.

In fact, after 30 minutes from the starting of the experiments with cecum content (Fig. 5a), the prodrug **4** released a maximum amount of 13% of hemiester **2** that rapidly decreased. On the contrary, increasing amount (up to 60%) of MTZ were released during the experiments. A similar release profile was obtained also in the colon content (Fig. 5b).

A different behaviour was shown by the prodrug **5** in both **B** contents. Just after 30 minutes from the starting of the experiments, approximately 45% of the corresponding hemiester **3** was released and its amount increased up to more than 60% at the end of the study in both cecum and colon content. The amount of released MTZ, on the contrary, was lower (30% in cecum, 25% in colon) even than that released from the prodrug **4** thus confirming the hypothesis of a slower conversion of the hemiester **3** in comparison with the **2** one (Fig. 7).

Therefore, overall results of the release experiments from the hemiesters **2** and **3** showed a reduced release process in media **B** in comparison to media **A** and they led us to suppose that the freezing procedure had reduced the activity of some enzymes [46,47].

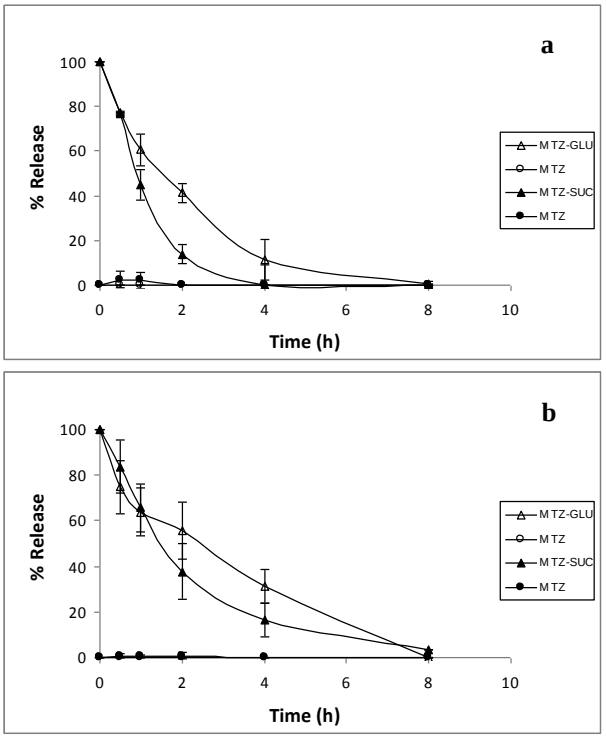

Figure 6. Metronidazole (MTZ) release and 2 (MTZ-SUC) and 3 (MTZ-GLU) disappearance during incubation of hemiesters 2 and 3 with freshly prepared contents A of cecum (a) and colon (b) at 37°C. Error bars represent standard deviation, *n* =3.

To verify the hypothesis of a different susceptibility to enzymatic hydrolysis of the amide and ester bonds, the drug release from the hemiesters **2** and **3** was also

studied. Results obtained in the presence of fresh cecum and colon content **A** are shown in Figure 6.

As can be seen, neither in cecum (Fig. 6a) nor in colon (Fig. 6b) MTZ was appreciably detected while the two hemiesters underwent hydrolysis and progressively disappeared. Therefore, the observed degradation of the two hemiesters confirms that the released MTZ is metabolized in the colon.

On the contrary, when the studies were performed with frozen contents **B,** MTZ could be quantified (Fig. 7) and degradation of the two hemiesters **2** and **3** occurred much more slowly than in fresh cecum and colon contents.

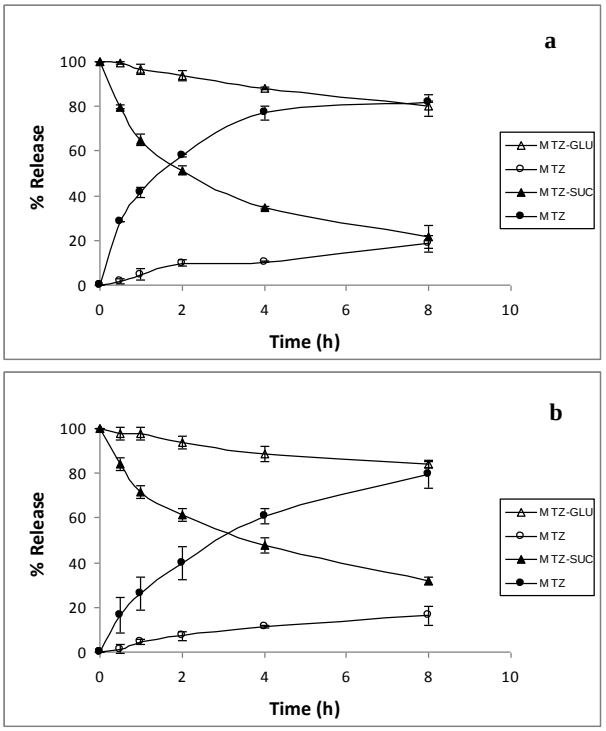

Figure 7. Metronidazole (MTZ) release and 2 (MTZ-SUC) and 3 (MTZ-GLU) disappearance during incubation of hemiesters 2 and 3 and with frozen contents B of cecum (a) and colon (b) at 37°C. Error bars represent standard deviation, *n* =3.

In particular, in both cecum and colon (Fig. 7) a good correlation between the hemiester disappearance and drug release could be found. Indeed, in cecum at the end of the experiments, ≅ 80% of hemiester **2** was hydrolyzed thus leading to ≅ 80%

of delivered MTZ while only ≅ 20% of hemiester **3** was degraded with a corresponding release of MTZ in the medium.

However, comparison of the figures 6 and 7 shows some differences in the behaviour of the two hemiesters. In fact, although the compounds **2** and **3** were rapidly converted to MTZ with both contents **A,** the enzymatic hydrolysis of **2** was a little bit faster than that of **3** especially in cecum where the hemiester **2** disappeared after only 4 hours. In addition, for both prodrugs **2** and **3,** the conversion rate was slightly faster in cecum content (Fig. 6a) than in that of colon (Fig. 6b) and MTZ was not detected in both systems **A**. When treated with both frozen contents **B**, the hemiester **2** showed again a MTZ release faster in cecum content (Fig. 7a) than in the colon one (Fig. 7b) while the hemiester **3** was very slowly converted to MTZ in both media (Fig. 7a-b). Furthermore, release experiments from the hemiesters confirmed a reduced release process in media **B** in comparison to media **A** and further support the hypothesis of a reduced activity of some enzymes as a consequence of the freezing procedure [46,47]. Nevertheless, the experiments in media **B** were useful to demonstrate the actual MTZ release in cecum and colon content from both prodrugs. In fact, when contents **A** (immediately used) were used the drug release rate was faster than in contents **B** as shown by the faster disappearance of MTZ-SUC and MTZ-GLU. However, in contents **A**, MTZ was metabolized and could not be detected. When the previously frozen contents **B** were tested, MTZ was detected thus showing that the drug was released both in cecum and colon contents.

In summary, results of these *ex vivo* experiments showed no substantial differences in the release behaviour of the two prodrugs in cecum and colon content: in both cases the hemiester conversion is slightly faster in the cecum than in the colon although a higher stability of the prodrug **5** can be observed in both media. Therefore, results obtained in this work show that both prodrugs can be potential colon specific delivery systems for MTZ since the prodrug **4** is able to give a fast and complete drug release by enzymatic hydrolysis in cecum and colon. On the other side, the slower conversion rate of the prodrug **5** could be useful for both delayed and sustained MTZ release.

6.4. Conclusion

In conclusion, the prepared prodrugs were adequately stable at acidic pH (pH=1.2) while the prodrug **5** was more sensitive to the alkaline hydrolysis than prodrug **4**. However, both **4** and **5** conjugates demonstrated their capability to release MTZ in the content of the cecum and the colon, showing that these compounds are susceptible to enzymatic hydrolysis although the glutaryl prodrug **5** showed slower drug release profiles. For this reason, both MTZ-SUC-CHT and MTZ-GLU-CHT seem to be suitable prodrugs for the development of a colonic drug delivery system for MTZ: the prodrug **4** could be used as a delayed drug delivery system while the second one (5) could guarantee a sustained drug release.

6.5. References

[1] J.F. Pinto. Site-specific drug delivery systems within the gastro-intestinal tract: from the mouth to the colon. Int. J. Pharm. 395 (2010) 44-52.

[2] P. Kumar, B. Mishra. Colon targeted drug delivery systems. An overview. Curr. Drug Deliv. 5 (2008) 186-198.

[3] M.K. Chourasia, S.K. Jain. Pharmaceutical approaches to colon targeted drug delivery systems. J. Pharm. Pharm. Sci. 6 (2003) 33-66.

[4] V.R. Sinha, R. Kumria. Polysaccharides in colon-specific drug delivery. Int. J. Pharm. 224 (2001) 19-38.

[5] M. Zou, H. Okamoto, G. Cheng, X. Hao, J. Sun, F. Cui, K. Danjo. Synthesis and properties of polysaccharide prodrugs of 5-aminosalicylic acid as potential colon-specific delivery systems. Eur. J. Pharm. Biopharm. 59 (2005) 155–160.

[6] Y. Jung, H. Kim, H. Kim, H. Kong, B. Choi, Y. Yang, Y. Kim. Evaluation of 5-aminosalicyltaurine as a colon-specific prodrug of 5-aminosalicylic acid for treatment of experimental colitis. Eur. J. Pharm. Sci. 28 (2006) 26-33.

[7] J. Varshosaz, J. Emami, N. Tavakoli, A. Fassihi, M. Minaiyan, F. Ahmadi, F. Dorkoosh. Synthesis and evaluation of dextran–budesonide conjugates as colon specific prodrugs for treatment of ulcerative colitis. Int. J. Pharm. 365 (2009) 69-76.

[8] K. Hoste, K. De Winne, E. Schacht. Polymeric prodrugs. Int. J. Pharm. 277 (2004) 119–131.

[9] V.R. Sinha, R. Kumria. Microbially triggered drug delivery to the colon. Eur. J. Pharm. Sci. 18 (2003) 3-18.

[10] T. Sousa, R. Paterson, V. Moore, A. Carlsson, B. Abrahamsson, A.W. Basit. The gastrointestinal microbiota as a site for the biotransformation of drugs. Int. J. Pharm. 363 (2008) 1-25.

[11] N. Bhattarai, J. Gunn, M. Zhang. Chitosan-based hydrogels for controlled, localized drug delivery. Adv. Drug Deliv. Rev. 62 (2010) 83–99.

[12] V.K. Mourya, N.N. Inamdar. Chitosan-modifications and applications: Opportunities galore. React. Funct. Polym. 68 (2008) 1013–1051.

[13] J. Vinsova, E. Vavrikova. Recent advances in drugs and prodrugs design of chitosan. Curr. Pharm. Des. 14 (2008) 1311-1326.

[14] J. Berger, M. Reist, J. M. Mayer, O. Felt, R. Gurny. Structure and interactions in chitosan hydrogels formed by complexation or aggregation for biomedical applications. Eur. J. Pharm. Biopharm. 57 (2004) 35–52.

[15] J.H. Park, G. Saravanakumar, K. Kim, I.C. Kwon. Targeted delivery of low molecular drugs using chitosan and its derivatives. Adv. Drug Delivery Rev. 62 (2010) 28–41.

[16] V.R. Sinha, A.K. Singla, S. Wadhawan, R. Kaushik, R. Kumria, K. Bansal, S. Dhawan. Chitosan microspheres as a potential carrier for drugs. Int. J. Pharm. 274 (2004) 1–33.

[17] Y. Kato, H. Onishi, Y. Machida. N-succinyl-chitosan as a drug carrier: water-insoluble and water-soluble conjugates. Biomaterials 25 (2004) 907–915.

[18] R. Hejazi, M. Amiji. Chitosan-based gastrointestinal delivery systems. J. Controlled Release 89 (2003) 151–165.

[19] Y. Xu, C. Zhan, L. Fan, L. Wang, H. Zheng. Preparation of dual crosslinked alginate–chitosan blend gel beads and in vitro controlled release in oral site-specific drug delivery system. Int. J. Pharm. 336 (2007) 329–337.

[20] H. Tozaki, T. Odoriba, N. Okada, T. Fujita, A. Terabe, T. Suzuki, S. Okabe, S. Muranishi, A. Yamamoto. Chitosan capsules for colon-specific drug delivery: enhanced localization of 5-aminosalicylic acid in the large intestine accelerates healing of TNBS-induced colitis in rats. J. Controlled Release 82 (2002) 51-61.

[21] K. Mladenovska, R.S. Raicki, E.I. Janevik, T. Ristoski, M.J. Pavlova, Z. Kavrakovski, M.G. Dodov, K. Goracinova. Colon-specific delivery of 5-aminosalicylic acid from chitosan-Ca-alginate microparticles. Int. J. Pharm. 342 (2007) 124–136.

[22] M.P. Patel, R.R. Patel, J.K. Patel. Chitosan mediated targeted drug delivery system: a review. J. Pharm. Pharm. Sci. 13 (2010) 536-557.

[23] M.N.V. Ravi Kumar, R.A.A. Muzzarelli, C. Muzzarelli, H. Sashiwa, A.J. Domb. Chitosan Chemistry and Pharmaceutical Perspectives. Chem. Rev. 104 (2004) 6017-6084.

[24] H. Zhang, S.H. Neau. In vitro degradation of chitosan by bacterial enzymes from rat cecal and colonic contents. Biomaterials 23 (2002) 2761–2766.

[25] C.L. Vernazza, G.R. Gibson, R.A. Rastall. In vitro fermentation of chitosan derivatives by mixed cultures of human faecal bacteria. Carbohydr. Polym. 60 (2005) 539–545.

[26] O. Felt, P. Buri, R. Gurny. Chitosan: a unique polysaccharide for drug delivery. Drug Dev. Ind. Pharm. 24 (1998) 979-993.

[27] C.D. Freeman, N.E. Klutman, K.C. Lamp. Metronidazole. A therapeutic review and update. Drugs 54 (1997) 679-708.

[28] S.L. Stanley. Amoebiasis. Lancet 361(9362) (2003) 1025-1034.

[29] A.H. Lau, N.P. Lam, S.C. Piscitelli, L. Wilkes, L.H. Danziger. Clinical pharmacokinetics of metronidazole and others nitroimidazole anti-infectives. Clin. Pharmacokinet. 23 (1992) 328-364.

[30] K.C. Lamp, C.D. Freeman, N.E. Klutman, M.K. Lacy. Pharmacokinetics and pharmacodynamics of the nitroimidazole antimicrobials. Clin. Pharmacokinet. 36 (1999) 353-373.

[31] W. Schreiber, J. Spernal. Metronidazole-induced psychotic disorder. Am. J. Psychiatry 154 (1997) 1170-1171.

[32] S Knowles, T Choudhury, N Shear. Metronidazole hypersensitivity, Ann. Pharmacother. 28 (1994) 325-326.

[33] S. Vermeersch, F. Vandoorne, D. Permentier, E. Schacht. Macromolecular prodrugs of metronidazole. Esterification of hydroxyl containing polymers with metronidazole monosuccinate. Bull. Soc. Chim. Belg. 94 (1985) 591-596.

[44] United States Pharmacopeia (USP 31, NF 26) Printed in the U.S. by Port City Press, Baltimore, 1 (2008) 814.

[35] Y. Kato, H. Onishi, Y. Machida. A novel water soluble N-succinyl-chitosan- mitomycin C conjugate prepared by direct carbodiimide coupling: physicochemical properties, antitumor characteristics and systemic retention. S. T. P. Pharm. Sci. 10 (2000) 133-142.

[36] A.A. De Angelis, D. Capitani, V. Crescenzi. Synthesis and ^{13}C CP-MAS NMR characterization of a New Chitosan-Based Polymeric Network. Macromolecules 31 (1998) 1595-1601.

[37] H-M. Kao, L-P. Lee, A. Palani. ^{13}C CPMAS NMR Spectroscopy as a Versatile and Quantitative Tool for Determination of Mercury Adsorption Capacity in Thiol-Functionalized. Mesoporous Silica SBA-1. Anal. Chem. 80 (2008) 3016-3019.

[38] V.V. Crescenzi, A. Francescangeli, A.L. Segre, D. Capitani, L. Mannina, D. Renier, D. Bellini. NMR Structural Study of Hydrogels Based on Partially Deacetylated Hyaluronan. Macromol. Biosci. 2 (2002) 272–279.

[39] S.M. Takai, Y. Shimizu, J. Hayashi, Y. Uraki, S. Tokura. NMR and Xray studies of chitin and chitosan in solid state, Chitin and Chitosan: Sources, Chemistry, Biochemistry, Physical Properties and Application; G. Skjak-Braek, T. Anthonsen, P. Sanfort. Eds, Elsevier Applied Science, New York (1989).

[40] J.G. Hexem, M.H. Frey, S.J. Opella. 13C NMR of Crystalline Morphine. J. Am. Chem. Soc. 105 (1983) 5717-5719.

[41] P. Agrawal, S. Kiihne, J. Hollander, D. Langosch, H. de Groot. ^{13}C and ^{15}N NMR evidence for peripheral intercalation of uniformly labeled fusogenic peptides incorporated in a biomimetic membrane. Biochim. Biophys. Acta 1768 (2007) 3020–3028.

[42] E.T. Olejniczak, J.E. Roberts, S. Vega, R.G. Griffin. Rotor frequency lines in multiple-pulse/magic-angle sample spinning NMR spectra. J. Magn. Reson. 56 (1984) 156-162.

[43] D. Kim, S. Hong, S. Jung, Y. Jung, Y.M. Kim. Synthesis and evaluation of N-nicotinoyl-2-[2-(2-methyl-5-nitroimidazol-1-yl)ethyloxy]-D,L-glycine as a colon specific prodrug of metronizole. J. Pharm. Sci. 98 (2009) 4161-4169.

[44] L. Koch, P. Goldman. The anaerobic metabolism of metronidazole forms N-(2-hydroxyethyl)-oxamic acid. J. Pharmacol. Exp. Ther. 208 (1979) 406-410.

[45] L Koch, E.J.T. Chrystal, B.B. Beaulieu, J.P. Goldman. Acetamide: a metabolite of metronidazole formed by the intestinal flora. Biochem. Pharmacol. 28 (1979) 3611-3615.

[46] E. Hajduk. Changes in some enzyme activities and DNA content in frozen stored and freeze-dried bovine thymus. Food Chem. 66 (1999) 235-239.

[47] S. Jiang, S.L. Nail. Effect of process conditions on recovery of protein activity after freezing and freeze-drying. Eur. J. Pharm. Biopharm. 45 (1998) 249-257.

7. METRONIDAZOLE-SUCCINYL-CYCLODEXTRIN ESTER AS COLON SPECIFIC PRODRUGS: SYNTHESIS, CHARACTERIZATION AND *EX VIVO* RELEASE STUDIES

7.1. Introduction

Native cyclodextrins (CDs) are cyclic oligosaccharides consisting of six (α-cyclodextrin), seven (β-cyclodextrin), eight (γ-cyclodextrin) glucopyranose units linked by β-(1,4) bonds [1]. They have been widely used in pharmaceutical field because of their ability to alter physical, chemical, and biological properties of guest molecules through the formation of inclusion complexes. Recently, various kinds of CD derivatives have been prepared so as to extend the physicochemical properties and inclusion capacity of natural CDs as novel drug carriers [2]. Among the chemically modified CDs, the hydrophilic or ionizable CDs will enhance drug absorption [3,4], while hydrophobic CDs may have broad applicability [5,6], and could serve as novel slow-release carriers of water soluble drugs, including peptide and protein drugs. Moreover, the biodegradation property of CDs is particularly useful for colon-targeting of drugs. CDs are known to undergo minimal hydrolysis in the stomach and small intestine, while they are selectively fermented into small saccharides by the colonic microflora [7]. These biodegradable properties of CDs make them to be good carrier candidates for preparation of colon specific delivery prodrugs. Indeed, prodrugs are designed to be neither hydrolysed nor absorbed in the upper gastrointestinal (GI) tract but to undergo enzymatic hydrolysis in the colon, releasing the active drug moiety from the carrier. [8]. For this reason several CD-drug conjugates have been prepared and studied as colon specific drug delivery systems [9-13].

Metronidazole (MTZ) is an antibiotic drug particularly used against anaerobic bacteria and protozoa. It is the drug of choice for intestinal amoebiasis [14], an infection of the large intestine caused by *Entamoeba histolytica*, a single celled protozoan parasite [15]. The trophozoites of *E. histolytica* can invade the colonic epithelium, causing amoebic colitis, resulting in hemorrhage and ulceration. MTZ must be delivered to the colon for its effective action against the parasite, but its pharmacokinetic profile indicates that the drug is completely and promptly absorbed after oral administration [16,17]. The administration of this drug in conventional tablet dosage forms provides minimal amount of metronidazole for local action in the colon, causing unwanted systemic effects. Thus, there is a strong clinical need

and a potential market for a delivery system capable of delivering maximum amount of MTZ to the colon in a controlled manner. Various approaches for colon specific drug delivery have been developed and they include: coating with pH sensitive polymer systems, design of timed release dosage forms, and use of prodrugs and carriers that are degraded exclusively by colonic bacteria [18-20].

In this work, metronidazole-CD prodrugs were prepared as colon specific drug delivery system. The strategy for the prodrug production consisted of linking the drug to CDs through a succinyl spacer.

Metronidazole hemiester [21] was firstly prepared and then the carboxyl group of this derivative and hydroxyl group of CDs were coupled via ester linkage. Therefore, MTZ-succinyl-α-, β-and γ-CD conjugates were prepared. The prodrugs were characterized by spectroscopic and analytical methods (IR, CHN, ^{1}H and ^{13}CNMR, and ROESY). In vitro stability studies of the prodrugs were performed at acid (pH=1.2) and alkaline (pH=7.4) pH values. Ex vivo drug release studies from the conjugates were carried out with cecum and colon content of rats.

7.2. Materials and methods

7.2.1. Materials

Metronidazole, succinic anhydride, 4-dimethylaminopyridine (DMAP), 1,1'-carbonyldiimidazole (CDI), α-, β- and γ-CD, Corning® Spin-X UF 500 (10 kDa MWCO) and DIAION HP-20 were obtained from Aldrich (Milan, Italy). All the products and solvents were of analytical grade.

Male Sprague-Dawley rats, weighing 250-275 g were purchased from Charles River (Calco, Italy) and were housed in a temperature- and humidity-controlled room with a 12-h light/dark cycle (light from 7:00 am to 7:00 pm). Animals used in this study were maintained in facilities fully accredited by the American Association for the Accreditation of Laboratory Animal Care and all experimentation was conducted in accordance with the guidelines of the Institutional Care and Use Committee of NIDA, NIH, and of the Guide for Care and Use of Laboratory Animals (National Res. Council, 1996) and the Council of the European Communities (86/809/EEC).

7.2.2. Methods

High-resolution liquid NMR ^{1}H and ^{13}C experiments were recorded at 25°C on a Varian Unity Inova spectrometer operating at 300 MHz in DMSO-d_6 using tetramethylsilane (TMS) as internal standard reference. Phase-sensitive rotating frame nuclear Overhauser effect (ROESY) spectra were recorded at 25 °C on Varian Unity INOVA 400 MHz spectrometer, operating at 400 MHz for ^{1}H and 100 MHz for ^{13}C respectively, and measured under the following conditions: sweep width, 3700 Hz; carrier frequency, 399.94 MHz; spin-lock field, 11 kHz; mixing time, 250 ms. Melting points were carried out in a Köfler apparatus. FTIR spectra were recorded on a Perkin Elmer System 2000 spectrophotometer using KBr mulls. CHNS analyses were carried out on a Fisons model EA 1108 Elemental Microanalyser. Eppendorf centrifuge was used for centrifugation. Thin layer chromatography (TLC) was performed on plates precoated with silica gel 60 F254 (Merck) and an eluent of ethyl acetate/2-propanol/water = 3,5 : 2,5 : 2,5 (indicator p-anisaldehyde).

The amount of released MTZ was assayed by HPLC at 320 nm, using a HP 1100 LC equipped with a Photodiode Array detector 996. The mobile phase consisted of citrate buffer (pH=2.6): acetonitrile (80:20 v/v) and was filtered through a 0.45 μm membrane filter before use. The mobile phase was eluted at a flow rate of 1 ml/min. The column was a Hypersil ODS 5.0 μm (4.6 x 200 mm, HP). Retention times of cyclodextrin conjugates, MTZ, and metronidazole hemisuccinate were 2.6, 3.5 and 5.5 minutes, respectively. Their concentrations in samples were calculated from the calibration curve constructed at the concentration range of 0.03-0.003 mg/ml for MTZ and metronidazole hemisuccinate and 0.1-0.01 mg/ml for CD conjugates (correlation coefficients, R^2 between 0.999 and 0.997).

7.2.3. General procedure for preparation of metronidazole-succinyl-α-, β-, and γ-cyclodextrin conjugates (**3, 4**, **5**)

Metronidazole hemisuccinate (MTZ-SUC, **2**) compound was obtained according to previously reported procedures [30]. The metronidazole-succinyl-cyclodextrin (MTZ-SUC-α-CD, **3**; MTZ-SUC-β-CD, **4**; MTZ-SUC-γ-CD, **5**) ester conjugates

were prepared by coupling CDs with carboxyl groups of hemiesters **2**. The hemiester (**2**, 1.2 mmol) was dissolved in 5 ml of anhydrous dimethyl sulfoxide and 1,1'-carbonyldiimidazole (CDI, 1.25 mmol) was added. The reaction mixture was stirred at room temperature for 90 minutes under N_2 flow to activate the carboxyl group of **2**, and then CDs and 5 ml of triethylamine were added. The reaction was left under stirring at room temperature for 48 hours. Subsequently, a large amount of acetone (200 ml) was added to the solution, and the resulting precipitates were collected by filtration through a 0.45 μm membrane filter (Alltech, Italy). The conjugates were purified by column chromatography using porous polystyrene resin DIAION HP-20 (5 x 20 cm) and eluting with methanol and 0.1 M acetic acid with increasing methanol content. The elutes were monitored by TLC and the prodrugs appeared in the 40-60% methanol in acetic acid fraction. The fractions containing the conjugates were collected, part of the solvent was removed under reduced pressure and the product was precipitated by adding 200 ml of acetone anhydrous; the resulting precipitate was collected by filtration (0.45 μm) and let to dry in a desiccator under vacuum. Finally, the ester conjugates **3**, **4** and **5** were obtained as white powders.

2-(2-methyl-5-nitro-1H-imidazol-1-yl)ethyl]-4-(α-cyclodextrin)-4-oxobutanoate **(3)**

Yield: 24.5%; m.p.: 260°C. IR (KBr mull) cm^{-1}: 3389 cm^{-1} (OH), 1731 cm^{-1} (ester CO), 1651 cm^{-1}, 1151 cm^{-1} 1023 cm^{-1}, 951 cm^{-1} (CD sugar structure). ^{1}H NMR (DMSO-d_6) δ (ppm) 2.59-2.62 (m, overlaps with DMSO- d_6, H_8-, H_9-, H_7-MTZ-SUC), 3.41-3.91 (m, 36 H, H_2-, H_4-, H_5-, H_6-, H_3-CD), 4.12 (t, H_3'-CD), 4.38-4.42 (dd, H_2'-CD), 4.49-4.51 (t, 2H, H_4-MTZ-SUC), 4.58-4.63 (d, 6H, OH_6-CD, D_2O exchange), 4.68-4.70 (t, 2H, H_5-MTZ-SUC), 4.89-4.95 (m, 5H, H_1-CD), 5.12-5.13 (d, 1H, H_1'-CD), 5.58-5.82 (m, 11H, OH_{2-3}-CD, D_2O exchange), 8.16 (s, 1H, H_2-MTZ-SUC)**.** ^{13}C NMR (ppm) 14.06 (C_7-MTZ-SUC), 28.46 (C_8-MTZ-SUC), 30.81 (C_9-MTZ-SUC), 44.83 (C_4-MTZ-SUC), 59.86-60.33 (C_6-CD), 62.50 (C_5-MTZ-SUC), 69.56 (C_3'-CD), 71.58 (C_5-CD), 72.23-72.48 (C_2-CD), 72.87-73.36 (C_3-CD), 73.67 (C_2'-CD), 81.86-82.50 (C_4-CD), 98.60 (C_1'-CD), 102.2-102.9 (C_1-CD), 133.9 (C_2-MTZ-SUC), 138.6 (C_3-MTZ-SUC), 151.8 (C_1-MTZ-SUC), 171.9 (C_6-MTZ-

SUC), 172.2 (C_{10}-MTZ-SUC). CHN: calculated from ($C_{46}H_{71}N_3O_{35}$) C: 45.05; H: 5.80; N: 3.43; found C: 44.59; H: 5.91; N: 3.37.

2-(2-methyl-5-nitro-1H-imidazol-1-yl)ethyl]-4-(β-cyclodextrin)-4-oxobutanoate **(4)**

Yield: 25.2%; m.p.: 278°C. IR (KBr mull) cm^{-1}: 3382 cm^{-1} (OH), 1740 cm^{-1} (ester CO), 1638 cm^{-1}, 1156 cm^{-1}, 1029 cm^{-1}, 947 cm^{-1} (CD sugar structure). ^{1}H NMR (DMSO-d_6) δ (ppm) 2.59-2.66 (m, overlaps with DMSO- d_6, H_8-, H_9-, H_7-MTZ-SUC), 3.44-3.75 (m, H_2-, H_4-, H_5-, H_6-, H_3-CD), 3.99 (t, H_3'-CD), 4.40-4.50 (t, 2H, H_4-MTZ-SUC), 4.58-4.60 (d, 7H, OH_6-CD, D_2O exchange), 4.69 (t, 2H, H_5-MTZ-SUC), 4.93 (s, 6H, H_1-CD), 5.15 (s, 1H, H_1'-CD), 5.58-5.62 (t, H_2'-CD), 5.7-6.04 (m, 13H, OH_{2-3}-CD, D_2O exchange), 8.16 (s, 1H, H_2-MTZ-SUC). ^{13}C NMR (ppm) 14.04 (C_7-MTZ-SUC), 28.47 (C_8-MTZ-SUC), 30.79 (C_9-MTZ-SUC), 44.81 (C_4-MTZ-SUC), 60.05 (C_6-CD), 62.49 (C_5-MTZ-SUC), 69.50 (C_3'-CD), 71.58 (C_5-CD), 72.12-72.5 (C_2-CD), 73.16 (C_3-CD), 73.20 (C_2'-CD), 81.22-81.81 (C_4-CD), 98.32 (C_1'-CD), 101.40-102.01 (C_1-CD), 133.12 (C_2-MTZ-SUC), 138.54 (C_3-MTZ-SUC), 151.70 (C_1-MTZ-SUC), 171.74 (C_6-MTZ-SUC), 172.03 (C_{10}-MTZ-SUC). CHN: calculated from ($C_{52}H_{81}N_3O_{40}$) C: 44.95; H: 5.83; N: 3.02; found C: 43.20; H: 6.89; N: 2.72.

2-(2-methyl-5-nitro-1H-imidazol-1-yl)ethyl]-4-(γ-cyclodextrin)-4-oxobutanoate **(5)**

Yield: 24.3%; m.p.: 280°C. IR (KBr mull) cm^{-1}: 3380 cm^{-1} (OH), 1737 cm^{-1} (ester CO), 1635 cm^{-1}, 1152 cm^{-1}, 1021 cm^{-1}, 950 cm^{-1} (CD sugar structure). ^{1}H NMR (DMSO-d_6) δ (ppm) 2.58-2.74 (m, overlaps with DMSO- d_6, H_7-, H_8-, H_9-MTZ-SUC), 3.32-3.72 (m, 48H, H_2-, H_3-, H_4-, H_5-, H_6-CD), 3.91 (t, H_3'-CD), 4.46-4.50 (t, 2H, H_4-MTZ-SUC), 4.55-4.62 (d, 8H, OH_6-CD, D_2O exchange), 4.67 (t, 2H, H_5-MTZ-SUC), 4.83 (s, 7H, H_1-CD), 5.15 (s, 1H, H_1'-CD), 5.58-5.62 (t, H_2'-CD), 5.71-6.00 (m, 15H, OH_{2-3}-CD, D_2O exchange), 8.16 (s, 1H, H_2-MTZ-SUC). ^{13}C NMR (ppm) 14.03 (C_7-MTZ-SUC), 28.50 (C_8-MTZ-SUC), 30.79 (C_9-MTZ-SUC), 44.83 (C_4-MTZ-SUC), 59.74 (C_6-CD), 62.54 (C_5-MTZ-SUC), 69.21 (C_3'-CD), 71.89 (C_5-CD), 72.26-73.00 (C_2-CD), 73.32 (C_3-CD), 73.84 (C_2'-CD), 78.38-81.49 (C_4-CD), 97.54 (C_1'-CD), 101.0-102.1 (C_1-CD), 133.1 (C_2-MTZ-SUC), 138.6 (C_3-MTZ-SUC), 151.7 (C_1-MTZ-SUC), 171.4 (C_6-MTZ-SUC), 171.9 (C_{10}-MTZ-SUC). CHN:

calculated from ($C_{58}H_{91}N_3O_{45}$) C: 44.91; H: 5.92; N: 2.71; found C: 44.68; H: 5.87; N: 2.73.

7.2.4. Stability studies

The conjugates stability was checked in two different media: acid (pH=1.2) and alkaline (pH=7.4) buffers [22] in a thermostatic bath at 37 °C. 3.5 mg of each conjugate were placed in a closed flat bottom tube containing 25 ml of the buffer solution. The solution was continuously stirred and the system was maintained at 37 °C for 24 hours. At appropriate time intervals, 1 ml solution was removed and replaced with the same buffer. 20 µl of the withdrawn solution was assayed by HPLC as reported above to determine the percentage of the released drug and the disappearance of the conjugates.

7.2.5. Drug release studies

Rats were anaesthetized by chloral hydrate (300 mg/Kg ip), the abdomen was opened and the cecum and colon were traced, legated at both ends, dissected and immediately transferred into pH=7.4 buffer. A portion of the cecal and colonic bag was immediately used for the experiment (content **A**) while another one was frozen and stored at -80 °C (content **B**). The cecal or colonic bags were opened and their contents were individually weighed, pooled, and then suspended in the buffer to give 10% w/v dilution. The release studies were performed by incubating each conjugate or hemiester with a 10% w/v cecal and colonic content of rats. These studies were carried out using both cecum and colon contents **A** and **B**. 2 mg of each conjugate were added to 5 ml of the 10% w/v suspension of cecal and colonic contents (**A** or **B)** and the mixture was stirred and incubated at 37 °C under N_2 flow to maintain the anaerobic condition as the cecum and the colon are naturally anaerobic. At appropriate time intervals, 0.5 ml of the suspension were withdrawn, acidified by addition of 1.0 M HCl solution (0.3 ml) and centrifuged at 7000 rpm for 5 minutes. 0.4 ml of the supernatant was ultrafiltered using a membrane filter (Corning® Spin-X®, a centrifugation of 5000 rpm for 20 min). The concentration of conjugates,

MTZ, and MTZ-SUC was determined in 20 μl of the filtrate by HPLC as described above. Each experiment was carried out in triplicate.

7.2.5. Statistical analysis

Data analysis was carried out with the software package R, version 2.10.1. Results are expressed as the mean ± standard deviation (S.D.). Multiple comparisons of means (Tukey test) were used to substantiate statistical differences between groups, while Student's t-test was used for comparison between two samples. Significance was tested at the 0.05 level of probability (p).

7.3. Results and discussion

7.3.1. Preparation and characterization of the ester conjugates and their intermediates

CDs are natural oligosaccharide with a considerable number of hydroxyl groups (α-CD: 18 OH; β-CD: 21 OH and γ-CD: 24 OH), which could be esterified with carboxylic groups of different drugs to prepare CD-drug conjugates. Since MTZ does not have any carboxylic acid group, succinic anhydride was used to insert a spacer capable of interacting with the OH group of MTZ [23]. This reaction was catalyzed by 4-dimethylaminopyridine (DMAP), as previously reported by other authors [21]. Then, MTZ-SUC was directly conjugated to CD by the activated ester method. Carbonyldiimidazole (CDI) was chosen as coupling agents because it allows one-pot ester formation (Scheme 1). Practically, the acylimidazole (activated species, **2'**) is formed in 1 hour by reacting the metronidazole hemiester and CDI in anhydrous dimethyl sulfoxide and then the cyclodextrin is added directly to the reaction mixture to give the final ester conjugate [24]. The reaction mixture should be kept under N_2 flow because both CDI and the acylimidazole are instable in water. It is believed that the excess of triethylamine activates the cyclodextrin hydroxyl groups through general base catalysis [21]. The MTZ-CD conjugate was separated by column chromatography. The chemical structure of the conjugates (**3**, **4**, **5**) (Figure 1) was determined by IR, CHN, and ^{1}H and ^{13}C NMR spectroscopy.

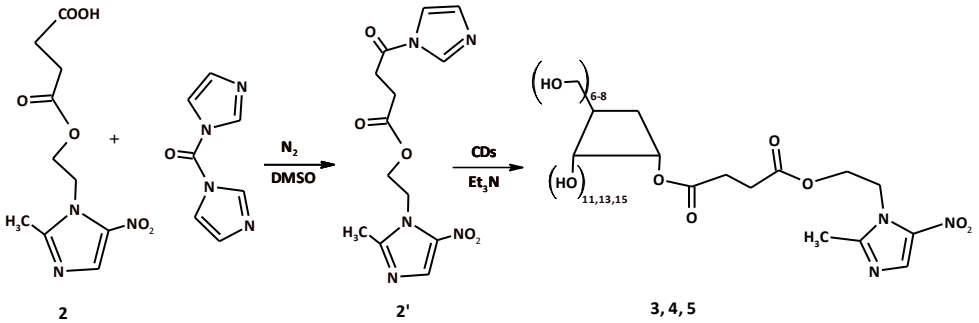

Scheme 1. Synthesis of metronidazole-succinyl-α-, β-, γ-CD conjugates (3, 4, 5).

Elemental analysis and NMR studies showed that the conjugate was monosubtituted and ^{1}H NMR spectroscopy indicated that MTZ-SUC was introduced at the secondary O_2 or O_3 hydroxyl group of the CD.

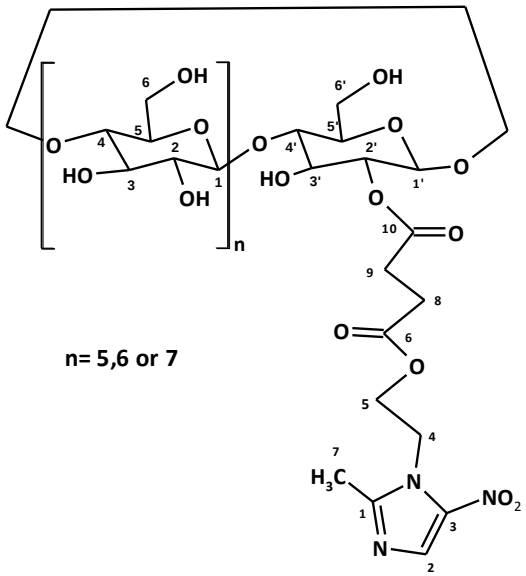

Figure 1. Chemical structures of metronidazole-succinyl-α-, β-, γ-CD conjugates (3, 4, 5).

This was demonstrated by the NMR. In fact, in the ^{1}H NMR spectrum of the α-CD derivative, the H_2 and H_3 protons of the CD gave new signals at 4.12 and 4.4 ppm (peaks H_3'-CD and H_2'-CD) respectively, in addition to the original signals at 3.412-3.9 ppm (H_3-CD and H_2-CD). In the ^{13}C NMR spectrum (Figure 2) the appearance

of new signals at 69.56 and 73.67 ppm (peaks C_3'-CD and C_2'-CD, respectively) besides the original signals at 72.3 and 73.0 ppm (peaks C_3-CD and C_2-CD, respectively) confirmed what ^{1}H NMR let us to suppose. Moreover, the C_6 carbon (C_6-CD) located at the primary hydroxyl side gave no additional ^{13}C signals. These results indicate that MTZ-SUC was introduced at the secondary O_2 (prevalently) and O_3 hydroxyl group of α-CD. Similar results were obtained with β-CD and γ-CD conjugates. They are in accordance with the results obtained by Yano et al. [11].

The esterification reaction involved mainly the secondary hydroxyl group in C_2 of CD [25] because it is more acid than that of C_6 [26] and it is not as sterically hindered as that of C_3 [27].

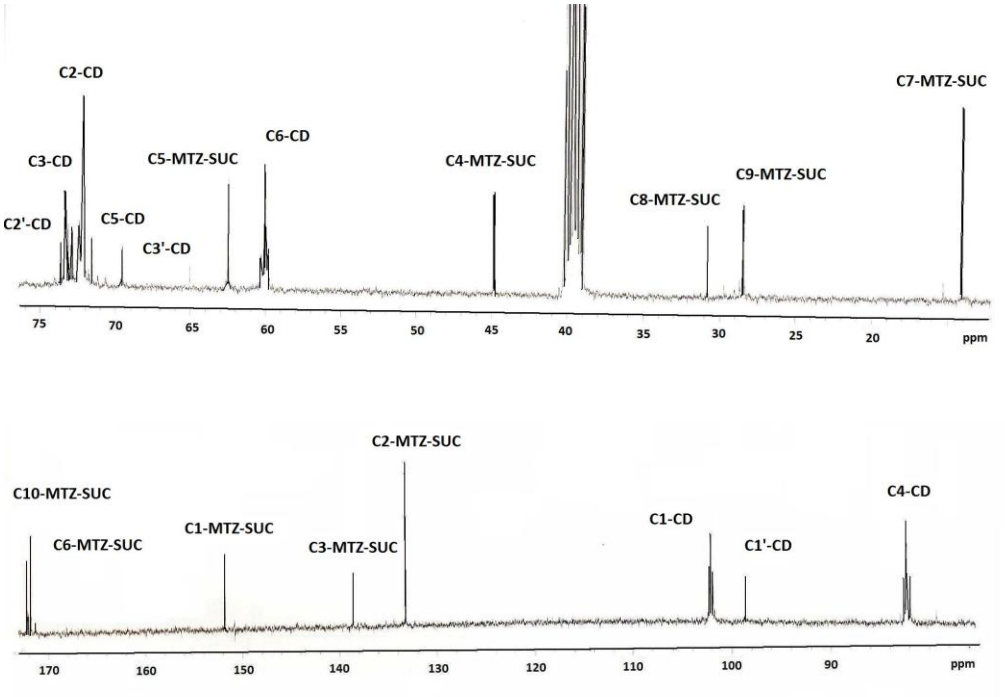

Figure 2. 13C NMR spectrum of MTZ-SUC-a-CD conjugate. See Figure 1 for the atom numbering of MTZ-SUC and CD.

To verify if the drug was completely or partially included in the cyclodextrin cavity, NMR ROESY spectroscopic studies were conducted. Figure 3 shows ROESY spectra of MTZ-SUC-α-CD. In particular, it was evaluated if the H_2 and the $-CH_3$ substituent of the imidazole ring gave correlation peaks with H_3-CD and H_5-CD

located inside the cyclodextrin cavity, indicating that the ring is included in the CD cavity. As can be seen, the interactions are too weak to conclude that the drug is completely or partially included in the CD.

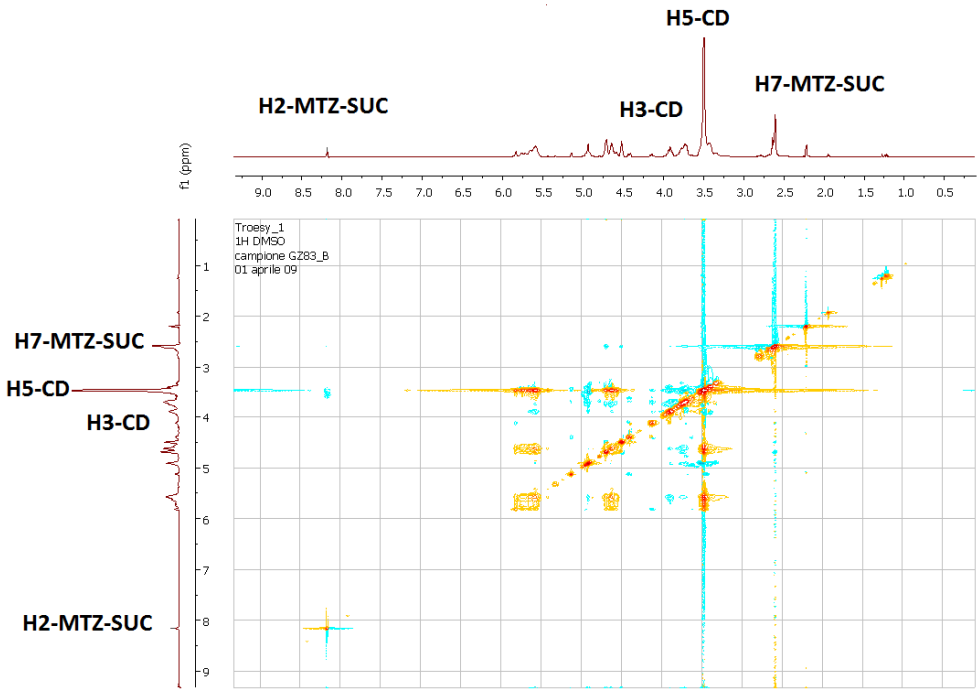

Figure 3. ROESY spectrum of MTZ-SUC-a-CD. See Figure 2 for the atom numbering of MTZ-SUC and CD.

This is confirmed by the 3D simulation (Chem 3D Ultra 8.0) of the conjugate that revealed that MTZ cannot be accommodated in the cyclodextrin cavity probably because of the steric hindrance of the two substituents in position 1 (methyl) and 3 (nitro) of the imidazole ring (Figure 4).

The physicochemical properties of MTZ, MTZ-SUC and **3**, **4** and **5** conjugates are presented in Table 1.

Table 1. Physicochemical properties of MTZ, MTZ-SUC and MTZ-SUC-CD conjugates (3, 4, 5).

Compound	*Molecular weight*	*Melting point (°C)*	*Yield %*
MTZ	171.13	160	-
MTZ-SUC	271.22	109	90.0
MTZ-SUC-α-CD	1225.22	260	24.5
MTZ-SUC-β-CD	1388.23	278	25.2
MTZ-SUC-γ-CD	1550.34	280	24.3

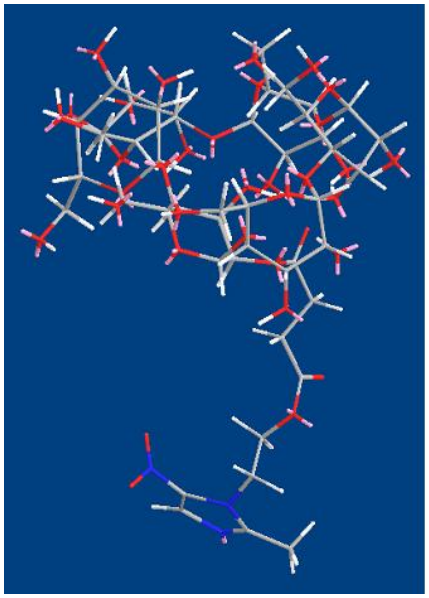

Figure 4. 3D simulation of MTZ-SUC-α-CD

7.3.2. Stability studies

Both esteric bonds of the prodrugs (between drug and spacer and between spacer and cyclodextrin) are susceptible to hydrolysis. The hydrolysis could be catalysed by acidic or alkaline media or by an enzyme. The colon targeting prodrug should be stable in the stomach and small intestine to pass unmodified and reach the colon, where the enzymes catalyze the drug-carrier bond hydrolysis thus releasing the drug in the site of action. Therefore, stability studies of the cyclodextrin conjugates in both acidic and alkaline media were firstly carried out in two different solutions

(pH=1.2 and 7.4). The disappearance of the cyclodextrin conjugate and the appearance of the released MTZ and MTZ-SUC were monitored during 24 hours experiments by HPLC. Results are shown in Figure 5, which shows results of the stability studies for α-CD conjugate (β- and γ-CD conjugates gave similar results). None of the prodrugs released the carried drug during the 24 h experiments in aqueous buffers (pH=1.2, Fig 5a and pH=7.4, Fig. 5b). Neither MTZ nor MTZ-SUC were released from the prodrugs, and only the MTZ-CD conjugate was detected by HPLC thus indicating that both the estereal bonds in conjugates **3**, **4** and **5** were stable in acid and alkaline pH and that the prepared prodrugs were chemically stable in the pH environment of the gastrointestinal tract.

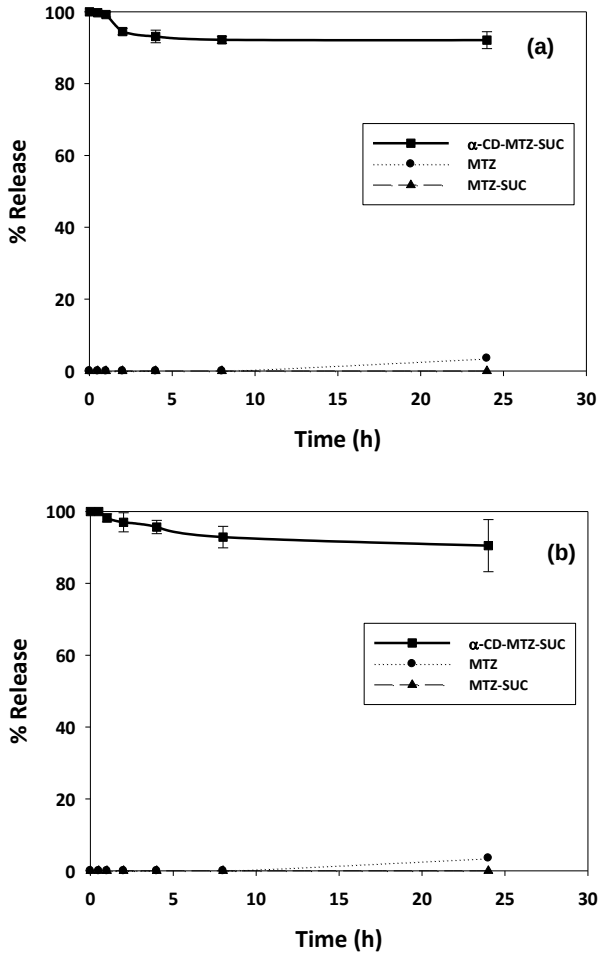

Figure 5. Stability studies of MTZ-SUC-α-CD in acid (pH=1.2) and alkaline (pH=7.4) buffers at 37°C. 5(a) buffer at pH 1.2; 5(b) buffer at pH 7.4. Error bars represent standard deviation, *n* =3.

7.3.3. Drug release studies

It is expected that the esteric bonds could be hydrolysed by the esterases of the cecum and colon. Therefore, we studied the drug release behaviour of the conjugates in cecum and colon contents of rats. In a previous work we found that when these studies were carried out in cecum or colon contents **A** (immediately used) neither MTZ nor MTZ-SUC were detected by HPLC. However, it is well known that MTZ is metabolized in the colon: N-(2-hydroxyethyl)-oxamic acid [28] and acetamide [29] are formed when the drug is reduced as a result of the colonic anaerobic bacteria activity. Also MTZ-SUC was found to disappear in cecum and colon content content **A**. On the other hand, when these studies were carried out in cecum or colon content **B** (previously frozen and stored at -80 °C) MTZ and MTZ-SUC were detected. We concluded that most likely the freezing procedure reduced the activity of some enzymes [30].

Also in this study, the drug release behaviour was studied in both contents **A** (immediately used) and **B** (previously frozen and stored at -80 °C). In this case the disappearance of the cyclodextrin conjugates was monitored. Figures 6, 7 and 8 show drug release from **3**, **4** and **5** in rat cecum and colon content **A.** As can be seen, the conjugates rapidly disappeared (after four hours) but no appreciable amounts of MTZ and MTZ-SUC were detected due to their fast metabolization by the colonic anaerobic bacteria activity. Release profiles indicated that the amount of MTZ and MTZ-SUC increased only up to 8% in the first two hours of the experiments to decrease and disappear after 4 hours. This is in accordance with the previously obtained results [30].

No substantial differences were observed in the release behaviour of the three prodrugs in cecum and colon content **A** but all the three products were rapidly hydrolysed.

However, some differences were observed in the hydrolysis rate of the three cyclodextrin conjugates during the first two hours and especially in the beginning of the experiments. In fact, after 30 minutes in the colon content **A,** α-CD conjugate amount was 65% (Fig. 6b), while β– (Fig.7b) and γ-CD (Fig.8b) conjugates were 60 and 40%, respectively. Therefore, it seems that as the cyclodextrin ring increases,

the rate of hydrolysis is faster (the bigger the CD ring is, the faster the rate of hydrolysis). It was no possible to gain insight the mechanism of hydrolysis due to the subsequent metabolization of MTZ and MTZ-SUC.

Preliminary overall obtained results showed that the conjugates are able to reach the cecum and colon without significant degradation, while they are selectively hydrolysed in the large intestine to release metronidazole.

Ex vivo hydrolysis studies in the content of cecum and colon of rats **B** are still in progress to verify the effective metronidazole release.

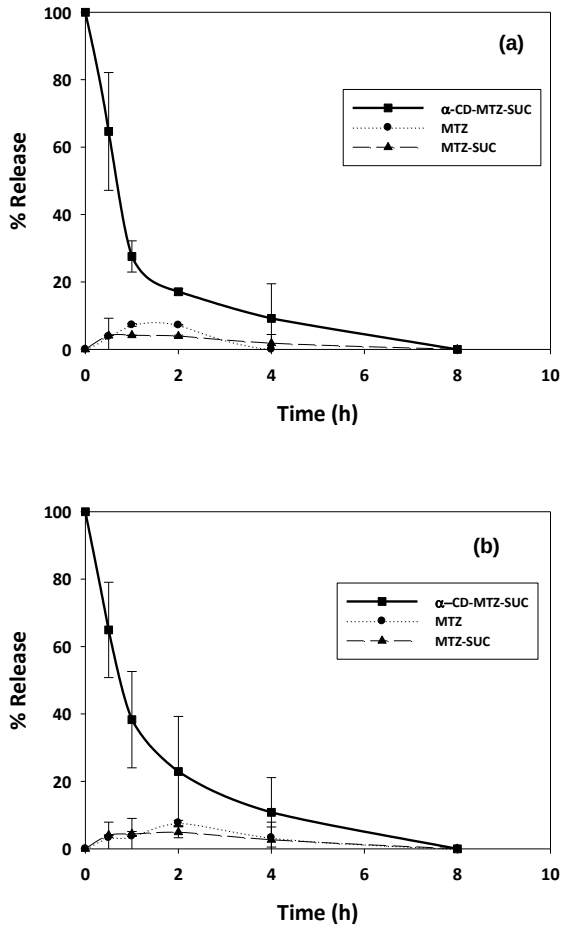

Figure 6. MTZ and MTZ-SUC release and MTZ-SUC-α-CD (3) disappearance during incubation of conjugate 3 with freshly prepared contents A of cecum (a) and colon (b) at 37°C. Error bars represent standard deviation, *n* =3

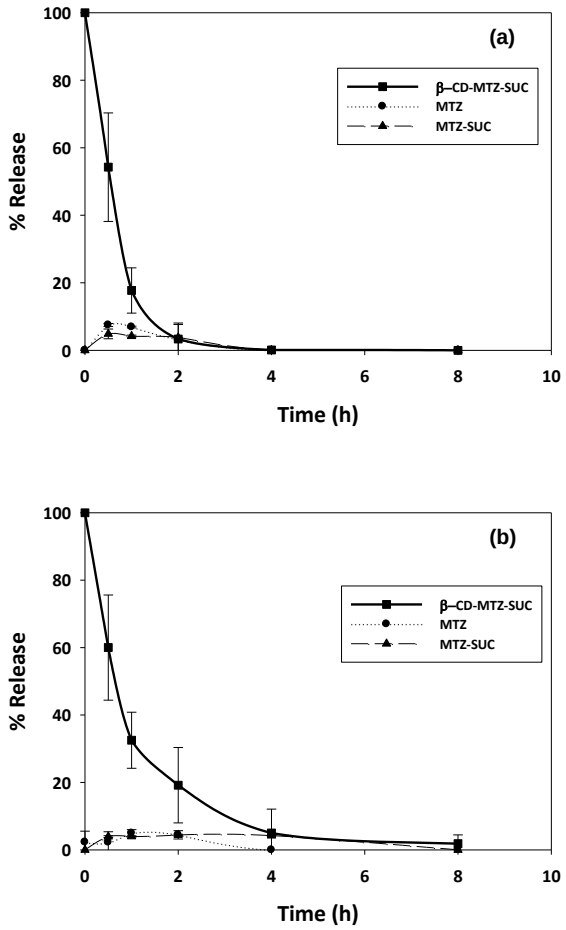

Figure 7. MTZ and MTZ-SUC release and MTZ-SUC-β-CD (4) disappearance during incubation of conjugate 4 with freshly prepared contents A of cecum (a) and colon (b) at 37°C. Error bars represent standard deviation, *n* =3

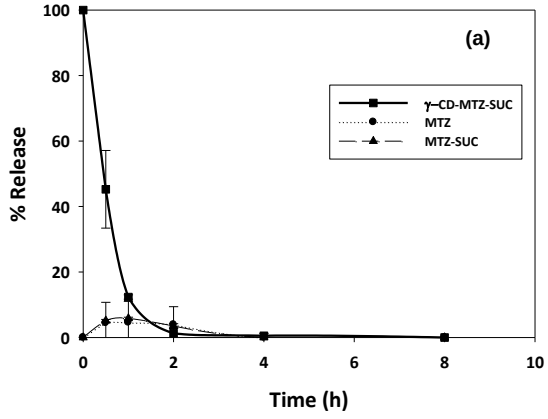

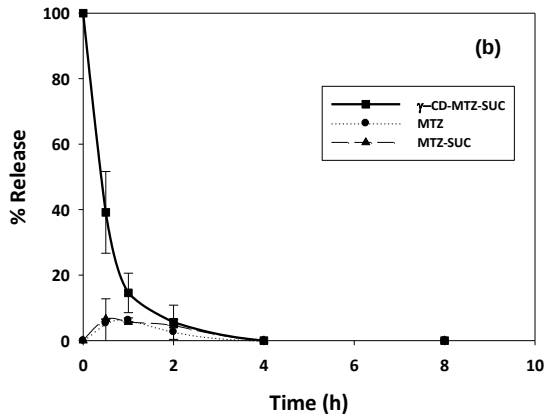

Figure 8. MTZ and MTZ-SUC release and MTZ-SUC-γ-CD (5) disappearance during incubation of conjugate 5 with freshly prepared contents A of cecum (a) and colon (b) at 37°C. Error bars represent standard deviation, *n* =3

7.4. Conclusion

MTZ-SUC was selectively conjugated via an ester bond to one of the secondary hydroxyl group of α-, β- and γ-CD. These conjugates were chemically stable in acid and alkaline media (pH=1.2 and 7.4), while they were hydrolyzed in cecum and colon contents of rats by the action of the enzymes produced by the microflora. In conclusion, the present data suggest that metronidazole-succinyl-cyclodextrin conjugates could serve as colon-specific prodrugs.

7.5. References

[1] K. Uekama, F. Hirayama, T. Irie. Cyclodextrin Drug Carrier Systems. Chem. Rev. 98 (1998) 2045-2076.

[2] F. Hirayama, K. Uekama. Cyclodextrin-based controlled drug release system. Adv. Drug Deliv. Rev. 36 (1999) 125–141.

[3] C.M. Fernandes, P. Ramos, A.C. Falcao, F.J.B. Veiga. Hydrophilic and hydrophobic cyclodextrins in a new sustained release oral formulation of nicardipine: in vitro evaluation and bioavailability studies in rabbits. J. Controlled Release 88 (2003) 127–134.

[4] O.A.E. Soliman, K. Kimura, F. Hirayama, K. Uekama, H.M. El-Sabbagh, A.E.H.A. El-Gawad, F.M. Hashim. Amorphous spironolactone-hydroxypropylated cyclodextrin complexes with superior dissolution and oral bioavailability. Int. J. Pharm. 149 (1997) 73-83.

[5] V. Lemsle-Lamache, D. Wouessidjewe, M. Cheron, D. Duchene. Study of β-cyclodextrin and ethylated β-cyclodextrin salbutamol complexes, in vitro evaluation of sustained-release behaviour of salbutamol. Int. J. Pharm. 141 (1996) 117-124.

[6] V.R. Sinha, A. Nanda, R. Kumria. Cyclodextrins as Sustained-Release Carriers. Pharmaceutical Technology (2002) 36-46.

[7] B. Van Ommen, A.T.H.J. De Bie, A. Barb. Disposition of ^{14}C-α-cyclodextrin in germ-free and conventional rats. Reg. Tox. Pharm. 39 (2004) S57-S66.

[8] V.R. Sinha, R. Kumria. Microbially triggered drug delivery to the colon. European Journal of Pharmaceutical Sciences 18 (2003) 3-18.

[9] K. Uekama, K. Minami, F. Hirayama. 6^{A}-*O*-[(4-Biphenylyl)acetyl]-α-, -*β*-, and -*γ*-cyclodextrins and *6*^{A}-Deoxy-*6*^{A}-[[(4-biphenylyl)acetyl]amino]-]-α-, -*β*-, and -*γ*-cyclodextrins: Potential Prodrugs for Colon-Specific Delivery. J. Med. Chem. 40 (1997) 2755-2761.

[10] H. Yano, F. Hirayama, M. Kamada, H. Arima, K. Uekama. Colon-specific delivery of prednisolone-appended α-cyclodextrin conjugate: alleviation of systemic side effect after oral administration. J. Controlled Release 79 (2002) 103–112.

[11] H. Yano, F. Hirayama, H. Arima, K. Uekama. Preparation of Prednisolone-Appended *α*-, β- and γ-Cyclodextrins: Substitution at Secondary Hydroxyl Groups and *In Vitro* Hydrolysis Behavior. J. Pharm. Sci. 90 (2001) 493-503.

[12] A.H. El-Kamel, A.A.-M. Abdel-Aziz, A.J. Fatani, H.I. El-Subbagh. Oral colon targeted delivery systems for treatment of inflammatory bowel diseases: Synthesis, in vitro and in vivo assessment. Int. J. Pharm. 358 (2008) 248–255.

[13] M. Zou, H. Okamoto, G. Cheng, X. Hao, J. Sun, F. Cui, K. Danjo. Synthesis and properties of polysaccharide prodrugs of 5-aminosalicylic acid as potential colon-specific delivery systems. European Journal of Pharmaceutics and Biopharmaceutics 59 (2005) 155–160.

[14] C.D. Freeman, N.E. Klutman, K.C. Lamp. Metronidazole. A therapeutic review and update. Drugs 54 (1997) 679-708.

[15] L. Stanley. Amoebiasis. Lancet 361(9362) (2003) 1025-1034.

[16] A.H. Lau, N.P. Lam, S.C. Piscitelli, L. Wilkes, L.H. Danziger. Clinical pharmacokinetics of metronidazole and others nitroimidazole anti-infectives. Clin. Pharmacokinet. 23 (1992) 328-364.

[17] K.C. Lamp, C.D. Freeman, N.E. Klutman, M.K. Lacy. Pharmacokinetics and pharmacodynamics of the nitroimidazole antimicrobials. Clin. Pharmacokinet. 36 (1999) 353-373.

[18] C.S. Leopold. Coated dosage forms for colon-specific drug delivery. PSTT 2 (1999) 197-204.

[19] M.K. Chourasia, S.K. Jain. Pharmaceutical approaches to colon targeted drug delivery systems. J. Pharm. Pharm. Sci. 6 (2003) 33-66.

[20] R. Kumar, M.B. Patil, S.R. Patil, M.S. Paschapur. Polysaccharides Based Colon Specific Drug delivery: A Review. Int. J. Pharm.Tech. Res. 1 (2009) 334-346.

[21] S. Vermeersch, F. Vandoorne, D. Permentier, E. Schacht. Macromolecular prodrugs of metronidazole. Esterification of hydroxyl containing polymers with metronidazole monosuccinate. Bull. Soc. Chim. Belg. 94 (1985) 591-596

[22] United States Pharmacopeia (USP 31, NF 26) Printed in the U.S. by Port City Press, Baltimore, 1 (2008) 814.

[23] J. Varshosaz, J. Emami, N. Tavakoli, A. Fassihi, M. Minaiyan, F. Ahmadi, F. Dorkoosh Synthesis and evaluation of dextran–budesonide conjugates as colon specific prodrugs for treatment of ulcerative colitis. Int. J. Pharm. 365, (2009) 69-76.

[24] C.A.G.N. Montalbetti, V. Falque. Amide bond formation and peptide coupling. Tetrahedron 61 (2005) 10827–10852.

[25] D. Icheln, B. Gehrcke, Y. Piprek, P. Mischnick, W.A. König, M.A. Dessoy and A.F. Morel. Migration of secondary *tert*-butyldimethylsilyl groups in cyclomalto-heptaose and -octaose derivatives. Carbohydr. Res. 280 (1996) 237-250.

[26] D. Rong and V.T. D'Souza. A convenient method for functionalization of the 2-position of cyclodextrins. Tetrahedron Lett. 31 (1990) 4275-4278.

[27] W. Saenger, M. Noltemeyer, P. G. Manor, B. Himgerty, B. Klar. "Induced-fit"-type complex formation of the model enzyme α-cyclodextrin. Bioorg. Chem. 5 (1976) 187-195.

[28] L. Koch, P. Goldman. The anaerobic metabolism of metronidazole forms N-(2-hydroxyethyl)-oxamic acid. J. Pharmacol. Exp. Ther. 208 (1979) 406-410.

[29] L Koch, E.J.T. Chrystal, B.B. Beaulieu, J.P. Goldman. Acetamide: a metabolite of metronidazole formed by the intestinal flora. Biochem. Pharmacol. 28 (1979) 3611-3615.

[30] C. Mura, D. Valenti, C. Floris, R. Sanna, M.A. De Luca, A. M. Fadda, G. Loy. Metronidazole Prodrugs: Synthesis, Physicochemical Properties, Stability, and *Ex Vivo* Release Studies. European Journal of Pharmaceutical Chemistry (submitted 2011).

8. CONCLUSION

Several colon specific delivery systems were prepared, characterized and subjected to *in vitro, ex vivo* and *in vivo* studies.

N-Succinyl-chitosan showed that it could be a good carrier candidate for the preparation of matrices for colon specific drug delivery. It showed pH-dependent swelling behaviour and good mucoadhesivness. Due to its favorable physicochemical properties it was able to release the loaded drug selectively at colonic pH (pH=7.4).

The introduction of CD into the matrices resulted in a reduction of drug release from the swollen polymeric matrices, while an increase of drug release from the inert polymers.

Moreover 5-ASA loaded *N*-Succinyl-chitosan microparticles and freeze-dried matrix markedly improved efficacy 5-ASA in the healing of induced colitis in rats, demonstrating the usefulness of these two formulations in the treatment of inflammatory bowel disease.

On the other hand chitosan and cyclodextrin resulted good carrier systems for the preparation of metronidazole-spacer prodrugs. They were basically stable at acidic and alkaline pH, while they selectively released the drug in the content of cecum and colon of rats, showing that these compounds are susceptible to enzymatic hydrolysis.

Both MTZ-SUC-CHT and MTZ-GLU-CHT seemed to be suitable prodrugs for the development of a colonic drug delivery system for MTZ: the first one could be used as a delayed drug delivery system while the second one could guarantee a sustained drug release.

MTZ-SUC-CD prodrugs were rapidly hydrolysed after incubation with cecum and colon contents of rats. Some differences were observed in the hydrolysis rate of the three conjugates especially in the beginning of the experiments. MTZ-SUC-α-CD conjugate hydrolysis rate was the slowest, while MTZ-SUC-γ-CD one was the fastest. Obtained results suggested that as the cyclodextrin ring increases, the rate of hydrolysis is faster.

Summarizing the results of this study we may conclude that all the prepared 5-ASA and MTZ drug delivery systems are potential carriers for targeting the model drug to colon.